Development and characterization of novel a TCRm antibody and its application as an immune checkpoint blocker

By

SOROUSH GHAFFARI.

Presented to the Faculty of the Graduate School of

The University of Texas at Arlington in Partial Fulfillment

of the Requirements

for the Degree of

DOCTOR OF PHILOSOPHY

THE UNIVERSITY OF TEXAS AT ARLINGTON

December 2021

Approved by Supervising Committee

_____

Dr. Jon Weidanz

Committee Chair

_____ _____

Dr. Michael Roner **Dr. Georgios Alexandrakis**

_____ _____

Dr. Shawn Christensen **Dr. Mark Pellegrino**

December 2021

ABSTRACT

Development and characterization of novel a TCRm antibody and its application as an immune checkpoint blocker

Soroush Ghaffari.

The University of Texas at Arlington, 2021

Supervising Professor: Dr. Jon Weidanz, MPH, Ph.D.

Immunotherapy, the treatment of diseases via targeted immune system activation, has recently shown extraordinary success in clinical trials for multiple malignancies. In contrast to a routine therapeutic regimen for cancer, effective immunotherapies can stimulate the innate and adaptive immune system to marsh specific and durable responses against tumors. Immunotherapies come in many shapes and forms. Immune checkpoint blockade (ICB) is an example of immunotherapy that revolutionized the field of immuno-oncology. Considering the recent success of ICB therapies, the scientific community tried to discover new inhibitory molecules and pathways as a new target for cancer immunotherapy.

Indeed, CD94/NKG2A receptor is an inhibitory checkpoint molecule with a high affinity for its ligand non-classical MHC-I, Qa-1^b (mouse), or HLAE (human). The result of this interaction is often a suppression of activated lymphocytes, natural kills cells, and antigen-presenting cells, along with the up-regulation of inhibitory T cells. Thus, this dissertation's general goal is to better understand the nature of this interaction and develop a new therapeutic agent to unleash

the suppressed immune system as a means of eliciting a more robust response. In other to reach out to this goal:

First, we developed a single domain (V_hH) TCR-like monoclonal antibody named EXX-1 with high affinity and selectivity for Qa-1^b/Qdm complex. We evaluated the specificity and avidity effect of our monoclonal antibodies in an in-vitro assay. We used a commercially available monoclonal antibody to Qa-1^b complex (clone 6a8.6f10.1a6) developed by Dr. Soloski's group (Johns Hopkins University, Baltimore, MD) as a positive control for our antibody. During this phase, we noticed that our commercial antibody (clone 6A8) only recognizes the Qa-1^b molecule regardless of the presence or absence of the Qdm peptide. Thus, interaction NKG2A to its ligand couldn't be blocked as the presence of the QDM peptide is crucial for this interaction. However, EXX-1 can recognize a Qdm peptide expressed by the Qa-1^b protein. We found that in the presence of EXX-1, Qa-1^b/ Qdm interaction with CD94/NKG2A will be interrupted. This blockade caused higher immune cell (NK and CD8+ T cell) proliferation and increased tumor kill rates.

Second, we tried to develop an in vivo model for this concept. Thus, we evaluated several mouse tumor models for the expression level of the Qa1^b/Qdm complex. During this phase, we realized that this expression is highly dependent on the cytokines such as IFN-γ. We also observed tumor regression and therefore extended life span of the mice treated with EXX-1 (ES) compared to its isotype control.

Third, we tried to enhance the efficacy of our therapy through. 1- Combination of EXX-1 with tumor vaccination, 2- Antibody dependent cellular cytotoxicity (ADCC). We observed tumor clearance in 40-45% of the mice treated with EXX-1 compared to its isotype. Moreover, we

noticed that EXX-1 treated mice were develop a tumor specific immunity compared to isotype control treated groups.

ACKNOWLEDGEMENTS

My journey to Ph.D. was both a challenging and rewarding process. But it is because of those people who cared, believed and supported me to overcome all challenges during graduate school. First, I would like to thank my supervising professor Dr. Jon Weidanz for giving me the opportunity to work with him and his incredible research team. Thank you for your wisdom, guidance, encouragement, and unwavering empathy throughout all the successes and numerous challenges I have faced. Your support has been above-and-beyond, and I am genuinely grateful to have worked with such an inspiring and kindhearted leader.

Second, I would like to thank my Ph.D. supervisory committee – Dr. Michael Roner, Dr. Shawn Christensen, Dr. Mark Pellegrino, and Dr. Georgios Alexandrakis for their thoughtfulness and continued support, advice, and engorgement throughout the past five years.

My sincere thanks also go to Abexxa biologics and the RSI management team of staff, including my supervisor at RSI, Ms. Debra Wawro and Susanne Gimlin, for their camaraderie and for allowing me to use their laboratory resources, space, and research facilities.

I would like to extend my deepest gratitude to Dr. Katherine Upchurch for all the challenges she gave me to shape me as an individual scientist. Thanks for taking me under your wing to train me for some of the basics of immunology. Thanks for all the help you provided me in past years, for reading my manuscript, and for providing me with constructive suggestions and sometimes funny critics. I also have had the great pleasure of working with Gizem Oter, who provided me with a lot of help and support during the past three years and became like my younger sister. I

cannot tell you guys enough how much your endless support, encouragement, love, and the laughter we all shared has meant to me.

I would like to thank Jean Philip (J.P) and the Flow Core Facility at Baylor institute of immunology for their expertise and help with my FACS Sorting projects. I would like to thank Dr. Trivendra Tripathi for providing me with an opportunity to improve my in vivo techniques. I also would like to thank all the past Weidnaz' lab members who were part of my training and development. Thank you to my current, and previous collogues at UTA and the department of Biology, including Dr. Laura Gough, Dr. Jeff Demuth, Dr. Anya Williford, Dr. Larura Mydlarz, Ms. Linda Taylor, Sherri Echols, Zaida Alsina, Xavier Aranda, Nick Pollock, Chris Magno Pollock, Kathleen Demuth, Alex Ferracuti, for all their support. Thanks to the Animal-Care Facility director Mr. Jeff Campbell, manager Ms. Christin Safieddine and the ACF staff for all the help and assistance during my in-vivo experiments.

Finally, I would like to thank my Dad, Mom and specially my younger sister Sarvi for all their support in this endeavor, I could not have done it with you.

My time at UTA and RSI have been critically constructive and has shaped me to become an individual immunologist. Thank you to everyone who has played a role, large or small, you have made a difference.

Soroush Ghaffari

Nov 8th, 2021

DEDICATION

This dissertation is dedicated to all those who believed in me and provided me with intellectual and emotional support over the past year. I could not have done it with you all.

LIST OF ABBREVIATIONS

µL	Microliter
µg	Microgram
mAb	Monoclonal antibody
HCAbs	Heavy chain associated antibodies
Ig	Immunoglobulin G
CH-1	constant region-1
FR	Framework
CDRs	Complementarity determining regions
TCRm	T cell receptor mimic
CAR	Chimeric antigen receptor
pMHC	Peptide-major histocompatibility complex
HLA	Human Leukocyte antigen
ADCC	Antibody-dependent cell-mediated cytotoxicity
IFN	Interferon gamma
TNF	Tumor necrosis factor
IL	Interleukin
GM-CSF	Granulocyte-Macrophage colony stimulating Factor
TME	Tumor microenvironment

TAM	Tumor associated macrophage
ICI	Immune checkpoint inhibitor
ICB	Immune checkpoint blockade
CM	Central memory
NK	Natural Killer cell
NKT	Natural Killer T cell
Tregs	T regulatory cell
DC	Dendritic cell
APC	Antigen presenting cell
MDSC	Myeloid derived suppressor cells
TIL	Tumor infiltrating lymphocyte
TRL	Toll like receptor
NDR	Node like receptor
TGF	Tumor growth factor
FoxP3	Forkhead box protein 3
CTLA-4	Cytotoxic T-lymphocyte associated protein 4
OX40L	OX40 ligand
PD-1	Program dead-1
PDL-1	Program dead ligand -1

GITR	Glucocorticoid induced TNF receptor
KIR	Killer immunoglobulin like receptor
PGE2	Prostaglandin E-2
COX2	Cyclooxygenase-2
VEGF	Vascular endothelial growth factor
N-CAM	Neural cell adhesion molecule
Aga1, 2	A-agglutinin binding subunits 1, 2
FACS	Fluorescent activated cell sorting
PBMC	Peripheral blood mononuclear cell
FDA	Food and Drug Administration

TABLE OF CONTENTS

LIST OF TABLES

LIST OF FIGURES

CHAPTER 1: INTRODUCTION

What we know about Cancer and its cure?

Cancer is known to be a disease of non-regulated cell growth due to some genetic mutation. Edwin Smith has recorded the first case of cancer in 3000 B.C, although it was Hippocrates in 400 B.C who scientifically described the cancer. Cancer cells can spread to adjacent or distant organs, which known as metastasis (1). Multiple metastases; ultimate failure of the affected organ resulting death in late-stage cancers. Indeed, cancer has no geographical boundaries and consider as second cause of death worldwide. According to the American Cancer Society, the number of death due to cancer is exciding tuberculosis, HIV/AIDS, and malaria. In fact, it is predicted by 2040, the global cancer burden would face an upsurge in the new cases (around 29.5 million new cases), resulting 16.4 million deaths annually.

Healthy tissue requires a mitogen signal (ex: the pRB, p53) for replication and growth, while cancer cells grow even without these signals. As a matter of fact, the tumor suppressor genes are expressed to cease cell division. In contrast, cancer cells have mutated forms of the suppressor gene resulting in skipped apoptosis and aberrant progression through the cell cycle. Moreover, cancer cells prevent normal aerobic respiration in mitochondria, reducing ATP production and reducing the ATP: ADP conversion ratio. Thus, mitochondria are getting deactivate and avoiding the triggering of apoptosis.

Apoptosis or program cell death is a standard feature of the nucleated cells and is considered a vital component for normal cell turnover, proper development, and functioning of the immune system (6). Normal cells have a limited number of divisions until they cannot divide, known as

senescence. Cancerous cells skip this capacity by maintaining telomerase and mislabeling the suppressor genes. The rapid growth of cancer cells and malignancy of tumors will only be achieved by a massive amount of vascularization (angiogenesis). Angiogenesis is typically present in tissue during the wound healing process or development of the embryo. While tumors are using angiogenesis to supply materials, they need for their rapid such as transportation of oxygen, nutrient. Moreover, they gain access to other healthy tissue for possible metastasis through angiogenesis.

When we talk about tumors, it includes not only malignant cells but also surrounding stromal cells such as epithelial cells, fibroblasts, and even more critical tumor-infiltrating immune cells, which are known as the tumor microenvironment (TME).

The standard cure for cancer includes tumor resection via surgery, systemic chemotherapy, and radiotherapy. Systemic chemotherapy was discovered by German chemist Paul Ehrlich in the 1900s and then became part of a routine anti-cancer therapy at the beginning of the 20th century (9). Tumor resection via surgery and radiotherapy dominated the field of cancer therapy up until 1960 which it became clear that combination therapy had an advantage over radical local treatment in some advanced tumors such as advanced Hodgkin lymphoma (9). Moreover, these methods are successful when a malignant tumor is solid, localized, and detected early (2).

Hanahan and his colleagues in 2000 defined six factors that have a direct impact on tumor biology, including limitless replication, insensitivity to anti-growth signal, evading apoptosis, invasion of healthy tissue or metastasis and sustained angiogenesis (1). Further studies lead to a better understanding of tumor biology at the molecular level and what can control cancer growth and its malignancy. This information helped scientists to discover the new generation of therapies such as targeted therapies and immunotherapy. In targeted therapy, therapeutic agents interact with the

specific protein in cancer and inhibit its crucial role in tumor propagation and survival, instead of being generally toxic to tumor cells like chemotherapies (10). Clinicians were able to use the benefit of this druggable protein to target the tumor cells proliferation directly; lead to better results in a patient with certain cancer such as BRAF driven melanoma, HER-2 positive breast cancer, and BCR-ABL driven leukemia. However, not all the tumors express these required proteins to be targeted, and even sometimes those who have these proteins can develop some compensatory mutation in protein' structure that renders the effectiveness of the targeted therapeutics.

The limited efficacy of exogenous therapies and modest benefits that they carried against metastatic cancers made scientists look for a new therapeutic approach to target the tumors. The Idea of using a patient's immune system to fight the disease has been around for about a decade, though with multiple false starts along the way. Cancer immunotherapy primarily focused on activating the T-cells with the implementation of stimulants such as antigenic vaccination and cytokines. However, future research showed that the communication between the immune system and cancer is a dynamic process. As a matter of fact, the immune system has a role of double-edged sword. It can promote tumor progression by targeting aggressive immune evasive subclones and modulating the tumor microenvironment to facilitate tumor propagation. It can also suppress tumors by destroying cancer cells and inhibiting outgrowth (11, 12). Thus, it is remains very important to understand the underlying mechanism of cancer outgrowth and their resistance to our immune system for the design and development of more effective therapies.

Immune system and its function

The idea of targeting tumors by a patient's immune system was proposed by Burnet and Thomas. They raise the points that the immune system should detect self from non-self, such as malignant

tumor (5). Initially, their hypothesis was rejected by the scientific community due to the development of new therapeutic agents such as chemo or radiation. Nowadays, innate immune cells such as natural killer cells (NK cells), macrophages and granulocytes, and adaptive immune systems such as lymphocytes have been shown to perform a significant role in tumor elimination.

The roles of innate and adaptive immune system in tumor microenvironment (TME)

The immune system has an important job to recognize and distinguish normal healthy cells from abnormalities such as a tumor. Innate and adaptive immune cells interact with tumor cells in the tumor microenvironment (TME). TME plays a vital role in the behavior of our immune system when they encounter different tumors. TME determines the migration and proliferation rate of the immune cells population at the tumor site (18, 19). TME cells also have some detrimental roles in tumor angiogenesis and its malignancy (20,21).

Innate immune cells are the first line of defense, and they create a rapid and non-specific response to the tumor. Antigen-presenting cells (APC) are one of the essential members of this family. APCs can get activated by binding to intra or extracellular receptors such as NOD-like receptors (NLR) or toll-like receptors (TLR) (22). Natural Killer cells (NK cells) are another important member of the innate immune system. NK cells directly kill their target by producing lytic protein such as perforin, granzyme, or cytokine like tumor necrosis factor alpha (TNF-α). Moreover, innate immune system can activate adaptive immune system in a specific manner.

During the tumor elimination phase, the release of the tumor antigens is a triggering signal to the innate immune system. Tumor-associated antigens are normal (unmutated) proteins that are either overexpressed or abnormally expressed on the surface of the tumors after embryonic development. A random mutation in the tumor genome also alters these typical tumor markers' protein sequence

or structure, and it forms new antigens known as neoantigens that are foreign to the immune system (30,31). Tumor antigens are released in the TME and captured by APC, primarily dendritic cells (DC). APCs phagocytize these proteins and process them into the small 9 to 10 amino acid peptides. Processed peptides loaded onto the major histocompatibility (MHC) molecule and expressed on their surface. Peptide/MHC complexes are then recognized by the adaptive immune system, such as CD8+ and CD4+ T cells. This recognition cause activation, proliferation, and differentiation of antigen-specific T cells. However, T cells need two additional signals for their activation including 1- co-stimulation of the T cell via interaction of the APC' ligand CD80/86 to T cell receptor CD28, 2- stimulation of the T cells with APC' cytokine (23). These stimulants are extremely important in the T cell's behavior toward anti-tumor response via T helper type I (Th1) or tumorigenic T regulatory cell (Treg) response (24). Activated CD4+ T cells and APCs then interact with B cells and activate them with cytokine production such as interleukin 21 (IL21) and/or CD40. Activated B cells then promote the production of the memory B cells as well as the production of the high avidity antibodies in plasma cells (25,26). Activated CD8+ T cells can produce cytolytic granules containing pore-forming protein (perforin) and granzyme (mediate apoptosis in their target) (27). Plus, activated T cells enhance the function of the tumor-specific T cells via the cytokine that shapes the pro-inflammatory environment in TME.

Suppressive mechanisms of the TME to inhibit the anti-tumor immune response

Previous research has shown that cellular, metabolic, and pathway changes associated with the immunosuppressive response in TME are the main reason for tumor-associated chronic inflammation (32, 33). In TME, anti-tumor effector and inhibitory immune cells must be balanced to prevent tumor progression and metastasis. One of the critical characters of cancer progression

is their ability to evade or resist immune surveillance (27). Some of the TME immune cells have an inhibitory role to paralyze immune cells to not perform their duties. Suppressive innate and adaptive immune cells modify TME and create an anti-inflammatory environment that abrogates the tumor-infiltrating immune cells and their anti-tumor effect (28,29). Recent studies showed that in TME, MHC expression was reduced in DCs. Also, DCs downregulate the expression of CD80/86 and thus cannot prime the T cells. Finally, DCs won't produce cytokines necessary to support the activity of the T cells. A sub-population of the T cells and B cells suppresses the immune system response to tumors named Tregs or B regs.

In 1995, a subpopulation of CD4+ T cells discovered that has a high IL-2 and CD25 receptor which is necessary for the immunologic self-tolerance process (53). They are known as regulatory T cells (Treg). Tregs are usually designed to stop the expansion of the T cells, which escaped the central deletion process in the thymus. They stopped the T cells propagation by binding to their priming signal, such as APC (34- 36).

Tregs express forkhead box transcription factor (FoxP3) and B regs expressing IL-10 and/or IL-35 receptor (28, 29). Foxp3 was also known as a master gene to regulate Treg cell function and development (54-56). In addition to the presence or absence of FoxP3 on T cells, the expression level of this molecule plays a crucial role in Treg function. In other words, when they have more FoxP3, they have more suppressive power (57).

CTLA-4, Il-2 receptor CD25, TGFβ, IL-10, IL35 are other means that help Tregs perform their function (58). Generally, with activation of the effector T-cells, expression of the CTLA-4 ligand will increase. In contrast, Tregs upregulate this ligand only during the resting condition. CTLA-4 competes with CD28, the co-stimulatory (activating signal) for the T-cell to bind to the CD80/86 on APCs.

CD25 is another suppressor marker that expresses by Tregs and has a high affinity for IL-2. IL-2 is a cytokine that considers as a critical mediator for the activation and proliferation of the T-cells. Recently, scientists found that Tregs expressed a high level of the Glucocorticoid-induced TNF receptor (GITR), which contributes to their suppressive behavior (59).

Tregs, alongside the tumor and stromal cells, cause immature myeloid cells recruited to the TEM (37- 39). These cells also suppress the T cells and are known as myeloid-derived suppressor cells (MDSCs). MDSCs are closely related to neutrophils and monocyte while they are only generate and differentiate during chronic inflammation of bone marrow. Generally, whenever a pathogen gets recognized by the immune system, we should expect expansion and activation of the neutrophile and monocyte. This incident caused a series of events such as robust phagocytosis, respiratory burst, and production of pro-inflammatory cytokines that led to the inflammation. Additionally, we can see an elevation of MDSCs's number with tumor progression (42). Generally, the high number of the MDSCs is a sign of the malignancy and poor prognosis of cancer such as melanoma. In general, MDSCs are considered an obstacle for immunotherapeutic agents.

Tumor-associated macrophages (TAMs) can also inhibit T cell activities and thus suppress the immune system. TAMs can exist in the form of the M1- like and can generate IL-12 and IFN-γ that suppress tumor growth , or M2-Like that produce IL-10 and have increased scavenger mannose, galactose E, and C-type receptor which facilitate the tumor growth. In other word, TAMs can either suppress the immune system or activate it.

The tumor-infiltrating dendritic cells (DCs) are another group of cells that reside in TME and influence tumor growth. It is known that CD103+ myeloid dendritic cell, creates a robust anti-tumor effect in TME. However, these cells are extremely rare, and tumor can find a way to reverse their impact (46). Tumor cells can produce vascular endothelial growth factor (VEGF), to prohibit

DCs maturation (50) since immature DCs can suppress the innate or adaptive immune system. For example, immature DCs degrade the arginine by arginase I receptor which is a requirement for T cell activation (51, 52).

Immunotherapy

The field of cancer immunotherapy, also known as immuno-oncology, created in the late 19th century, when a physician in New York treated his patient for the first time with immunotherapy. Dr. William B. Coley injected a mixture of the killed bacteria at the tumor site and named it Coley's toxin (43). Although Dr. Coley's method was successful in some of his patients, immunotherapy did not become popular for the next several decades due to the discovery of other forms of therapy such as chemotherapy.

In 2013 cancer immunotherapy was nominated by science magazine as the breakthrough in the field of cancer. In recent years, immuno-oncology has found its way as a most promising therapeutic technique that provides a paradigm shift for cancer treatment. Unlike traditional cancer interventions such as surgery, chemotherapy, and radiation, immunotherapy works with an individual's immune system. Also, it has the potential for generating long-term responses against the primary, metastatic, and recurring tumor after initial therapy. This effect of immunotherapy is possible only if 1) tumor-associated antigen released in the TME, 2) APCs take up this neo-antigen, 3) naïve lymphocytes get activated by primed APCs and migrate to TME, and finally 4) activated the lymphocyte that can recognize and destroy the tumor (60). If this process is interrupted or not executed accordingly tumor can evade the immune system and continue to grow.

In general, the immune system will react against tumors in three sequential steps: elimination, equilibration, and escape (Fig 1). In the elimination step, both innate and adaptive immune systems

such as Natural killer cells (NK), macrophages, lymphocytes are engaged to destroy cancer before it gets clinical. These steps required cytotoxic mechanisms such as perforin, TNF-2 related apoptosis-inducing ligands, and reactive oxygen species. However, some cancers can skip this phase and enter the next stage, “equilibrium,” in which they become dormant due to the presence of immune cells such as T cells. During this phase, the tumor starts to edit its genome and change its immunogenicity. As a result, tumors cannot be recognized by the force of adaptive immunity. So, they become insensitive to immune effectors and create an immunosuppressive environment in the tumor microenvironment. Next, these immune-insensitive cells can enter the skip phase and form a new tumor that immune system cannot maintain (13,14,15). Based on this finding, immunotherapies need to re-induce the anti-tumor immunity to eliminate these insensitive immune cells. Thus, most of these treatments attempt to activate the tumor-infiltrating T cells that become nonfunctional in the TME (44). These days immunotherapies consider as 5th pillar of cancer therapy due to their effect. Immunotherapy comes in many shapes and forms. Immunotherapies can be proteins, such as aforementioned cytokine therapies IL2 and IFN-α, adoptive cellular therapies like CAR-T cells, cancer vaccines, or the checkpoint blockade such as PD-1 or CTLA-4.

Cytokine therapy

One of the first cytokine that got approved by U.S Food and Drug Administration (FDA) in 1995 was IFN-α (2b). Physician used cytokine as an adjuvant therapy for resected stage IIB/III melanoma, due to its stimulatory roles on various immune cells such as lymphocytes and dendritic cells. Later in 1998, FDA recognized and approved usage of the IL-2 for the treatment of the metastatic melanoma. IL-2 is an anchor cytokine and is used as T cells’ growth stimulant.

Adoptive cellular therapies

Adoptive cell transfer is another method to stimulate patient immune system. Example of this method is isolation, ex-vivo modification and re-infusion of the T cell for each individual known as adaptive T cell transfer. One of the famous examples of this category is chimeric antigen receptor T cell therapy know as CAR- T cells therapy. In this method immune cells can be extracted from either tumor cells or from patient's blood. One of the advantages of tumor infiltrating lymphocytes (TIL) in compare to patient's blood mono nuclear cells (PBMC) is that they already being primed with tumor neo-antigens so they can act more specific against tumor. However, we won't be able to isolate many TIL cells from TME (61, 62, 63).

Dr. Zelig Eshhar designed and used CAR-T cells for the first time to treat invitro tumor and named the cells "T-bodies" (64). Dr. Eshhar's CAR-T cells incorporated with intracellular motif from CD3 zeta chain to simulate the phosphorylation signals from the TCR complex that initiates T cell activation. Later, scientist advanced this technology and developed other generation of the CAR-T cells (65). Although CAR-T cell therapy has shown enormous success for treatment of some cancers such as hematopoietic cancers, they have limited efficacy in solid tumors (66).

Cancer vaccines

Cancer vaccine is another format of the immunotherapy. Rational behind this method is that in addition to boosting immune system via vaccine's adjuvant, inoculation with tumor neo-antigens will allow patient's adaptive immune system to develop a response against them which can end up to tumor clearance. cancer vaccines can be classified into three groups including 1- cellular, 2-viral, 3-molecular.

Sipuleucel-T is an example of the cellular vaccine that got FDA approval and has improved patient' survival time up to 4.5 months. In this method patient' dendritic cells utilize with granulocyte-macrophage colony-stimulating factor (GM-CSF) and prostatic acid phosphatase, and then reinfused back into the patient (67).

Viral vaccine takes advantage of the nature of patient's immune response to virus. In this method Viral vector is engineered to express tumor antigen and thus its prime the innate and adaptive immune system against these proteins (68, 69). One of the limitation factors for this method is that when adaptive immune system got stimulated against the viral vector, they produce neutralizing antibody. In this case viral vector don't have enough time to reach and infect the cells and reach out to their purpose, depositing tumor antigens. TroVax vaccine is an example for this method that is under trial for treatment of the metastatic renal carcinoma.

Molecular base vaccines use the peptide, RNA or DNA that encode the tumor antigens as a triggering point for immune system. This protein can be natural protein that tissue express in abnormal way or can be neo-antigens. One of the main challenges of this method is that TIL that strongly react to antigen and remove it during central and peripheral tolerance. Therefore, presence of the adjuvant is necessary to stimulate the low affinity T cells (70, 71). Other downfall of the molecular based vaccine is antigen expression in non-cancerous cells can lead to on-target off-tumor toxicity (72).

Immune Check-point Blockade (ICB) mechanism of effect

The idea of using immune system to fight the cancer has been around for more than a decade and faced a lot of ups and downs along the way. Late19th century was the first time that the concept of using patient's own immune system to fight the cancer was used in medicine and immuno-

oncology was mostly focused on the way to activate the T cells. Since then, advancement in science allows us to better understand how this system operates. Based on these studies, scientists were able to revolutionize the immune checkpoint modulators and field of immuno-oncology and transform immunotherapy as a 5th pillar in cancer therapy regimen. These fundamental studies also revealed that inhibitory pathways can be modulated to generate powerful T cell responses with subsequent tumor elimination. That led to the successful development of immune checkpoint blockade (ICB) as a potential curative cancer therapy.

Immune checkpoints (IC) are the co-inhibitory target or ligands on the surface of immune cells or tumors that disable the innate or adaptive immune system. Upon engagement of these proteins, immune cells are generally suppressed, either at the tumor killing stage or the activation stage in the case of T cell checkpoint pathways. Thus, by blocking these immunomodulatory complexes (checkpoint pathways), we can harness the immune power to wipe out the tumors and create a long-term immunity (16,17).

Cytotoxic T-lymphocyte–associated antigen 4 (CTLA-4) discovered by Dr. James P Allison in late 1990 and programmed death-1 (PD-1)/programed death ligand-1 (PD-L1) discovered by Dr. Tasuku Honjo 1991, are some of the examples of the known ICB. Their discoveries led to a Nobel prize in field of physiology in 2018.

Monoclonal antibodies that block these co-inhibitory receptors can reactivate T cells and destroy cancer cells. Many of these antibodies have shown unprecedented success in the clinical trials of wide range of advanced stage malignancies. To date, FDA has approved some of these antibodies such as Lipilimumab (CTLA-4 blockade) and Pembrolizumab and Nivolumab (PD-1 blockade) for melanoma cancer treatment. FDA even designate the “breakthrough therapy” title for PD-1 blockade antibodies. These therapeutic agents create an exceptional improvement in the field of

cancer therapy and often were able to create a durable response with low toxicity in most patients. However, only a small fraction of the cancer patients' tumors are responding to this therapy. Therefore, one of the big challenges in the field of immuno-oncology is to understand the mechanisms of resistance to ICI and learn how to increase the proportion of patients benefiting from it, while controlling the treatment toxicity (73). One way to overcome this challenge is to evaluate tumor genomics and discover another immune-modulator pathway that trigger and boost anti-tumor immunity. Hence, other inhibitory effectors such as T cells or NK cells and the roles they play to suppress the immune system is attracting considerable research interest.

NK cells

In early 1970 a new subset of lymphocyte had been discovered in mice and it got famous because of its spontaneous cytotoxic capacity against tumor without the help of other cells such APCs. These cells are known as natural killer cells (NK cells) (74). 5-20% of the circulating lymphocytes consist of NK cells. NK cells are like granular lymphocytes, they can produce memory cells without having random mutation capability in their germline. (75). They will be abundant in lymphoid tissue such as lymph node, spleen, and tonsils (76). NK cell can be differentiated from lymphocyte through some phenotypic features like presence of CD56 or absence of T cell marker (CD3). CD56 is an isoform of the neural cell adhesion molecule (N-CAM) that express by NK cells, some T cells and cancer cells (Lanier et al., 1989). NK cells are also expressing low-affinity receptor for the Fc portion of IgG known as CD16 (FcγRIIIA).

Natural killer cells can kill the virus-infected and transformed cells without any priming signal through secretion of cytokines like IFN-γ, Tumor necrosis factor-α (TNF-α). NK cell activation is tightly regulated by the balance between signals (activation or inhibition) they received. They

particularly get activated when they recognize stress induces ligand, and as a result, they can eliminate the potential threat. NK cells can bind to their ligands via two mains mechanistic: 1-the Antibody Dependent Cell Cytotoxicity (ADCC) and 2- the Natural Cytotoxicity.

Antibody Dependent Cell Cytotoxicity (ADCC)

Complete activation NK cells require a combined signal of two or more activation receptor on NK cells. CD16 (FcγRIIIA) is one of these receptors that normally present by mice and sub population of the human ($CD56^{Dim}$) NK cells. CD16 is a low affinity receptor for the Fc portion of the mouse or human IgG class antibodies. This interaction activates NK cells and enable them to exert ADCC against their antibody coated targets (81, 82). In the presented research, I conducted an experiment to demonstrate the importance of CD16-mediated ADCC in anti-cancer immunity and innate memory formation (83).

Natural Killer cell Group 2

Natural killer cell group 2 (NKG2) receptors are considered as C-type lectin-like family receptor and they can activate or inhibit the NK cells (84, 85). NKG2A has inhibitory roll while NKG2C and NKG2D have activating functions. NKG2A and NKG2C are forming a heterodimer via disulfide bond with CD94 receptors whereas NKG2D does not associated with CD94. In healthy individual (under the normal condition), NKG2A receptor has higher affinity to bind to is ligand compared to NKG2C/D. Thus, inhibitory condition always dominates the activation signals. Although NKG2A consider as extra-cellular receptor but transmit its signal through cytoplasmic immune tyrosine-based activating motif (ITAM) (86, 87). NKG2A complex has two ITIMs which helps to

relay inhibitory signal of NKG2A by recruiting the phosphatases SHP-1 and SHP-2 (88- 90). SHP-1 and SHP-2 are dephosphorylated and thus deactivate the activation signaling cascade of NK cells.

NKG2A/CD94 heterodimer binds to non-classical MHC-I (HLAE/Human or Qa1/mouse). HLA-E and Qa-1^b normally present short (9 amino acid) proteins (peptides) on their surface. These peptides are derived from the leader segments of other MHC-I proteins. Since HLA-E and Qa-1^b are consider as surface marker, and their peptide derived from MHC-I molecules, we can monitor the total expression of MHC-I on tissues. This is often gotten impaired upon viral infection or malignant transformation of cells.

MHC-I is expressed on all nucleated cells, preventing the normal cell from being lysed by NK cells. When cells get infected by a virus, MHC-I expression will down-regulate, and CD8+ T cells can no longer recognize the abnormal cells. However, this downregulation can initiate NK cell activation. MHC-I alone is not sufficient to activate the NK cell. Thus, co-expression of the other ligand such as Killer Immunoglobulin-like Receptor (KIR) is necessary for NK cell activation. CD94/NKG2C/E/H and NKG2D are members of the KIR ligand.

KIR are type-I transmembrane glycoprotein and they composed of multiple Ig-like D domain in their structure as KIR2D/KIR3D (91, 92). They also expressed a cytoplasmic tail for their roles in inhibition or activation signal transduction (93). Inhibitory KIR normally have the long tail which include ITAM and suppress NK effectors upon their binding to their ligand. The importance of NK cells in anti-tumoral immunity exploited in clinical application of new therapeutic such as NK mediated ICB antibodies.

NK cell-based immune checkpoint blockade

By development of numerus ICB such as α-PD1 or α-CTLA-4, field of immuno-oncology have seen substantial advances. However, due to some intrinsic resistance, only a small proportion of patients have benefited from ICB. Recent studies demonstrated that NK cells as innate lymphoid

cells play an important role in tumor surveillance and prevention of the malignancy recurrence. According to these researches, NK cell based immuno-therapies showed great potential against solid and hematologic tumors. KIRs, LIRs, and NKG2A are classical NK cell receptors that can hinder the efficacy of the NK cells in TME. Thus, blocking of other inhibitory pathways create a significant research success in the field of ICB.

CD94/NKG2A interaction with its ligand non-classical MHC-I (HLAE/Human or Qa1/mouse), is one the mechanistic for tumor to evade the immune system. Thus, by blocking this interaction, we can aid our patients in their battle with tumors through unleashing the power of NK cells. In the presented research, we discovered a single domain monoclonal antibody (mAb) that recognizes the non-classical peptide MHC-I complex of the mouse (Qa-1^b/Qdm). With the help of this antibody, we tried to block the axis points mentioned above and answer a lot of unknown questions.

Monoclonal antibody (mAb) therapy

Monoclonal antibody (mAb) is considered as established modality for cancer immunotherapy due to their selectivity and specificity. Antibodies can be used to inhibit growth of tumor cells via targeting moieties of effector domains. Many mAbs are designed to recognize the tumor cell markers and interfere with the function of these targeted proteins, e.g., blocking growth factor receptor or inducing apoptosis. mAbs can also opsonize the tumor cell and the mark them to be attacked by the Macrophages, NK cells and complement system. Since the approval of Rituximab in 1997, more than a dozen mAbs have been approved for cancer treatment. Ipilimumab mAb which binds to CTLA-4 protein was the first mAb that got FDA' approval as an ICB.

Monoclonal antibodies depend to their mode of action, can be classified into 4 different groups:

1- antibody make their target more susceptible to be recognized and attacked by immune system

(94, 95). For example, Rituximab can bind to its target CD20 protein on B cell lymphoma and make it more susceptible to immune attacks. 2- antibodies that slow and eventually stop the tumor growth upon binding to their target. Cetuximab is binding to epidermal growth factor on head and neck tumor and slow tumor growth. 3- anti-angiogenic mAb that reduce the oxygen and nutrient supply in tumor such as Bevacizumab targets the vascular endothelial growth factor (VEGF) on tumor. 4- mAb that can transfer the drug payload to the tumor. ibritumomab, approved for non-Hodgkin's lymphoma, and trastuzumab-emtansine, which is approved for treatment of HER2-positive breast cancer is example of this group.

mAbs can also be classified based on their structure: naked, conjugated, and bi-specific categories. Bi-specific particularly has the capability to recognize two different targets at the same time, even on two different cells. For example, blinatumomab can binds to CD3 on T cells and CD19 on tumor to enhance the immune mediated tumor destruction.

Naked antibodies have a capability to bind to their target and activate tumor destruction via immune-mediated mechanisms such as antibody-dependent cellular cytotoxicity (ADCC) (96).

Single domain monoclonal antibody (Nano body/V_hH)

Monoclonal antibodies have changed the field of cancer therapy with impressive achievements in the treatment of both hematological malignancies and solid tumors (3). However, their delivery path to tumor in vivo is hampered by the large size (150 kDa) of conventional antibodies.

In 1989, Professor Raymond Hamers team at the Vrije Universiteit Brussel (VUB) changed the perspective of canonical antibody. His team analyzed total and fractionated immunoglobulin G (IgG) molecules in the serum of a dromedary camel and concluded that their antibodies lack the light chain. There is unforeseen discovery of antibodies with only heavy chain (HCAbs) was the

result of a student's project in Dr. Hamer's groups. He tried to develop a diagnostic assay for trypanosomiasis infection in water buffalos and camel. Hamer' groups later introduce the V_hH terminology for the first time to the word. V_hH means a VH domain derived from camelid heavy chain antibody.

With this new finding it become essential for the scientist to evaluate and characterize this newly found IgG in the sera of new word camel (Lama pacos and Lama glama). Their first aim was to understand and compare the binding capability of these newly found IgG with their counterpart conventional IgG.

The presence of the truncated form of heavy chain antibody with no light chain so called heavy chain only antibody previously been reported in human (97-99). However, due to the massive mutation and deletion in heavy chain's framework (VH) and constant region-1(CH-1), these antibodies have no functional activity in human (100, 101). By contrast, llama' antibodies showed to have strong affinity for their target antigens. Therefore, possibility of being able to isolate stable and soluble V_hH antibody with nanomolar affinities against their target, creates a very early-on promise of these molecules as high-affinity binding moieties.

Camelid antibodies have a unique anatomical structure compared to the so-called conventional antibodies. Single domains mAbs are considered as homodimer by their nature and have only variable domains of heavy chain (V_hH). Also, they don't have a first constant region (CH1), as they don't process the light chain. Published data on genomic and cDNA of camelid antibody (V_hH genes) have shown that they have homology to the human VH3 family of clan III. However, there are several key amino acids substituted in their FR2, namely, Val37 → Phe/Tyr, Gly44 → Glu, Leu45 → Arg, and Trp47 → Gly (Kabat numbering), and they are encoded by a distinct subset of germline V genes (102, 103). Furthermore, recent published studies showed the

presence of genes belonging to IGHV families 1, 3, and 4 (human clan I and III) in alpaca and llama. They uncovered new camelid genes (V gene) which are highly homologous to the human IGHV5 and IGHV7 families (human clan II). Although, they couldn't find any similarity between human clan I and camelid antibody (104), V genes in camelids identified to have close relation to the human VH4 family (clan I). These VH4 homology contribute a lot to the solubilizing V_hH residues in FR2 and classical antibody repertoire structure in camelid family. Like these published data, several structural studies have suggested that due to the loss of light chain (VL region), V_hH have gained complexity in their structure through involving more residues in antigen binding compared to classical VHs that create some new features for them (105).

Some of these unique feature carries by V_hH mAbs makes them a novel candidate for immunotherapy. Compared to conventional antibody, they are very small (2.5 nm in diameter and about 4 nm in length, ~15 kDa) and for that reason they named nanobody (Fig. 2). They have longer complimentary determining region-3 (CDR-3) compared to conventional antibodies (106). Because of this feature, they would be able to interact with broad range of the protein target that normally are not antigenic to canonical antibodies (107-109). Camelid antibodies have high affinity and specificity (equivalent to conventional antibodies), high thermostability, relatively low production cost, ease of genetic engineering, format flexibility or modularity, low immunogenicity, and a higher penetration rate into tissues (110-112). Good solubility and strictly monomeric behavior are another characteristic of single domain antibodies. This is due to replacement of the large, bulky, and hydrophobic residue of their frameworks with small, hydrophilic amino acids (113, 114). They also have more disulfide bond between their CDR regions. These bonds stabilize the CDR regions and counteracts the destabilization by the

framework region-2 hallmark amino acids. Second, they rigidify the long third antigen-binding loop, leading to a stronger antigen interaction.

V_hHs have short half-life in blood circulation which makes them suitable candidate to certain applications such as delivery of radioisotopes or drug payload to tumor or tumor imagining where rapid clearance is required. However, the pharmacokinetic behavior of V_hHs can improved and extend their half-lives via using different techniques, including fusion to serum albumin or PEGylation or an anti-serum albumin moiety (115-117).

V_hHs antibodies can also undergo certain modification to reduce their immunogenicity such as humanization while maintaining their affinity and specificity (118-119). However, like any other antibodies that has non-human origin (even though fully humanized), immunogenicity and toxicity of these antibodies still must be investigated empirically.

Since 2016, more than 120 different V_hH antibodies have been developed against important therapeutic targets relevant to in vivo imaging, hematology, oncology, infectious diseases, neurological, and inflammatory disorders which with some of them being successful in their clinical trials (104).

One of the unique characteristics of V_HHs is their ability to target antigenic epitopes at locations which are difficult to access by large molecules such as conventional monoclonal antibodies (mAbs). For example, intracellular targets or epitopes concealed from mAbs in protein structures such as G protein-coupled receptors (120-124).

V_hHs can be very useful for the generation of the bispecific antibodies due to their simple design and relatively small size compared to other antibody fragments. This will result in better penetration rates in solid tumor, ease of fusion to a heterodimerization motif and avoid issues related to some linker peptides such as aggregation and immunogenicity (127-130). Based on

recent research published by Li T et al, some V_hH antibodies, can pass through human brain endothelial cell layers “blood brain barrier” (105, 131). Therefore, V_hH antibodies can be engineered to carries a payload (e.g., chemotherapy drug or radioisotope) to deliver their cargo to the brain malignancy (132).

Although the vast majority of engineered V_hH domains were obtained using phage display as platform technology (104,105), it has been shown that such antigen-specific single-domain antibodies can readily be isolated using yeast surface display (YSD) (133).

Expression and selection of the V_hH antibody using yeast display technologies

Antibody display on the surface of the yeast is known as an established method in discovery of the new therapeutic agent. In particular, yeast display has been effective tools in expression and development of single domain antibody (V_hH) against various targets such as single chain T-cell receptor (134), carcinoembryonic antigen (135) and calmodulin (136). Moreover, yeast display is a robust system for development of the antibodies with some advantages compere to other types of display technologies such as Phage display, Ribosome display and E-coli periplasmic display. Simultaneous screening against multiple antigens (protein, peptide or hapten) and stable propagation without expression bias are some of yeast display benefit.

Yeasts have a secretory pathway like the higher eukaryotes, and they have post translational modification which is needed for most of eukaryotic function proteins. This capability enables them to produce proteins that are folded in their endoplasmic reticulum, where chaperones, foldases and a quality-control mechanism ensure that only properly folded proteins are secreted by yeast display.

Particularly selection of high affinity antibodies in phage display system is often hindered by different variables that selection procedures is dependent on such as antibody expression levels. However, yeast display system can overcome this issue because their antibody repertoires expressed on them can be screened by both affinity and display level using fluorescent-activated cell sorting "FACS" (137**)**. Also, by using FACS selection in the antibody discovery procedure, we can determine the affinity of antibodies, their stability and their extracellular expression directly in one display format without relying on the time-consuming procedure of subcloning, expression and purification of phage display system (138).

Saccharomyces cerevisiae, Pichia pastoris, Yarrowia lipolitica and Hansenula polymorpha are some of the yeast strains that can be used as display system for antibody discovery system. In this work, we used S. cerevisiae to display our nanobodies. The alpha agglutinin proteins (Aga-1 and Aga-2) are complementary cell adhesion glycoproteins in the Saccharomyces cerevisiae that is anchored to the cell wall. We fused display nanobodies to the C-terminus of the Aga-2 protein which bound via two disulfide bond Aga1 (parts of yeast genome). Aga-1then serves as an anchor for expressed nanobodies to the yeast cell wall (Fig. 3).

FIGURES

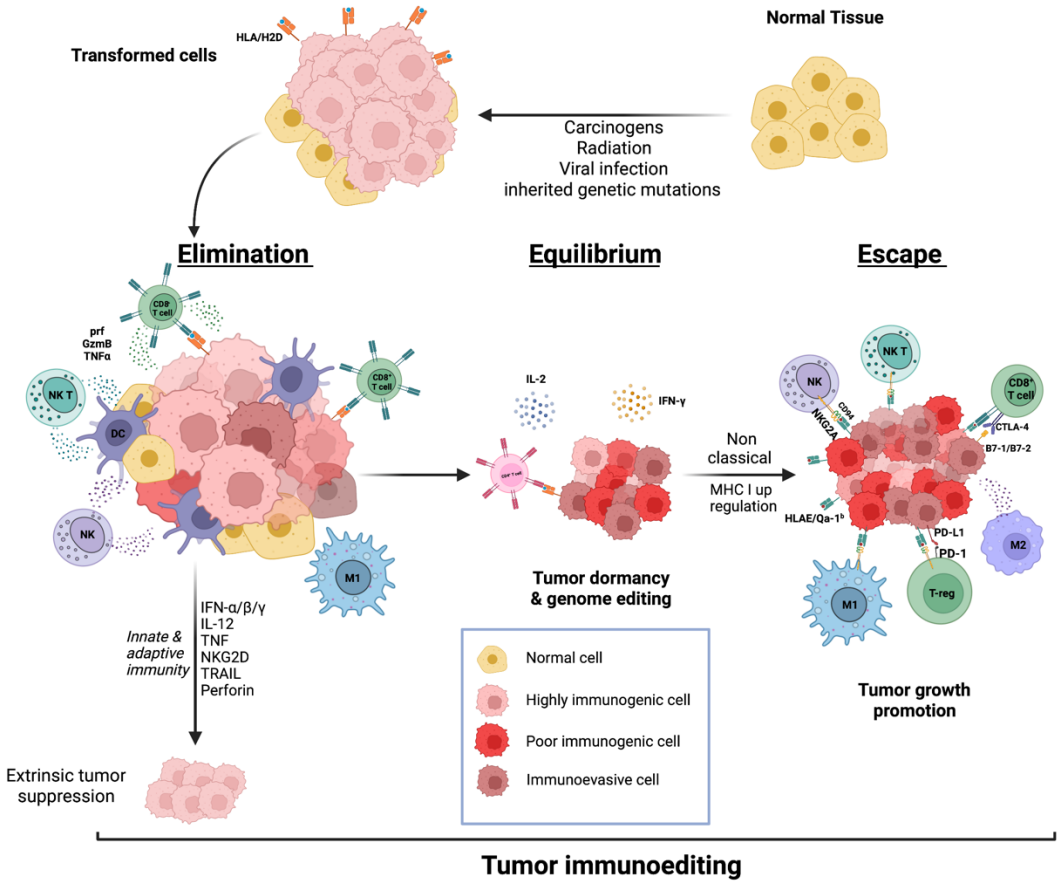

Chapter 1 1: The cancer immunoediting concept.

Three sequential steps of cancer development: phase 1: elimination: control of cell growth associated with induction of tumor-specific immune responses; phase 2: equilibrium: latency where cancer growth is prevented by several immunologic mechanisms; and phase 3: escape: uncontrolled tumor growth, due to genetic instability related to cancer. (DC dendritic cell, NK natural killer cell, Mϕ macrophage, NKT natural killer T cell, CTL cytotoxic T lymphocyte, Th1 T helper 1, PD-L1 programmed death-ligand 1, IDO indoleamine 2,3-dioxygenase, IL interleukin, IFN interferon, TGF transforming growth factor)

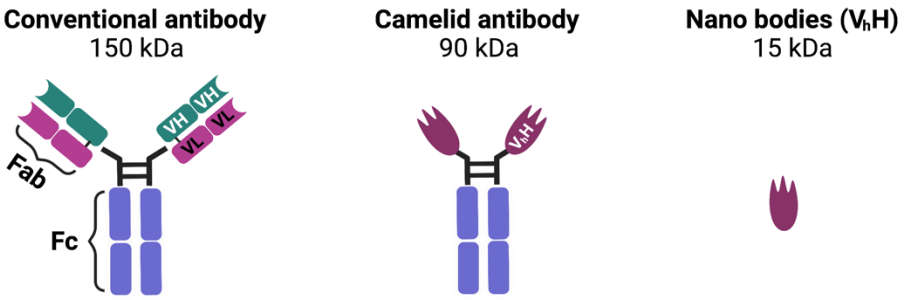

Chapter 1 2: Schematic comparison of the conventional, heavy chain only (HcAbs) and V_hH antibodies

Schematics represent the structural difference of the (right) conventional immunoglobulin, (middle) camelid heavy chain immunoglobulin, and (left) VhH derivative of camelid antibody (Nanobody). The molecular weights for each antibody (in kDa) are also featured.

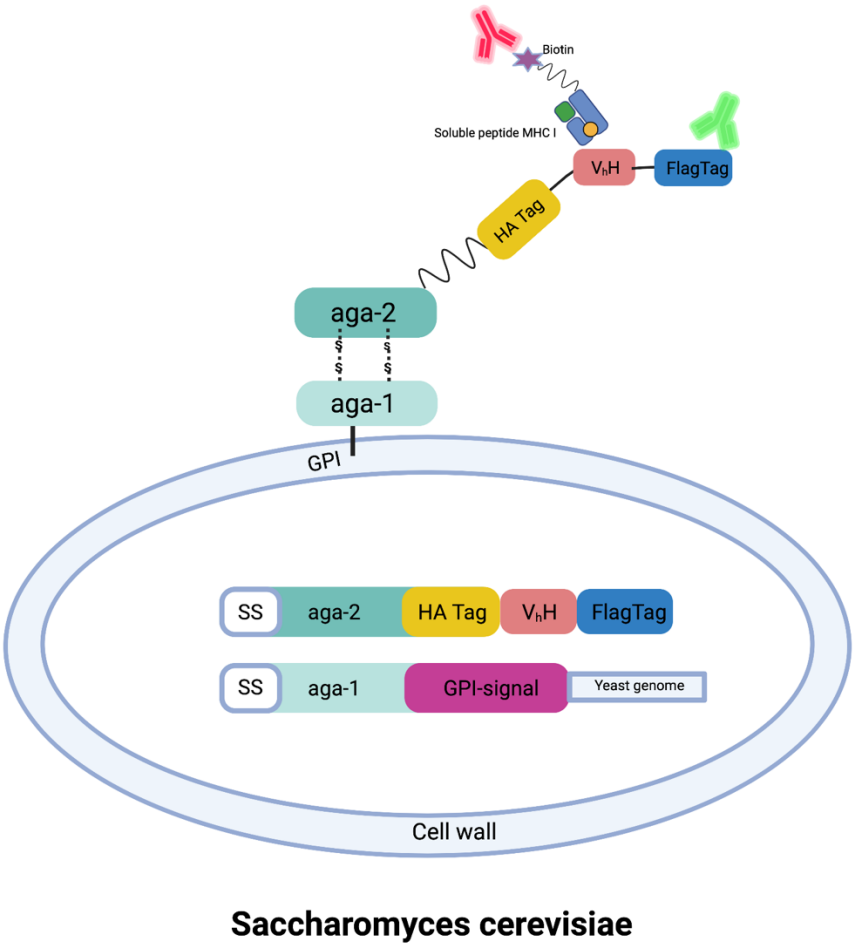

Chapter 1 3: The principle of using a-agglutinin in the yeast surface display.

The V_hH (pink) is displayed as an Aga-2 (green) fusion protein on the surface of yeast. Expression can be detected by using fluorescent antibodies binding to the epitope tags (blue), and binding of the V_hH to a biotinylated antigen can be detected using fluorescent avidin (red). HA, hemagglutinin; V_hH, variable heavy chain; GPI, glycosylphosphatidylinositol linker.

REFERENCES

1. Hanahan D, Weinberg RA. The hallmarks of cancer. Cell. 2000;100(1):57-70.
2. Bach PB, Kelley MJ, Tate RC, McCrory DC. Screening for Lung Cancer: A Review of the Current Literature. Chest. 2003;123(90010):72S-82.
3. Jemal A, Siegel R, Ward E, Hao Y, Xu J, Murray T, et al. Cancer statistics, 2008. CA Cancer J Clin. 2008;58(2):71-96.
4. Hanahan D, Weinberg RA. Hallmarks of cancer: the next generation. Cell. 2011;144(5):646-74.
5. Burnet M. Cancer; a biological approach. I. The processes of control. Br Med J. 1957;1(5022):779-86.
6. Elmore, Susan. “Apoptosis: a review of programmed cell death.” Toxicologic pathology vol. 35,4 (2007): 495-516. doi:10.1080/01926230701320337
7. Burnet FM. The concept of immunological surveillance. Prog Exp Tumor Res 1970;13:1-27.
8. Thomas L. Discussion In: Lawrence HS, ed. Cellular and Humoral Aspects of the Hypersensitive States. New York: Hoeber-Harper, New York, 1959:529-32.
9. DeVita, V. T., Jr. & Chu, E. A history of cancer chemotherapy. Cancer research **68**, 8643-8653, doi:10.1158/0008-5472.CAN-07-6611 (2008).
10. Baudino, T. Targeted Cancer Therapy: The Next Generation of Cancer Treatment. Curr Drug Discov Technol **12,** 3–20 (2015).
11. Schreiber, R. D., Old, L. J. & Smyth, M. J. Cancer immunoediting: integrating immunity's roles in cancer suppression and promotion. Science **331**, 1565-1570, doi:10.1126/science.1203486 (2011).
12. O'Donnell, J. S., Teng, M. W. L. & Smyth, M. J. Cancer immunoediting and resistance to T cell-based immunotherapy. Nature reviews. Clinical oncology **16**, 151-167, doi:10.1038/s41571-018-0142-8 (2019).
13. Schreiber, R. D., Old, L. J. & Smyth, M. J. Cancer immunoediting: integrating immunity's roles in cancer suppression and promotion. Science **331**, 1565-1570, doi:10.1126/science.1203486 (2011).

14. O'Donnell, J. S., Teng, M. W. L. & Smyth, M. J. Cancer immunoediting and resistance to T cell-based immunotherapy. Nature reviews. Clinical oncology **16**, 151-167, doi:10.1038/s41571-018-0142-8 (2019).
15. Dunn, G. P., Old, L. J. & Schreiber, R. D. The three Es of cancer immunoediting. Annual review of immunology **22**, 329-360, doi:10.1146/annurev.immunol.22.012703.104803 (2004).
16. Le, D. T. et al. PD-1 Blockade in Tumors with Mismatch-Repair Deficiency. The New England journal of medicine **372**, 2509-2520, doi:10.1056/NEJMoa1500596 (2015).
17. Le, D. T. et al. Mismatch repair deficiency predicts response of solid tumors to PD-1 blockade. Science **357**, 409-413, doi:10.1126/science.aan6733 (2017).
18. Joyce, J.A. and D.T. Fearon, T cell exclusion, immune privilege, and the tumor microenvironment. Science, 2015. 348(6230): p. 74-80.
19. Spill, F., et al., Impact of the physical microenvironment on tumor progression and metastasis. Current opinion in biotechnology, 2016. 40: p. 41-48.
20. Tsai, J.H. and J. Yang, Epithelial–mesenchymal plasticity in carcinoma metastasis Genes & development, 2013. 27(20): p. 2192-2206.
21. Ziani, L., S. Chouaib, and J. Thiery, Alteration of the antitumor immune response by cancer-associated fibroblasts. Frontiers in immunology, 2018. 9: p. 414.
22. Kumar, H., T. Kawai, and S. Akira, Pathogen recognition by the innate immune system. International reviews of immunology, 2011. 30(1): p. 16-34.
23. Ahrends, T., et al., CD4+ T cell help confers a cytotoxic T cell effector program including coinhibitory receptor downregulation and increased tissue invasiveness. Immunity, 2017. 47(5): p. 848-861. e5.
24. Hall, A.O.H., et al., The cytokines interleukin 27 and interferon-γ promote distinct Treg cell populations required to limit infection-induced pathology. immunity, 2012. 37(3): p.511-523.
25. Ma, C.S., et al., The origins, function, and regulation of T follicular helper cells. Journal of Experimental Medicine, 2012. 209(7): p. 1241-1253.

26. Tangye, S.G., Cytokine-mediated regulation of plasma cell generation: IL-21 takes center stage. Frontiers in immunology, 2014. 5: p. 65.
27. Barry, M. and R.C. Bleackley, Cytotoxic T lymphocytes: all roads lead to death. Nature Reviews Immunology, 2002. 2(6): p. 401-409.
28. Wang, R.-X., et al., Interleukin-35 induces regulatory B cells that suppress autoimmune disease. Nature medicine, 2014. 20(6): p. 633-641.
29. Rosser, E.C. and C. Mauri, Regulatory B cells: origin, phenotype, and function. Immunity, 2015. 42(4): p. 607-612
30. Finnigan Jr, J.P., et al., Mutation-derived tumor antigens: novel targets in cancer immunotherapy. Oncology, 2015. 29(12).
31. Coulie, P.G., et al., Tumour antigens recognized by T lymphocytes: at the core of cancer immunotherapy. Nature Reviews Cancer, 2014. 14(2): p. 135-146.
32. Coussens, L.M. and Z. Werb, Inflammation and cancer. Nature, 2002. 420(6917): p. 860-867.
33. Gonzalez, H., C. Hagerling, and Z. Werb, Roles of the immune system in cancer: from tumor initiation to metastatic progression. Genes & development, 2018. 32(19-20): p. 1267-1284.
34. Shevach, E.M., Mechanisms of foxp3+ T regulatory cell-mediated suppression. Immunity, 2009. 30(5): p. 636-645.
35. Sakaguchi, S., et al., Regulatory T Cells and Immune Tolerance. Cell, 2008. 133(5): p.775-787.
36. Akkaya, B., et al., Regulatory T cells mediate specific suppression by depleting peptide–MHC class II from dendritic cells. Nature Immunology, 2019. 20(2): p. 218-231.
37. Chun, E., et al., CCL2 Promotes Colorectal Carcinogenesis by Enhancing Polymorphonuclear Myeloid-Derived Suppressor Cell Population and Function. Cell Reports, 2015. 12(2): p. 244-257
38. Holmgaard, Rikke B., et al., Tumor-Expressed IDO Recruits and Activates MDSCs in a Treg-Dependent Manner. Cell Reports, 2015. 13(2): p. 412-424.
39. Gabrilovich, D.I., S. Ostrand-Rosenberg, and V. Bronte, Coordinated regulation of myeloid cells by tumours. Nature Reviews Immunology, 2012. 12(4): p. 253-268.

40. Kumar, V., et al., The Nature of Myeloid-Derived Suppressor Cells in the Tumor Microenvironment. Trends in Immunology, 2016. 37(3): p. 208-220.
41. Gabrilovich, D.I. and S. Nagaraj, Myeloid-derived suppressor cells as regulators of the immune system. Nature Reviews Immunology, 2009. 9(3): p. 162-174.
42. Ostrand-Rosenberg, S. and P. Sinha, Myeloid-derived suppressor cells: linking inflammation and cancer. Journal of immunology (Baltimore, Md. : 1950), 2009. 182(8): p. 4499-4506.
43. Kienle, G.S., Fever in Cancer Treatment: Coley's Therapy and Epidemiologic Observations. Global advances in health and medicine, 2012. 1(1): p. 92-100.
44. Kruger, S., et al., Advances in cancer immunotherapy 2019 – latest trends. Journal of Experimental & Clinical Cancer Research, 2019. 38(1): p. 268.
45. Levings MK, Sangregorio R, Roncarolo MG. Human cd25(+) cd4(+) t regulatory cells suppress naive and memory T cell proliferation and can be expanded in vitro without loss of function. J Exp Med 2001;193(11):1295-302 doi: 10.1084/jem.193.11.1295.
46. Broz ML, Binnewies M, Boldajipour B, et al. Dissecting the Tumor Myeloid Compartment Reveals Rare Activating Antigen-Presenting Cells Critical for T Cell Immunity. Cancer Cell 2014;26(6):938 doi: 10.1016/j.ccell.2014.11.010.
47. Harimoto H, Shimizu M, Nakagawa Y, et al. Inactivation of tumor-specific CD8(+) CTLs by tumor-infiltrating tolerogenic dendritic cells. Immunol Cell Biol 2013;91(9):545-55 doi: 10.1038/icb.2013.38.
48. Krempski J, Karyampudi L, Behrens MD, et al. Tumor-infiltrating programmed death receptor-1+ dendritic cells mediate immune suppression in ovarian cancer. J Immunol 2011;186(12):6905-13 doi: 10.4049/jimmunol.1100274.
49. Watkins SK, Zhu Z, Riboldi E, et al. FOXO3 programs tumor associated DCs to become tolerogenic in human and murine prostate cancer. J Clin Invest 2011;121(4):1361-72 doi: 10.1172/JCI44325.
50. Michielsen AJ, Hogan AE, Marry J, et al. Tumour tissue microenvironment can inhibit dendritic cell maturation in colorectal cancer. PLoS One 2011;6(11):e27944 doi: 10.1371/journal.pone.0027944.

51. Curiel TJ, Wei S, Dong H, et al. Blockade of B7-H1 improves myeloid dendritic cell-mediated antitumor immunity. Nat Med 2003;9(5):562-7 doi: 10.1038/nm863.
52. Kusmartsev S, Nefedova Y, Yoder D, Gabrilovich DI. Antigen-specific inhibition of CD8+ T cell response by immature myeloid cells in cancer is mediated by reactive oxygen species. J Immunol 2004;172(2):989-99 doi: 10.4049/jimmunol.172.2.989.
53. Sakaguchi S, Sakaguchi N, Asano M, Itoh M, Toda M. Immunologic self-tolerance maintained by activated T cells expressing IL-2 receptor alpha-chains (CD25). Breakdown of a single
54. Khattri R, Cox T, Yasayko SA, Ramsdell F. An essential role for Scurfin in CD4+CD25+ T regulatory cells. Nat Immunol 2003;4(4):337-42 doi: 10.1038/ni909.
55. Fontenot JD, Gavin MA, Rudensky AY. Foxp3 programs the development and function of CD4+CD25+ regulatory T cells. Nat Immunol 2003;4(4):330-6 doi: 10.1038/ni904.
56. Hori S, Nomura T, Sakaguchi S. Control of regulatory T cell development by the transcription factor Foxp3. Science 2003;299(5609):1057-61 doi: 10.1126/science.1079490
57. Chauhan SK, Saban DR, Lee HK, Dana R. Levels of Foxp3 in regulatory T cells reflect their functional status in transplantation. J Immunol 2009;182(1):148-53 doi: 10.4049/jimmunol.182.1.148.
58. Schmidt A, Oberle N, Krammer PH. Molecular mechanisms of treg-mediated T cell suppression. Front Immunol 2012;3:51 doi: 10.3389/fimmu.2012.00051.
59. Shimizu J, Yamazaki S, Takahashi T, Ishida Y, Sakaguchi S. Stimulation of CD25(+)CD4(+) regulatory T cells through GITR breaks immunological self-tolerance. Nat Immunol 2002;3(2):135-42 doi: 10.1038/ni759.
60. D. S. Chen, I. Mellman, Oncology Meets Immunology: The Cancer-Immunity Cycle, Immunity 39, 1– 10 (2013).
61. Jump up to: a b Casucci, Monica; Attilio Bondanza (2011). "Suicide Gene Therapy to Increase the Safety of Chimeric Antigen Receptor-Redirected T Lymphocytes". Journal of Cancer. 2: 378–382. PMC 3133962. PMID 21750689. doi:10.7150/jca.2.378. Retrieved 30 April 2012.

62. Jump up ^ Rudd, Christopher E.; Schneider, Helga (July 2003). "Unifying concepts in CD28, ICOS and CTLA4 co-receptor signalling". Nature Reviews Immunology. 3 (7): 544– 556. PMID 12876557. doi:10.1038/nri1131.
63. Jump up ^ Rudd, Christopher E. (1999-01-08). "Adaptors and Molecular Scaffolds in Immune Cell Signaling". Cell. 96 (1): 5–8. ISSN 0092-8674. doi:10.1016/S0092- 8674(00)80953-8.
64. Eshhar, Z., et al., Specific activation and targeting of cytotoxic lymphocytes through chimeric single chains consisting of antibody-binding domains and the gamma or zeta subunits of the immunoglobulin and T-cell receptors. Proc Natl Acad Sci U S A, 1993. 90(2): p. 720-4.
65. Maher, J., et al., Human T-lymphocyte cytotoxicity and proliferation directed by a single chimeric TCRzeta /CD28 receptor. Nat Biotechnol, 2002. 20(1): p. 70-5.
66. Junghans, R.P., The challenges of solid tumor for designer CAR-T therapies: a 25-year perspective. Cancer Gene Ther, 2017. 24(3): p. 89-99
67. Gardner TA, Elzey BD, Hahn NM. Sipuleucel-T (Provenge) autologous vaccine approved for treatment of men with asymptomatic or minimally symptomatic castrate-resistant metastatic prostate cancer. Hum Vaccin Immunother 2012;8(4):534-9 doi: 10.4161/hv.19795.
68. Brown M, Davies DH, Skinner MA, et al. Antigen gene transfer to cultured human dendritic cells using recombinant avipoxvirus vectors. Cancer Gene Ther 1999;6(3):238-45 doi:10.1038/sj.cgt.7700014.
69. Bonini C, Lee SP, Riddell SR, Greenberg PD. Targeting antigen in mature dendritic cells for simultaneous stimulation of CD4+ and CD8+ T cells. J Immunol 2001;166(8):5250-7 doi:10.4049/jimmunol.166.8.5250
70. Kaiser J. Personalized tumor vaccines keep cancer in check. Science 2017;356(6334):122 doi: 10.1126/science.356.6334.122.
71. Pedersen SR, Sorensen MR, Buus S, Christensen JP, Thomsen AR. Comparison of vaccineinduce effector CD8 T cell responses directed against self- and non-self-tumor antigens: implications for cancer immunotherapy. J Immunol 2013;191(7):3955-67 doi: 10.4049/jimmunol.1300555.

72. Overwijk WW. Cancer vaccines in the era of checkpoint blockade: the magic is in the adjuvant. Curr Opin Immunol 2017;47:103-09 doi: 10.1016/j.coi.2017.07.015.
73. André P, Denis C, Soulas C, et al. Anti-NKG2A mAb Is a Checkpoint Inhibitor that Promotes Anti-tumor Immunity by Unleashing Both T and NK Cells. Cell. 2018;175(7):1731-1743.e13. doi:10.1016/j.cell.2018.10.014
74. Herberman RB, Nunn ME and Lavrin DH (1975). "Natural cytotoxic reactivity of mouse lymphoid cells against syngeneic acid allogeneic tumors. I. Distribution of reactivity and specificity." Int J Cancer 16(2): 216-229
75. O'Leary JG, Goodarzi M, Drayton DL and von Andrian UH (2006). "T cell- and B cell-independent adaptive immunity mediated by natural killer cells." Nat Immunol 7(5): 507-516.
76. Gregoire C, Chasson L, Luci C, Tomasello E, Geissmann F, Vivier E, et al. (2007). "The trafficking of natural killer cells." Immunol Rev 220: 169-182.
77. Fauriat, C., Long, E. O., Ljunggren, H.-G. G. & Bryceson, Y. T. Regulation of human NK-cell cytokine and chemokine production by target cell recognition. Blood 115, 2167–76 (2010).
78. Long, E. O. et al. Controlling Natural Killer Cell Responses: Integration of Signals for Activation and Inhibition. Annu. Rev. Immunol. 31, 227–258 (2013).
79. Lanier, L. L. Up on the tightrope: natural killer cell activation and inhibition. Nat. Immunol. 9, 495–502 (2008).
80. Long, E. O. Regulation of immune responses through inhibitory receptors. Annu. Rev. Immunol. 17, 875–904 (1999).
81. Perussia, B., Starr, S., Abraham, S., Fanning, V. & Trinchieri, G. Human natural killer cells analyzed by B73.1, a monoclonal antibody blocking Fc receptor functions. I. Characterization of the lymphocyte subset reactive with B73.1. J. Immunol. 130, 2133–2141 (1983).
82. Perussia, B. et al. The Fc receptor for IgG on human natural killer cells: phenotypic, functional, and comparative studies with monoclonal antibodies. J. Immunol. 133, 180–9 (1984).

83. Pahl, J. H. W. et al. CD16A Activation of NK Cells Promotes NK Cell Proliferation and Memory-Like Cytotoxicity against Cancer Cells. Cancer Immunol. Res. 6, 517–527 (2018)
84. Borrego, F., Masilamani, M., Marusina, A. I., Tang, X. & Coligan, J. E. The CD94/NKG2 Family of Receptors: From Molecules and Cells to Clinical Relevance. Immunol. Res. 35, 263–278 (2006).
85. López-Botet, M., Llano, M., Navarro, F. & Bellon, T. NK cell recognition of non-classical HLA class I molecules. Semin. Immunol. 12, 109–119 (2000).
86. Watzl, C. & Long, E. O. in Current Protocols in Immunology 90:11.9B, 11.9B.1-11.9B.17 (John Wiley & Sons, Inc., 2010).
87. Long, E. O. et al. Inhibition of natural killer cell activation signals by killer cell immunoglobulin-like receptors (CD158). Immunol. Rev. 181, 223–233 (2001).
88. Carretero, M. et al. Specific engagement of the CD94/NKG2-A killer inhibitory receptor by the HLA-E class Ib molecule induces SHP-1 phosphatase recruitment to tyrosine-phosphorylated NKG2-A: evidence for receptor function in heterologous transfectants. Eur. J. Immunol. 28, 1280–1291 (1998).
89. Le Dréan, E. et al. Inhibition of antigen-induced T cell response and antibody-induced NK cell cytotoxicity by NKG2A: association of NKG2A with SHP-1 and SHP-2 protein-tyrosine phosphatases. Eur. J. Immunol. 28, 264–276 (1998).
90. Long, E. O. Negative signaling by inhibitory receptors: the NK cell paradigm. Immunol. Rev. 224, 70–84 (2008).
91. Lanier, L. L. NK cell recognition. Annu. Rev. Immunol. 23, 225–74 (2005).
92. Rajalingam, R. in Methods in Molecular Biology (eds. Christiansen, F. T. & Tait, B. D.) 882, 391–414 (Humana Press, 2012).
93. Lopez-Vergès, S. et al. CD57 defines a functionally distinct population of mature NK cells in the human CD56dimCD16+ NK-cell subset. Blood 116, 3865–3874 (2010).
94. Breedveld, F.C., Therapeutic monoclonal antibodies. The Lancet. 355(9205): p. 735-740.
95. Carter, P., Improving the efficacy of antibody-based cancer therapies. Nat Rev Cancer, 2001. 1(2): p. 118-29.

96. Weiner, G.J., Building better monoclonal antibody-based therapeutics. Nat Rev Cancer, 2015. 15(6): p. 361-70.
97. Hamers-Casterman C, Atarhouch T, Muyldermans S, Robinson G, Hamers C, Songa EB, et al. Naturally occurring antibodies devoid of light chains. Nature(1993) 363:446–8. doi:10.1038/363446a
98. Wernery U. Camelid immunoglobulins and their importance for the new-born – a review. J Vet Med B Infect Dis Vet Public Health (2001) 48:561–8. doi:10.1111/j.1439-0450.2001.00478.x
99. Muyldermans S. Nanobodies: natural single-domain antibodies. Annu Rev Biochem (2013) 82:775–97. doi:10.1146/annurev-biochem-063011-092449.
100. Franklin EC, Lowenstein J, Bigelow B, Meltzer M. Heavy chain disease – a new disorder of serum gamma-globulins: report of the first case. Am J Med(1964) 37:332–50. doi:10.1016/0002-9343(64)90191-3
101. Alexander A, Steinmetz M, Barritault D, Frangione B, Franklin EC, Hood L, et al. gamma heavy chain disease in man: cDNA sequence supports partial gene deletion model. Proc Natl Acad Sci U S A (1982) 79:3260–4. doi:10.1073/pnas.79.10.3260
102. Vu KB, Ghahroudi MA, Wyns L, Muyldermans S. Comparison of llama VH sequences from conventional and heavy chain antibodies. Mol Immunol (1997) 34:1121–31. doi:10.1016/S0161-5890(97)00146-6
103. Conrath KE, Wernery U, Muyldermans S, Nguyen VK. Emergence and evolution of functional heavy-chain antibodies in Camelidae. Dev Comp Immunol(2003) 27:87–103. doi:10.1016/S0145-305X(02)00071-X
104. Klarenbeek A, El Mazouari K, Desmyter A, Blanchetot C, Hultberg A, de Jonge N, et al. Camelid Ig V genes reveal significant human homology not seen in therapeutic target genes, providing for a powerful therapeutic antibody platform. MAbs (2015) 7:693–706. doi:10.1080/19420862.2015.1046648
105. Nguyen VK, Su C, Muyldermans S, van der Loo W. Heavy-chain antibodies in Camelidae; a case of evolutionary innovation. Immunogenetics (2002) 54:39–47. doi:10.1007/s00251-002-0433-0

106. van der Linden R, de Geus B, Stok W, Bos W, van Wassenaar D, Verrips T, et al. Induction of immune responses and molecular cloning of the heavy chain antibody repertoire of Lama glama. J Immunol Methods (2000) 240:185–95. doi:10.1016/S0022-1759(00)00188-5

107. Rothbauer U, Zolghadr K, Tillib S, Nowak D, Schermelleh L, Gahl A, et al. Targeting and tracing antigens in live cells with fluorescent nanobodies. Nat Methods (2006) 3:887–9. doi:10.1038/nmeth953

108. Maass DR, Sepulveda J, Pernthaner A, Shoemaker CB. Alpaca (Lama pacos) as a convenient source of recombinant camelid heavy chain antibodies (V_HHs). J Immunol Methods (2007) 324:13–25. doi:10.1016/j.jim.2007.04.008

109. De Simone EA, Saccodossi N, Ferrari A, Leoni J. Development of ELISAs for the measurement of IgM and IgG subclasses in sera from llamas (Lama glama) and assessment of the humoral immune response against different antigens. Vet Immunol Immunopathol (2008) 126:64–73. doi:10.1016/j.vetimm.2008.06.015

110. Muyldermans S. Nanobodies: natural single-domain antibodies. Annu Rev Biochem (2013) 82:775–97. doi:10.1146/annurev-biochem-063011-092449

111. Wesolowski J, Alzogaray V, Reyelt J, Unger M, Juarez K, Urrutia M, et al. Single domain antibodies: promising experimental and therapeutic tools in infection and immunity. Med Microbiol Immunol (2009) 198:157–74. doi:10.1007/s00430-009-0116-7

112. Fernandes CFC, Pereira SDS, Luiz MB, Zuliani JP, Furtado GP, Stabeli RG. Camelid single-domain antibodies as an alternative to overcome challenges related to the prevention, detection, and control of neglected tropical diseases. Front Immunol (2017) 8:653. doi:10.3389/fimmu.2017.00653

113. Blanc MR, Anouassi A, Ahmed Abed M, Tsikis G, Canepa S, Labas V, et al. A one-step exclusion-binding procedure for the purification of functional heavy-chain and mammalian-type gamma-globulins from camelid sera. Biotechnol Appl Biochem (2009) 54:207–12. doi:10.1042/BA20090208

114. Franklin EC, Lowenstein J, Bigelow B, Meltzer M. Heavy chain disease – a new disorder of serum gamma-globulins: report of the first case. Am J Med(1964) 37:332–50. doi:10.1016/0002-9343(64)90191-3

115. Chakravarty R, Goel S, Cai W. Nanobody: the “magic bullet” for molecular imaging? Theranostics (2014) 4:386–98. doi:10.7150/thno.800

116. Holt LJ, Herring C, Jespers LS, Woolven BP, Tomlinson IM. Domain antibodies: proteins for therapy. Trends Biotechnol (2003) 21:484–90. doi:10.1016/j.tibtech.2003.08.007

117. Harmsen MM, van Solt CB, Fijten HP, van Keulen L, Rosalia RA, Weerdmeester K, et al. Passive immunization of guinea pigs with llama single-domain antibody fragments against foot-and-mouth disease. Vet Microbiol (2007) 120:193–206. doi:10.1016/j.vetmic.2006.10.029

118. Vaneycken I, D’Huyvetter M, Hernot S, De Vos J, Xavier C, Devoogdt N, et al. Immuno-imaging using nanobodies. Curr Opin Biotechnol (2011) 22:877–81. doi:10.1016/j.copbio.2011.06.009

119. Vincke C, Loris R, Saerens D, Martinez-Rodriguez S, Muyldermans S, Conrath K. General strategy to humanize a camelid single-domain antibody and identification of a universal humanized nanobody scaffold. J Biol Chem (2009) 284:3273–84. doi:10.1074/jbc.M806889200

120. McGonigal K, Tanha J, Palazov E, Li S, Gueorguieva-Owens D, Pandey S. Isolation and functional characterization of single domain antibody modulators of caspase-3 and apoptosis. Appl Biochem Biotechnol (2009) 157:226–36. doi:10.1007/s12010-008-8266

121. Staus DP, Wingler LM, Strachan RT, Rasmussen SG, Pardon E, Ahn S, et al. Regulation of β2-adrenergic receptor function by conformationally selective single-domain intrabodies. Mol Pharmacol (2014) 85:472–81. doi:10.1124/mol.113.089516

122. Stijlemans B, Conrath K, Cortez-Retamozo V, Van Xong H, Wyns L, Senter P, et al. Efficient targeting of conserved cryptic epitopes of infectious agents by single domain antibodies: African trypanosomes as paradigm. J Biol Chem (2004) 279:1256–61. doi:10.1074/jbc.M307341200

123. Bradley ME, Dombrecht B, Manini J, Willis J, Vlerick D, De Taeye S, et al. Potent and efficacious inhibition of CXCR2 signaling by biparatopic nanobodies combining two distinct modes of action. Mol Pharmacol (2015) 87:251–62. doi:10.1124/mol.114.094821

124. Manglik A, Kobilka BK, Steyaert J. Nanobodies to study G protein-coupled receptor structure and function. Annu Rev Pharmacol Toxicol (2017) 57:19–37. doi:10.1146/annurev-pharmtox-010716-104710.

125. Li J, Zhu Z. Research and development of next generation of antibody-based therapeutics. Acta Pharmacol Sin (2010) 31:1198–207. doi:10.1038/aps.2010.120

126. Mazor Y, Sachsenmeier KF, Yang C, Hansen A, Filderman J, Mulgrew K, et al. Enhanced tumor-targeting selectivity by modulating bispecific antibody binding affinity and format valence. Sci Rep (2017) 7:40098. doi:10.1038/srep40098

127. Holt LJ, Herring C, Jespers LS, Woolven BP, Tomlinson IM. Domain antibodies: proteins for therapy. Trends Biotechnol (2003) 21:484–90. doi:10.1016/j.tibtech.2003.08.007

128. Mazor Y, Sachsenmeier KF, Yang C, Hansen A, Filderman J, Mulgrew K, et al. Enhanced tumor-targeting selectivity by modulating bispecific antibody binding affinity and format valence. Sci Rep (2017) 7:40098. doi:10.1038/srep40098

129. Holliger P, Winter G. Engineering bispecific antibodies. Curr Opin Biotechnol (1993) 4:446–9. doi:10.1016/0958-1669(93)90010-T

130. Rozan C, Cornillon A, Petiard C, Chartier M, Behar G, Boix C, et al. Single-domain antibody-based and linker-free bispecific antibodies targeting FcγRIII induce potent antitumor activity without recruiting regulatory T cells. Mol Cancer Ther (2013) 12:1481–91. doi:10.1158/1535-7163.MCT-12-1012

131. Muruganandam A, Tanha J, Narang S, Stanimirovic D. Selection of phage-displayed llama single-domain antibodies that transmigrate across human blood-brain barrier endothelium. FASEB J (2002) 16:240–2.

132. Webster CI, Caram-Salas N, Haqqani AS, Thom G, Brown L, Rennie K, et al. Brain penetration, target engagement, and disposition of the blood-brain barrier-crossing bispecific antibody antagonist of metabotropic glutamate receptor type 1. FASEB J (2016) 30:1927–40. doi:10.1096/fj.201500078

133. Deschacht N, De Groeve K, Vincke C, Raes G, De Baetselier P, Muyldermans S. A novel promiscuous class of camelid single-domain antibody contributes to the antigen-binding repertoire. J Immunol (2010) 184:5696–704. doi:10.4049/jimmunol.0903722

134. Michele C.Kieke[1], Bryan K.Cho[1], Eric T.Boder[2], David M.Kranz[1] and K.Dane Wittrup[2] Isolation of anti-T cell receptor scFv mutants by yeast surface display Protein Eng., 10 (1997), pp. 1303-1310

135. Christilyn P Graff, K. Chester, R. Begent, K.D. Wittrup Directed evolution of an anti-carcinoembryonic antigen scFv with a 4-day monovalent dissociation half-time at 37 degrees C

136. Ryckaert S, Pardon E, Steyaert J, Callewaert N. Isolation of antigen-binding camelid heavy chain antibody fragments (nanobodies) from an immune library displayed on the surface of Pichia pastoris. J Biotechnol. 2010;145(2):93-98. doi:10.1016/j.jbiotec.2009.10.01

137. M.J. Feldhaus, R.W. Siegel, L.K. Opresko, J.R. Coleman, J.M. Feldhaus, Y.A.Yeung, J.R. Cochran, P . Heinzelman, D. Colby, J. Swers, C. Graff, H.S. Wiley, K.D.Wittrup Flow-cytometric isolation of human antibodies from a nonimmune Saccharomyces cerevisiae surface display library Nat. Biotechnol., 21 (2003), pp. 163-170

138. G. Chao, W.L. Lau, B.J. Hackel, S.L. Sazinsky, S.M. Lippow, K.D. Wittrup Isolating and engineering human antibodies using yeast surface display Nat. Protoc., 1 (2006), pp. 755-768

CHAPTER 2

A single-domain TCR-like antibody selective for the Qa-1b/Qdm peptide complex enhances tumoricidal activity of NK cells via the NKG2A immune checkpoint

Authors: Soroush Ghaffari[a], Katherine Upchurch-Ange[b], Susanne Gimlin[b], Trivendra Tripathi[b], Marjolein Sluijter[c], Jim Middelburg[c], Thorbald van Hall[c] and Jon Weidanz[b,d,+]

Affiliations:

[a]Department of Biology, College of Science

The University of Texas at Arlington, TX, USA.

[b]Abexxa Biologics Inc. 500 S Cooper St, Arlington, TX, USA.

[c]Department of Medical Oncology, Oncode Institute, Leiden University Medical Center, Albinusdreef 2, 2333 ZA Leiden, the Netherlands.

[d]College of Nursing and Health Innovation

The University of Texas at Arlington, Arlington, TX, USA

[+]Contact: Jon Weidanz

Email: weidanz @uta.edu,

College of Nursing and Health Innovation,

The University of Texas at Arlington, Arlington, TX, USA

One Sentence Summary: A high affinity TCR-like antibody with binding selectivity for the non-classical MHC Qa-1^b/Qdm peptide complex enhances NK lysis of tumor cells by blocking the NKG2A: Qa-1^b (HLAE) axis

ABSTRACT

The NKG2A/HLA-E axis is an immune checkpoint that suppresses immune effector activity in the tumor microenvironment. In mice, the ligand for the NKG2A/CD94 inhibitory receptor is the non-classical MHC molecule Qa-1^b, the HLA-E ortholog, which presents the peptide AMAPRTLLL, referred to as Qdm (for Qa-1 determinant modifier). This dominant peptide is derived from the leader sequences of murine classical MHC class I encoded by the H-2D and -L loci. To investigate Qa-1^b/Qdm expression and its tumor protective role, we identified a T-cell receptor-like (TCRL) antibody from a single domain VHH library using yeast surface display. The TCRL antibody (EXX-1) binds to the Qa-1^b/Qdm complex and not to Qa-1^b alone or Qa-1^b loaded with control peptides. Flow cytometric results revealed EXX-1 selectively bound to Qa-1^b/Qdm positive B16F10 and TC-1 tumor cells; no binding was observed following genetic knockdown of Qa-1^b or Qdm peptide. Furthermore, EXX-1 antibody blockade promoted NK-mediated tumor cell lysis in vitro. Our findings show that EXX-1 has exquisite binding specificity for the Qa-1^b/Qdm peptide complex making it a valuable tool for further investigation of Qa-1^b/Qdm biology and for evaluation as an immune checkpoint blocking antibody in syngeneic mouse tumor models.

Keywords: Qdm peptide, Qa-1^b, HLA-E VL9 peptide, immune checkpoint inhibitor, cancer, tumor, B16, TC-1, NKG2A, CD94, NK cells, $CD8^+$ T-cells, Effector cells

INTRODUCTION

The NKG2A axis is a novel immune checkpoint believed to control the cytolytic activity of effector cells in the tumor microenvironment (1, 2). Blocking this inhibitory pathway has been shown to promote anti-tumor immunity in cancer patients and in murine tumor models by enhancing the lysis activity of NK and $CD8^+$ T-cells (3, 4). Findings from a recent phase II study showed clinical benefit in head and neck cancer patients treated with anti-NKG2A antibody, Monalizumab, in combination with Cetuximab (anti-EGFR mAb) (3). Additionally, a monoclonal antibody targeting mouse NKG2A receptor has shown efficacy in murine tumor models when used in combination with PD-L1 therapy or cancer vaccines (3, 4). The ligand for the NKG2A/CD94 heterodimeric receptor in mice is Qa-1^b, the HLA-E ortholog.

The non-classical MHC molecule (MHC class Ib), Qa-1^b is an essentially monomorphic protein with similar tissue expression as classical MHC class I molecules (MHC class Ia), albeit at lower levels (5, 6). The Qa-1^b molecule presents the dominant nonameric peptide AMAPRTLLL, referred to as Qdm (for Qa-1 determinant modifier) that is derived from the leader sequence of murine MHC class Ia from the H-2D and -L loci (7-9)). In human cells, HLA-E presents dominant peptides ('VL9' peptides) having sequences nearly identical to AMAPRTLLL that are derived from leader sequences of MHC class Ia antigens and the non-classical MHC, HLA-G (1). These leader peptides are even conserved among the larger mammalian family (10). When cellular conditions change (i.e., a defect in the antigen processing machinery (APM) such as during infection or cellular transformation) the diversity of peptides presented by Qa-1^b can expand markedly (11, 12). For example, peptides derived from viruses and bacteria have been reported to be presented by Qa-1^b in infected cells (13, 14) In cancer cells with a defective APM, Qa-1^b has been shown to present immunogenic alternative peptides (9, 15) for recognition by CTLs. Since

Qdm peptide presentation by Qa-1^b directly correlates with MHC Ia expression and APM integrity, loss of either one results in reduction or even absence of Qdm peptide, indicating that the display of Qa-1^b/Qdm complexes at the surface of cells can act as a barometer for MHC Ia and APM integrity (16).

More than two decades ago Qa-1^b/Qdm (HLA-E/VL9) was found to be the ligand for the NKG2A receptor (17, 18). The inhibitory NKG2A receptor belongs to the NKG2 family of C-type lectin-like receptors that also includes two activating variants, NKG2C and NKG2E. NKG2 molecules pair with CD94 to form functional heterodimeric receptors that interact with Qa-1^b (HLA-E) when complexed with Qdm and VL9 peptides, respectively (19). Interaction of the NKG2A/CD94 heterodimeric inhibitory receptor to Qa-1^b or HLA-E molecules recruits SHP-1 (protein tyrosine phosphatase, non-receptor type 6 (PTPN6)) that promotes an inhibitory signaling cascade in the effector cells to suppress immune activities.(2, 7, 20-22) In addition to NK cells, recent reports have shown tissue resident and tumor localized CD8$^+$ T-cells express NKG2A/CD94 receptor at markedly higher frequencies compared to circulating CD8$^+$ T-cells (23, 24). The currently held belief is that Qa-1^b or HLA-E engage with the NKG2A/CD94 inhibitory receptor when presenting peptides Qdm or VL9 peptides, respectively, to protect cells from lysis by NK and CD8$^+$ T-cells (25, 26).

Even though healthy cells are expected to express Qa-1^b loaded with Qdm peptide, during infections or in tumor cells alternative peptides can be presented by Qa-1^b molecules (9, 27). Currently, no distinction can be made between the different peptides, including Qdm, that are presented by Qa-1^b complexes in healthy and diseased cells. Novel research tools that could directly recognize the Qa-1^b/Qdm complex or Qa-1^b loaded with other peptides, in normal or tumor tissue would be particularly useful. Such tools would be invaluable in furthering our understanding

of Qa-1^b/Qdm expression and regulation in normal and tumor cells. Additionally, because of the growing importance of the NKG2A immune checkpoint in cancer immunity, an antibody that selectively bound to Qa-1^b/Qdm complex could be used to explore the potential therapeutic effect of blocking the ligand side of the NKG2A axis.

To address these points, we generated a T-cell receptor-like (TCRL) or TCR mimicking (TCRm) antibody to the Qa-1^b/Qdm complex. TCRL antibodies have been made to many different HLA/peptide complexes (28-30), however, to the best of our knowledge, none exist to peptides presented by non-classical MHC, including the Qa-1^b/Qdm complex. To this end, we constructed a single-domain antibody library for yeast surface display after immunizing a llama with recombinant Qa-1^b/Qdm protein. Screening of the single-domain antibody library for binders to Qa-1^b/Qdm yielded a unique clone, EXX-1. Here we characterize EXX-1 and show this TCRL antibody staining of cancer cells is Qa-1^b dependent and Qdm peptide specific and displays functional activity in vitro by disrupting the NKG2A/Qa-1^b axis to unleash NK cytolysis of tumor cells.

METHODS and MATERIALS

Library Generation and Yeast Library Construction

Immunization of a Lama glama with Qa-1^b/Qdm was performed by Capralogics Inc. as described previously (32) and followed by the construction of a phage display library by Creative BioLabs. (The immunization protocol was reviewed and approved by the IACUC committee at Capralogics, and all work was performed under veterinary oversight with strict adherence to standard operating procedures). To convert from a phage display library to a yeast display library, an appropriate amount of phagemid was used to cover at least 10x excess of the expected

diversity. The VHH genes were amplified from phagemid using the forward primers Lla_04, Lla_05 and Lla_06 and the reverse primer Lla_07 (primer sequence shown in Table I). The primers were modified to allow for cloning into the yeast display vector. The yeast strain EBY100 (ATCC) was transformed with pYES3/Aga2 vector (modified from pYES3/CT, ThermoFisher) containing cloned V_hH genes according to the protocol of Van Deventer and Wittrup (33). Multiple electroporations were pooled, with 200 ng of vector and 2 μg of V_hH used in each electroporation. Dilution plates indicated the number of transformants, and colony PCR was used to quantify inserted sequence quality.

Screening for binders to Qa-1^b/Qdm complex

For staining and selection purposes, the V_hH single-domain antibody library was incubated overnight in galactose rich media at 30℃ to induce expression of antibody molecules for display on the surface of yeast. Yeasts were resuspended in blocking buffer (5% BSA, 0.05% Tween-20 in PBS) for 30 to 60 min at RT with rotation. Yeasts were then incubated with biotinylated antigen (Qa-1^b /QDM, Qa-1^b /GroEL, Qa-1^b /DDX5, Qa-1^b /Q001 and Qa-1^b/Q002) followed by incubation for 30 to 90 min at 4℃, with incubation time dependent on 1 antigen concentration. Yeasts were washed with staining buffer (0.5% BSA, 0.05% Tween-20 in PBS) and resuspended in staining buffer containing anti-flag tag (DYKDDDDK) antibody conjugated with fluorescein isothiocyanate (FITC) and streptavidin (SA) conjugated to R-phycoerythrin (PE). After a 30 min incubation at 4℃ yeasts were washed 3x and resuspended in staining buffer. Yeasts were analyzed on a Beckman Coulter CytoFLEX S. Data were analyzed using FlowJo software version 10. Yeasts were first gated based on FSC and SSC to remove debris, followed by selection of singlets before analyzing antigen binding (PE) vs V_hH expression (FITC). For

MACS selection, after blocking, yeasts were resuspended in 0.5-1 mL of Qa-1^{b}/Qdm at 1 μM and incubated for 30 min at 4℃. After washing, yeasts were resuspended in 5 mL of staining buffer with 400 μL of SA microbeads (Miltenyi Biotec, cat#130-048-101) for 20 min at 4℃. Yeast were selected for binding to SA microbeads using LS columns (Miltenyi Biotec, cat#130-042-401). MACS selection was performed once, followed by two rounds of sorting on a FACS Aria II (BD Biosciences). For sorting, yeasts were stained as described above.

Mouse tumor cell lines and reagents

The tumor cell lines B16F10, B16F10 Qa-1$^{b\ ko}$, TC-1, TC-1 Qa-1$^{b\ ko}$, RMA, RMA Qa-1$^{b\ ko}$ have been described previously (4). 4T1 and EL-4 were purchased from ATCC. The C1498 cell line was purchased from Imanis Life Sciences. B16F10.D^{b} knock out cells were described before (22). Tumor cells were cultured in recommended medium. Cell lines were authenticated and confirmed free of rodent viruses and Mycoplasma by routine testing by IDEXX.

Antibodies for flow cytometry and peptides

Antibodies specific for anti-mouse NKp46-1 BV421 (29A1.4; cat#137612), SA-APC (405204), Zombie Aqua Fixable Viability Kit (cat#423101/423102) and calcein-AM (cat#425201), TrueStain FcX plus (cat#156604), FluoroFix buffer (cat#422101) were purchased from BioLegend. SA-PE (cat#12-4317-87) was purchased from eBioscience. Anti-Flag-AF488 (cat#IC8529G), anti-mFcg RI/CD64 (cat#290322) were purchased from R&D Systems. Anti-mouse NKG2A/C/E-PE (20d5; cat#130-105-620) was purchased from Miltenyi Biotech. Anti-mouse H2D^{b}-PE (28-14-8; cat#A15443), CellTrace CFSE Cell Proliferation kit (cat#C34554) were purchased from Thermofisher. Antibodies specific for anti-mouse CD3-BV421 (17A2;

cat#555276), biotin-labeled anti-mouse Qa-1^b (6A8.6F10.1A6; cat#559829) were purchased from BD Pharmingen. AffiniPure Goat Anti-Human (GAH) IgG, Fcγ fragment specific (cat#109-115-098) and AffiniPure Goat Anti-Mouse (GAM) IgG subclasses 1+2a+2b+3 (cat#115-115-164), GAM-APC (cat#115-135-164), GAM-PE (cat#115-115-164), GAH-APC (cat#109-135-098), GAH-PE (cat#1150098) were purchased from Jackson ImmunoResearch. InVivoMAb anti-mouse NKG2A/C/E (20d5; cat#BE0321) was purchased from Bio X cell. CytoFLEX S V4-B2-Y4-R3 Flow Cytometer (Beckman Coulter) was used, and flow cytometry data were analyzed with FlowJo software version 10.

Peptide Qdm (AMAPRTLLL) was synthesized by MBL International. Peptides D^k (AMVPRTLLL), K^d (MAPCTLLLL), K^b (MVPCTLLLL), Q001 (AQAERTPEL, DENN domain containing protein 3), Q002 (IINTHTLLL, IQ motif containing GTPase activating protein 1), GroEL (GMQFDRGYL, heat shock protein 60), EPH (TLADFDPRV, erythropoietin-producing human hepatocellular receptor), DDX5 (ATPGRKDFL, DEAD box protein 5), glycine/alanine substituted Qdm peptides (p1A→G, p3A→G, p4P→1 A, p5R→A, p6T→A, p7L→A, and p8L→A), and lysine-substituted Qdm peptides (Lys-P5 and Lys-P8) were synthesized by GenScript USA.

Production of Qa-1^b peptide monomers

The extracellular domain of mouse Qa-1^b containing a C-terminus BirA peptide sequence for biotinylation and human β2M genes were cloned in pET21(+) vector purchased from Sigma-Aldrich and transformed into BL21(DE3) Escherichia coli (New England Biolabs). Proteins were produced, purified from inclusion bodies, and used in refolding reactions with synthesized peptides to produce Qa-1^b/peptide complex as described previously (34). The Qa-1^b/peptide

mixture was concentrated, and correctly folded complex was isolated from impurities using size exclusion chromatography (SEC) and a Superdex 75 (S75) column (GE Healthcare Bio-Sciences AB). A portion of the purified refolded complex, designated as active monomer, was biotinylated using the BirA biotin ligase enzyme (Avidity) and purified a second time on the S75 column. Purified material (unbiotinylated and biotinylated) was analyzed by mass spectrometry to detect Qa-1^b heavy chain, β2M, peptide (indicating peptide loading) and the percentage of material that was biotinylated (for biotin-labeled molecules). All mass spectrometry work was performed at the Proteomics Core Lab at the University of Texas Southwestern Medical Center.

Antibody production

The expression tests in mammalian cells were performed in Expi293Fcells (Thermo Fisher, cat#A14527). The VHH region of EXX-1 or its isotype control, anti-hCD3e VHH, was cloned into either human pFUSE- hIgG1-Fc2 (cat#pfuse-hg1fc2) or mouse pFUSE-mIgG2a-Fc2 (cat#pfuse-mg2afc2) vector purchased from InvivoGen. Cells were transfected transiently with expression vectors according to the manufacturer's instruction. Five days 1 post-transfection, antibody containing supernatants were harvested. The antibodies were captured and purified using protein-A beads (Genscript Inc cat#L00210.). After buffer exchange into PBS using Amicon Ultra-4 Centrifugal Filters (EMD Millipore), antibodies were analyzed for correct size and purity. SDS PAGE was performed under either reducing or non-reducing conditions using mini-protein TGX stain-free polyacrylamide gels and the mini-protein tetra system purchased from Bio-Rad. SDS PAGE gels were stained with Coomassie blue for visualization. Additional purified samples were run on an analytical-grade Superdex-200 column (GE Healthcare BioSciences AB) for size and purity determination. Larger scale production of EXX-1 mFc and

associated controls and production of EXX-1 hFc (ES) and EXX-1 mFc (ES) and associated controls were done by ATUM.

Elisa

High protein binding flat-bottom 96-well plates (Nunc MaxiSorp) were coated with 50 µl of neutravidin (50 mg/mL in PBS) in each well and incubated overnight at 4℃. Plates were washed 3x with wash/assay buffer (0.1% BSA, 0.05% Tween-20 in PBS). Available protein binding sites were blocked with 100 µL/well of blocking buffer (5% BSA, 0.05% Tween-20 in PBS) and incubated for 1 hr at RT. Buffer was discarded, plate washed 3x in wash buffer, and 50 µL of biotinylated monomer (Qa-1^b/peptide complex) was diluted in wash/assay buffer with final concentrations of 5, 2.5, 1.25 and 0.625 µg/mL and incubated for 1 hr at RT. Plates were washed 4x with assay buffer (200 µL/well) and allowed to soak for 1-2 min before the addition of antibodies. Antibodies were diluted in the assay buffer with the concentrations of 2.5, 1.25 and 0.625 µg/mL and 50 µL of diluted antibodies (anti-β2m (Thermofisher, clone B2M-01 cat#MA1-23 19141) and anti-mouse Qa-1^b (BD Biosciences, clone 6A8.6F10.1A6 cat#744390) (positive controls) and isotype control hFc (negative control) and EXX-1 1 hFc (both antibodies were produced in-house) were added to their designated wells and incubated for 1 hr at RT. Plates were washed 5x (200 µL/well) before adding anti-human-horseradish peroxidase ((HRP) cat#109-035-088) or anti-mouse-HRP conjugates (cat#115-035-003, Jackson ImmunoResearch Laboratories) diluted 1:5000 in assay buffer to designated wells and allowed to incubate for 1 hr at RT to detect bound antibody. The plate was washed 5x (200 µL/well), and 50 µL of 1-step Ultra TMB-ELISA substrate solution (BD Biosciences) was added into each well, incubated for

30 min at RT, followed by the addition of 50 µL of stop solution (1M Hydrochloric Acid) and read at 450 nm on a Synergy 2 Multi-Mode Microplate Reader (Bio-Tek Instruments, Inc.).

Affinity and binding specificity determined using label-free bioassay system

The binding affinity of EXX-1 was determined using label-free technology (ResoSens instrument, Resonant Sensors, Incorporated). The dissociation equilibrium constant (K_D) was determined as follows. Thermofisher Capture Select™ Biotin anti-human-IgG-Fc (cat#7103262100) diluted in PBS buffer) was immobilized on neutravidin coated Bionetic label-free microarray plate at 5 µg/mL until binding reached equilibrium. The plate was subsequently washed 3x with dilution/wash buffer (0.1% BSA, 0.05% Tween-20) in PBS). EXX-1 hFc (10 µg/mL in dilution/wash buffer) was captured by anti-human IgG-Fc until binding reached equilibrium. The plate was subsequently washed 3x in dilution/wash buffer. The Qa-1^b/Qdm monomer complex (serial dilutions starting at 20 µg/mL in dilution/wash buffer) was added to wells and allowed to incubate for 20 min to determine the binding association. Then excess antigen was removed, replaced with fresh wash buffer, and immediately incubated on reader for approximately 25 min to determine dissociation rate. Binding affinity calculated using Tracedrawer 1 kinetic analysis software.

Binding specificity was also determined by ResoSens label-free bioassay system using Integrated ResoVu software was used for data acquisition and statistical analysis (Resonant Sensors Incorporated).

Staining of tumor cells

When cultured target cells reached ~70–80% confluence, 20 ng/mL of recombinant mIFNg (R&D System) was added to the cells and further incubated for 48 hr at 37℃. Adherent cells were treated using Trypsin-EDTA Solution (Millipore Sigma) and recovered cells were washed 3x with FACS buffer (PBS supplemented with 2% FBS (Gibco) and 2mM EDTA (Invitrogen)). 100,000 to 200,000 cells/well were used for staining

Fc block (mouse TruStain FcX plus) was added to wells with cells and incubated for 15 min at 4℃ before adding 50 µL of primary antibody and incubated for 30 min at 4℃. Cells were washed with addition of 100-150 µL/well of FACS buffer before the addition of secondary antibody conjugates. GAH-Fc/PE or GAM-Fc/PE was added to wells at 1:100 dilution in FACS buffer. For detection of biotin-labeled antibodies, SA-PE was added at a 1:50 dilution in FACS buffer. All samples were stained using zombie aqua viability stain and washed 3x with FACS buffer. Cells were fixed by adding 100-200 µL/well of FluoroFix buffer before analysis. For gating, cells were first selected based on FSC and SSC, followed by selection of singlets and live cells.

Cytotoxic assays with mouse NK cells

The effector cells used were NK cells enriched (EasySep Mouse NK cell isolation kit, StemCell Technologies) from spleens of na.ve C57Bl/6 mice (The Jackson Laboratory, USA), with a purity >90%. NK cells were incubated at $1x10^6$/mL with recombinant mouse IL-2 (20 ng/mL) for 24 hr. NK cells were co-cultured at a ratio of 3:1with target cell lines, B16 Qa-1^{b+} or B16 Qa-$1^{b\,ko}$ that had been previously incubated with mIFN-γ for 48 hrs and which were labeled with calcein AM. Antibodies were added at 10 µg/mL. Plates were incubated for 24 hrs at 37ÅãC and

read at 490nm on a Synergy 2 Multi-Mode Microplate Reader (Bio-Tek Instruments, Inc.). Cell lysis was calculated according to the formula: [(test release - spontaneous release)/(maximum release - spontaneous release)] x 100. Spontaneous release represents calcein-AM release from untreated target cells and maximum release represents calcein-AM release from target cells lysed with 2%Triton X-100 (Millipore Sigma).

Statistical analysis

The data are expressed as the mean ± SEM and were analyzed with unpaired Student's t-tests and one-way ANOVA Tukey's multiple comparisons test. Significance was assumed with *$p<0.05$, **$p<0.01$, ***$p<0.001$ and ****$p<0.0001$.

RESULTS

Identification of anti-Qa-1^b/Qdm TCRL antibody EXX-1

To generate TCRL antibodies with specificity for Qa-1^b/Qdm, a llama was first immunized with complexes of recombinant Qa-1^b/Qdm following the protocol described previously (31). One week after the final immunization, blood was collected, B-cells enriched, mRNA isolated, and a yeast display library was constructed and screened for binders. A MACS selection was done (R1 out) using target antigen (Qa-1^b/Qdm) at 1μM. The R1 library was checked for binders recognizing target, and a substantial enrichment was observed in the number of binders recognizing the Qa-1^b/Qdm complex compared to controls (Qa-1^b:b2M not containing peptide (Qa-1^b no peptide) and Qa-1^b loaded with one of the following control peptides: Q001, Q002, and DDX5. To select for binders with enhanced affinity through selective gating, the R1 library was sorted using FACS (R2 out). This was repeated a final time for a total of three selections (R3 out). The R3 library was

then analyzed for unique binders specific for Qa-1^b/Qdm. In total five unique binders were found and tested for specificity using the panel of control peptides loaded into Qa-1^b. One clone, termed EXX-1 showed the best combination of binding sensitivity (1nM antigen) and specificity for Qa-1^b/Qdm (Fig. 1).

Characterization of the top clone, EXX-1

EXX-1 was cloned into the pFUSE-IgG-Fc expression vector containing either human IgG1 (hFc), human IgG1 with mutations at Leu234Ala and at Leu235Ala "LALA mutations" (hFc Effector Silent; ES), mouse IgG2a (mFc) or mouse IgG2a with LALA mutations (mFc ES) and produced in Chinese Hamster Ovary (CHO) cells or Expi293 cells using a transient transfection protocol followed by purification by Protein-A affinity chromatography. An example of sample purity was shown for the EXX-1 mFc molecule by SDS-PAGE under reduced (a single band at 41 kD representing monomer VHH-IgG) and non-reduced conditions (single band at ~100kD) (Fig. 2A) and by observing a single peak by size exclusion chromatography (Fig. 2B). The binding affinity of EXX-1 hFc was determined with a dissociation equilibrium constant (K_D) of 1.73 nM.

EXX-1 specifically recognizes the Qa-1^b/Qdm complex

We next evaluated by ELISA the binding specificity of the EXX-1 hFc to recombinant mouse Qa-1^b loaded with specific peptide Qdm, control peptide Q001 or Qa-1^b no peptide. The Qa-1^b monomer samples were coated at 0.25 mg/mL and EXX-1 hFc binding was evaluated at various concentrations (0.125, 0.062 and 0.031 mg/mL) and shown to be selective for the Qa-1^b/Qdm complex in a dose dependent manner (Fig. 2C**)**. In contrast, EXX-1 hFc displayed little to no

binding to control antigens, Qa-1^b/Q001 and Qa-1^b no peptide. Anti-hβ2M antibody bound to Qa-1^b/Qdm, Qa-1^b/Q001 and Qa-1^b no peptide indicating the presence of β2M associated with Qa-1^b. In addition, anti-Qa-1^b antibody (clone 6A8.6F10.1A6 or clone 6A8) demonstrated presence of Qa-1^b heavy chains in all complexes **(**Fig. 2C**)**. Next, we assessed by ELISA the detection sensitivity of EXX-1 hFc. Plates were coated with Qa-1^b/Qdm, Qa-1^b/Q001 or Qa-1^b no peptide starting at 0.25 mg/mL with 2-fold serial dilutions down to 0.0312 mg/mL. EXX-1 hFc added to wells at 1 mg/mL showed detection of Qa-1^b/Qdm complex, titrating down to background signal (~0.1 OD_{450nm}) at 0.0312 mg/mL. Only background signal was detected for EXX-1 hFc binding to controls, Qa-1^b/Q001 and Qa-1^b no peptide, supporting the specificity of EXX-1 binding for Qa-1^b/Qdm peptide complex **(**Fig. 2D**)**. Additionally, clone 6A8 and anti-b2M antibody demonstrated the presence of Qa-1^b heavy chain and b2m, respectively. The isotype control antibody, a VHH single-domain specific for human CD3e containing hFc, did not bind to Qa-1^b/Qdm or control Qa-1^b molecules, as anticipated. Taken together, our findings demonstrate that EXX-1 antibody binding is highly specific even at low antigen concentration for the Qa-1^b/Qdm peptide complex.

We next modified the EXX-1 antibody by replacing the hFc domain with a mFc (ES) domain and characterized its binding specificity. As expected, the EXX-1 mFc (ES) antibody bound to Qa-1^b/Qdm complex and not to Qa-1^b no peptide **(**Fig. 2E**)**. These data demonstrate that EXX-1 antibody binding is specific for Qa-1^b/Qdm peptide complex and binding specificity is not altered when mFc (ES) is used in place of hFc.

To further characterize EXX-1 mFc (ES), we assessed binding through flow cytometry using 293T cells transfected with Qa-1^b plasmid (293T Qa-1^{b+}) and parent 293T cells. Cells were either not

pulsed (unpulsed) or pulsed with 1 mM concentration of peptides Qdm, Q001, GroEL or EPH for 3 hrs at 37^{o}C before staining with anti-Qa-1^{b}-biotin (clone 6A8) plus streptavidin (SA)-PE or SA-PE alone (control) or EXX-1 mFc (ES) plus goat-anti-mouse (GAM)-PE conjugate or GAM-PE conjugate alone (control). High frequencies (45-56%) of 293T Qa-1^{b+} cells stained with the 6A8 antibody, irrespective of peptide pulsing (Fig. 3A), indicating that approximately half of the 293T cells expressed the Qa-1^{b} molecule. In contrast, the EXX-1 mFc (ES) antibody only stained 293T-Qa-1^{b+} cells following pulsing with the Qdm peptide, as shown in Fig. 3B. Moreover, EXX-1 mFc (ES) showed high staining intensity (MFI ~2,000 after subtracting isotype) for Qdm-pulsed 293T Qa-1^{b+} cells, whereas staining of all control peptides was comparable to parent 293T (Fig. 3B). To expand our investigation into the binding selectivity of EXX-1, 293T Qa-1^{b+} cells were pulsed with different concentrations of peptide (Qdm, Q001and Q002), stained with EXX-1 hFc and assessed by flow cytometry. EXX-1 hFc exhibited significant dose-dependent binding to 293T Qa-1^{b+} cells pulsed with Qdm peptide at all concentrations (5.0 to 0.0097 mM) and only background staining to cells pulsed with peptides Q001 and Q002 (Fig. 3C). These results indicate that EXX-1 antibody retains binding selectivity even in the presence of low target density.

Interferon-γ (IFN-γ) is required for EXX-1 binding to mouse tumor cell lines in vitro

Next, clone 6A8 and EXX-1 antibodies were used to stain several in vitro cultured murine tumor cell lines B16, TC-1, RMA, 4T1, EL-4, and C1489 for expression of Qa-1^{b} and Qa-1^{b}/Qdm, respectively. The results, shown in Fig. 4 A and B, clearly demonstrate a lack of antibody staining, indicating these mouse tumor cell lines do not constitutively express Qa-1^{b} or Qa-1^{b}/Qdm molecules. This was not unexpected, as it was previously reported by van Montfoort et al.(4) that

exposure of cells to recombinant IFNγ was needed to induce expression of Qa-1^b on tumor cells in vitro. We thus treated this tumor panel and their Qa-1^b knockdown variants (Qa-$1^{b\ ko}$) with recombinant mouse IFN-γ (m-IFN-γ) before flow cytometric analysis. Results shown in Fig. 4A reveal that m-IFNγ induced Qa-1^b expression only in wild type (Qa-1^{b+}) tumor cells and not in Qa-$1^{b\ ko}$ tumor cells. Moreover, we observed EXX-1 mFc (ES) staining of wild type B16, TC-1, and RMA tumor cells and not Qa-$1^{b\ ko}$ tumor cells after overnight treatment with m-IFN-γ, indicating that IFN-γ regulates the expression of not only Qa-1^b molecules but also the Qa-1^b/Qdm complex (Fig. 4B). Additionally, only after m- IFN-γ treatment did we observed significant tumor cell staining with EXX-1 hFc. Collectively, these data show that EXX-1 is Qa-1^b dependent and Qa-1^b/Qdm complex expression in tumor cells in vitro is dependent on IFN-γ.

EXX-1 mFc (ES) binding is specific for the Qdm peptide presented by Qa-1^b

To provide additional evidence of Qdm peptide specificity for EXX-1, murine tumor cell lines B16F10 (wild type) and B16F10.Db ^{ko} (MHC Db gene knockout) were treated overnight with m-IFN-γ and stained with either anti-Db, clone 6A8 or EXX-1 antibodies. B16F10 tumor cells were shown to express high levels of MHC class Ia Db, but genetic knockout of this gene indeed led to absence of the Db protein (Fig. 5). Since H-2Db is the only classical MHC molecule delivering the Qdm in C57BL/6 cells, B16F10.Db ko cells are deficient for Qdm peptide presentation by Qa-1^b (10). Importantly, the B16F10.Db ko cells were not stained with EXX-1, though staining was still observed with 6A8. Taken together, these data demonstrate that EXX-1 specifically recognizes Qdm peptide in Qa-1^b and that B16F10.Db ko cells express Qa-1^b alone or potentially Qa-1^b with other peptides in addition to expressing Qa-1^b/Qdm peptide complex.

Alanine scan analysis to determine EXX-1 interaction with residues of Qdm peptide

To determine which residues of Qdm peptide are critical for EXX-1 interaction, seven mutated forms of the peptide were synthesized. Each variant contained a single residue substitution with either alanine or glycine (G1, G3, A4, A5, A6, A7, and A8) and was used to pulse 293T Qa-1^{b+} cells. Peptides with alanine mutations in residues p2 and p9 were not used since these are primary anchor residues for Qdm peptide binding to Qa-1^{b} (35-37). EXX-1 staining of peptide-pulsed 293T Qa-1^{b+} cells revealed a marked reduction (>95%) in staining signal when cells were pulsed with variant peptides G3, A6, A7 or A8 compared to Qdm peptide (Fig. 6A). Additionally, a more modest reduction of 20% to 60% was observed for EXX-1 staining signal when 293T Qa-1^{b+} cells were pulsed with peptides G1, A4 or A5 compared to Qdm peptide (Fig. 6A). We concluded that the EXX-1 antibody has broad interaction across the Qdm peptide, but making 1 particularly critical contact with residues p3, p6, p7, and p8.

Miller et al. (36) demonstrated that only residues p5 and p8 in the Qdm peptide serve as major contact residues for NKG2/CD94 receptors using variant peptides substituted at p5 or p8 with lysine. Though both lysine and arginine have basic sides chains, arginine has a bulkier side chain that engages CD94 and to a lesser degree NKG2A. Leucine at p8 in the peptide is hydrophobic and substituting lysine for leucine is not tolerated by the CD94/NKG2A receptor (36). To further assess the mode of interaction for EXX-1 with Qdm peptide, residues p5 and p8 were individually substituted with lysine and then used to pulse 293T Qa-1^{b}+ cells (Fig. 6B). Like the observed total disruption of EXX-1 binding to Qdm peptide A8 (alanine substitution for leucine), substitution of the hydrophobic leucine for positively charged lysine, resulted in clear reduction in EXX-1 staining signal ($p < 0.05$) suggesting EXX-1 binding requires contact with the sidechain of leucine. In contrast, substitution at p5 with either an alanine or lysine residue

yielded an ~50% reduction in EXX-1 binding ($p < 0.05$) compared to Qdm peptide (Fig. 6B). As anticipated EXX-1 did not bind to unpulsed 293T Qa-1^{b+} cells (Fig. 6B). In total, these results show EXX-1 contacts multiple residues across the peptide reinforcing the notion that EXX-1 binding is highly selective for the Qdm peptide in Qa-1^{b}.

Blockade of the NKG2A/Qa-1^{b} axis using EXX-1 antibody unleashes NK cell mediated lysis of tumor cells in vitro

Having established that EXX-1 binding was specific for the Qa-1^{b}/Qdm complex, we attempted to determine whether EXX-1 could unleash NK cell lysis of B16 tumor cells by disrupting the NKG2A/Qa-1^{b} axis. Enriched mouse NK cells cultured in the presence of recombinant mouse interleukin-2 (r-mIL-2) for 24hr were tested for cytolytic activity using m-IFN-γ-stimulated B16 Qa-1^{b+} or B16 Qa-$1^{b\,ko}$ cells as targets. As shown in Fig. 7, NK cells with PBS control displayed significantly greater killing (>30%) of B16 Qa-$1^{b\,ko}$ cells compared to B16 Qa-1^{b+} cells, exhibiting the inhibitory power of Qa-1^{b}. When NK cells were treated with blocking NKG2A antibody, target cell lysis was restored to the level of Qa-1 knockout B16F10 cells. Importantly, EXX-1 mFc (ES) showed identical improvement in tumor cell killing (~30%) as compared with NKG2A blockade. Because EXX-1 mFc (ES) was an Fc-inert variant, killing was not FcR-mediated but rather the result of disrupting the NKG2A axis. Furthermore, the isotype control for EXX-1 mFc (ES) did not restore target cell lysis. Collectively, these findings indicate that EXX-1 is effective at enhancing NK cell cytolytic activity by blocking the NKGA2/Qa-1^{b} axis.

DISCUSION

In this report we describe a novel research tool, a single-domain TCRL antibody for investigating the Qa-1^b/Qdm complex. The antibody, EXX-1, was characterized for binding affinity, specificity and blocking activity in vitro. EXX-1 antibody binding selectivity was demonstrated using several methods, including genetic knockout approaches and alanine scanning analysis. EXX-1 stained IFN-γ treated wild-type B16, TC-1, and RMA tumor cells; conversely IFN-γ treated B16 and TC-1 cells lacking Qa-1^b and B16 cells lacking D^b, which is the exclusive source of Qdm peptide, were not stained, demonstrating that EXX-1 is Qa-1^b dependent and Qdm peptide specific, respectively. Furthermore, several additional murine tumor cells, 4T1, EL-4, and C1498, were stained with EXX-1 but only after overnight incubation with IFN-γ, suggesting that Qa-1^b/Qdm expression is tightly regulated by IFN-γ in tumor cells. Results from alanine scanning analysis showed EXX-1 has broad interactions across the Qdm peptide, providing further evidence that EXX-1 binding is associated with greater peptide selectivity. Moreover, when the EXX-1 antibody was engineered with an inactive mFc, it was found to be effective at blocking the NKG2A/Qa-1^b inhibitory axis and promoting NK cytolysis of tumor cells in vitro.

Multiple reports, including those from our laboratory, have described TCRL antibodies and their use as novel research tools (30, 38-41). TCRL antibodies are generally endowed with high affinity and target selectivity and because of this have been widely used to detect in real-time specific peptide loaded Major Histocompatibility Complexes (pMHC) on the cell surface, helping to further our understanding of antigen presentation and regulation of pMHC complex expression (39, 42, 43). Though previous reports have described single-domain TCR-like antibodies (44, 45), to the best of our knowledge the EXX-1 antibody is the first TCRL antibody

identified that displays specificity for the Qdm peptide presented by Qa-1^{b}. A major challenge of TCRL antibodies is their tendency to exhibit binding modes focused towards hot spots on the HLA surface that can lead to a greater degree of cross-reactivity (46). To overcome this potential limitation, we constructed a single-domain V_hH library and screened for binders having broad interactions across the peptide. V_hH single-domain antibodies have the smallest antigen-binding domain amongst antibodies and can have a unique convex paratope architecture that prefers to associate with concave surfaces of the antigen compared to conventional antibodies (47). The EXX-1 antibody identified using yeast surface display contacted multiple residues across the peptide indicating a highly selective interaction with the Qdm peptide in the Qa-1^{b} molecule. Interestingly, our attempts to find binders from either immunized or naïve mouse libraries were unsuccessful since the binders identified exhibited cross-reactivity, indicating a binding mode biased toward hotspots in the Qa-1^{b} molecule. Further analysis of EXX-1's antigen binding domain is being pursued to determine whether the exquisite selectivity of EXX-1 is due to the unique nature of the antigen binding pocket afforded by V_hH single-domain antibodies. The small size and unique features of V_hH antibodies could be beneficial attributes for generating highly selective TCRL antibodies. Regardless, EXX-1 provides a unique selective research tool for pursuing studies into the biology and function of Qa-1^{b}/Qdm complex in healthy and diseased cells.

Early studies performed by the labs of Drs. Forman, Soloski, and others dissected the dominant presence of Qdm peptide (AMAPRTLLL) in Qa-1^{b} in mouse tumor cells using alloreactive CTL clones specific for Qa-1b/Qdm complex and mass spectrometry (7, 21). They reported that CTL clones specific for Qa-1b/Qdm recognized Qa-1^{b+} /H-2^{d+} target cells but not Qa-1^{b+}/H-2^{k+} target

cells (21). Using genetic analysis Forman et al showed that the Qdm peptide mapped to the leader sequence of D^d, D^b and L^d antigens (7). These same groups observed that cells deficient in antigen processing machinery (e.g., deletion of transporter associated with antigen processing 1 (TAP1)) were not lysed (21). Taken together, these findings provided support for Qdm being the single dominant peptide loaded in Qa-1^b in cells having intact APM expressing MHC class Ia antigens, H2-D.

Additionally, the Qa-1^b/Qdm complex is a ligand for the NKG2A/CD94 inhibitory receptor (17) expressed mainly on a subset of tissue resident or tumor trafficking CD8+ T cells and on NK cells (48, 49). Antibodies recognizing Qa-1^b have been used to show healthy cells and tissues express Qa-1^b, however, direct evidence for Qdm peptide loaded on Qa-1^b in healthy cells has not been conclusively confirmed. A recent study performed by our laboratory found Qa-1^b expression in resting C57BL/6 splenocytes; conversely, little if any EXX-1 staining of splenocytes was observed suggesting that under homeostatic conditions Qdm peptide may not be presented by Qa-1^b or alternatively, its density could fall below the detection threshold of EXX-1. This raises questions regarding Qa-1^b/Qdm expression and its role in protecting cells against lysis from NK cells or CD8+ T-cells.

The human ortholog, HLA-E, is loaded with VL9 peptides and serves as the ligand for the NKG2A/CD94 inhibitory receptor. Like Qa-1^b/Qdm complex, HLA-E/VL9 peptide expression in healthy cells is speculated and hypothesized to protect against lysis from NK cells and a subset of CD8+ T-cells (18, 50, 51). To test this hypothesis with human cells, our team recently generated a TCRL antibody that recognizes HLA-E loaded with VL9 peptides (US Patent No. 10981996). Staining studies have shown this novel research tool is able to recognize most if not all the leader sequence peptides derived from human MHC class Ia molecules presented by

HLA-E. In a preliminary study surveying immune cells for HLA-E/1 VL9 peptide expression, only human monocytes and monocyte-derived macrophages appeared to express the HLA-E/VL9 peptide complex, though all immune cell populations express HLA-E as demonstrated by staining cells with clone 3D12, an antibody that binds to HLA-E independent of peptide loaded (US Patent No.10981996). Though conclusion of these studies is pending, our early findings have raised several important questions related to HLA-E/VL9 complex expression and the biological relevance of HLA-E/VL9 complexes in healthy cells. Parallel studies are now underway by our group using the EXX-1 antibody to survey murine immune and non-immune cells as well as various tissues to determine Qa-1^b/Qdm expression levels in healthy mice. An absence of EXX-1 antibody staining of immune and non-immune cells from healthy mice would challenge the hypothesis that Qa-1^b/Qdm complexes protect normal cells from lysis by NKG2A+ NK and CD8+ T cells and raise additional questions regarding the role of Qa-1^b/Qdm in healthy cells.

An equally important application for the EXX-1 antibody will be to characterize Qa-1^b/Qdm expression and its regulation during inflammation, infection, and cancer. It has been previously described that Qa-1^b (HLA-E) is upregulated under inflammatory conditions (52). It has been shown that Qa-1^b expression can be increased during viral infection, likely regulated by pro inflammatory cytokines such as IFN-γ and IFN-α (53, 54). In fact, Zhou et al., showed that Qa-$1^{b\,ko}$ mice infected with influenza were able to respond to the virus but were not able to effectively terminate the CD8+ T-cell response leading to immunopathology (25). This study and others suggest that Qa-1^b/Qdm is upregulated during stress or inflammatory conditions to downregulate the effector immune response mediated by CD8+ T-cells and NK cells to protect uninfected cells from unwanted lysis. Recently it has been demonstrated that the regulation of

Qa-1^b expression in tumor cells is IFN-γ dependent (4). However, in that study, it was 1 not known whether Qa-1^b/Qdm complexes were being expressed. In our study, we observed EXX-1 binding to all mouse tumor cells evaluated but only after overnight incubation with m-IFN-γ, suggesting this cytokine has an important role in regulating Qa-1^b/Qdm complex expression. It also raises questions regarding Qa-1^b/Qdm regulation by IFN-γ and perhaps other cytokines in the tumor microenvironment. To this end, EXX-1 antibody may prove to be an invaluable tool for detecting and quantifying Qa-1^b/Qdm complexes and for elucidation of regulatory pathways controlling its expression in tumor tissue.

An exciting translational application for the EXX-1 antibody will be to explore its potential as a checkpoint blocking antibody. Several recent studies have shown that in tumor mouse models the expression of NKG2A is associated with worse clinical outcome (3, 4). For example, van Montfoort et al. (4) showed improved anti-tumor effects using B16, TC-1 and RMA tumor models by combining cancer vaccines with a monoclonal antibody to the NKG2A receptor. Andr. P et al. (3) reported that antibody blockade of mouse or human NKG2A combined with anti-PD-(L)1 promotes anti-tumor immunity by unleashing both T and NK cells functions in vivo as well as in vitro. We show here that EXX-1 mFc (ES) can disrupt the NKG2A/Qa-1^b axis in vitro by binding to Qa-1^b/Qdm to enhance NK cell-mediated killing of target cells. Our findings support further evaluation of EXX-1 as an immune checkpoint blocking antibody in tumor models. If healthy tissues do not express Qa-1^b/Qdm complex, since Qdm is likely the dominant peptide loaded in Qa-1^b in tumor cells, these Qa-1^b/Qdm peptide complexes appear to be the primary ligands for NKG2A/CD94 heterodimeric receptors (17, 18), and because the expression of Qa-1^b/Qdm complex is inducible by IFN-γ in tumor cells, Qa-1^b/Qdm could be a superior target over NKG2A. One potential caveat to targeting Qa-1^b/Qdm or HLE/VL9

peptides, is that these molecules also serve as ligands for the related activating receptor, NKG2C. Regardless, 1 there might be benefits to targeting tumor cells with TCRL antibodies to Qa-1^b/Qdm or HLA-E/VL9 peptide complexes to disrupt the NKG2A axis. TCRL blocking antibodies could be modified into potentially more potent molecules by engineering enhanced Fc binding affinity for CD16 (Fc receptor) to mediate antibody-dependent cellular cytotoxicity (ADCC) or by developing antibodies to carry payloads (cytotoxic or immunomodulatory agents) while still retaining blocking activity. To assess the potential therapeutic benefits of targeting Qa-1^b/Qdm, future studies will be aimed at evaluating NKG2A axis blockade with EXX-1 antibody or derivative forms of EXX-1 alone or in combination with cancer vaccines, oncolytic viruses, or other checkpoint blocking antibodies in mouse syngeneic tumor models.

FIGURES

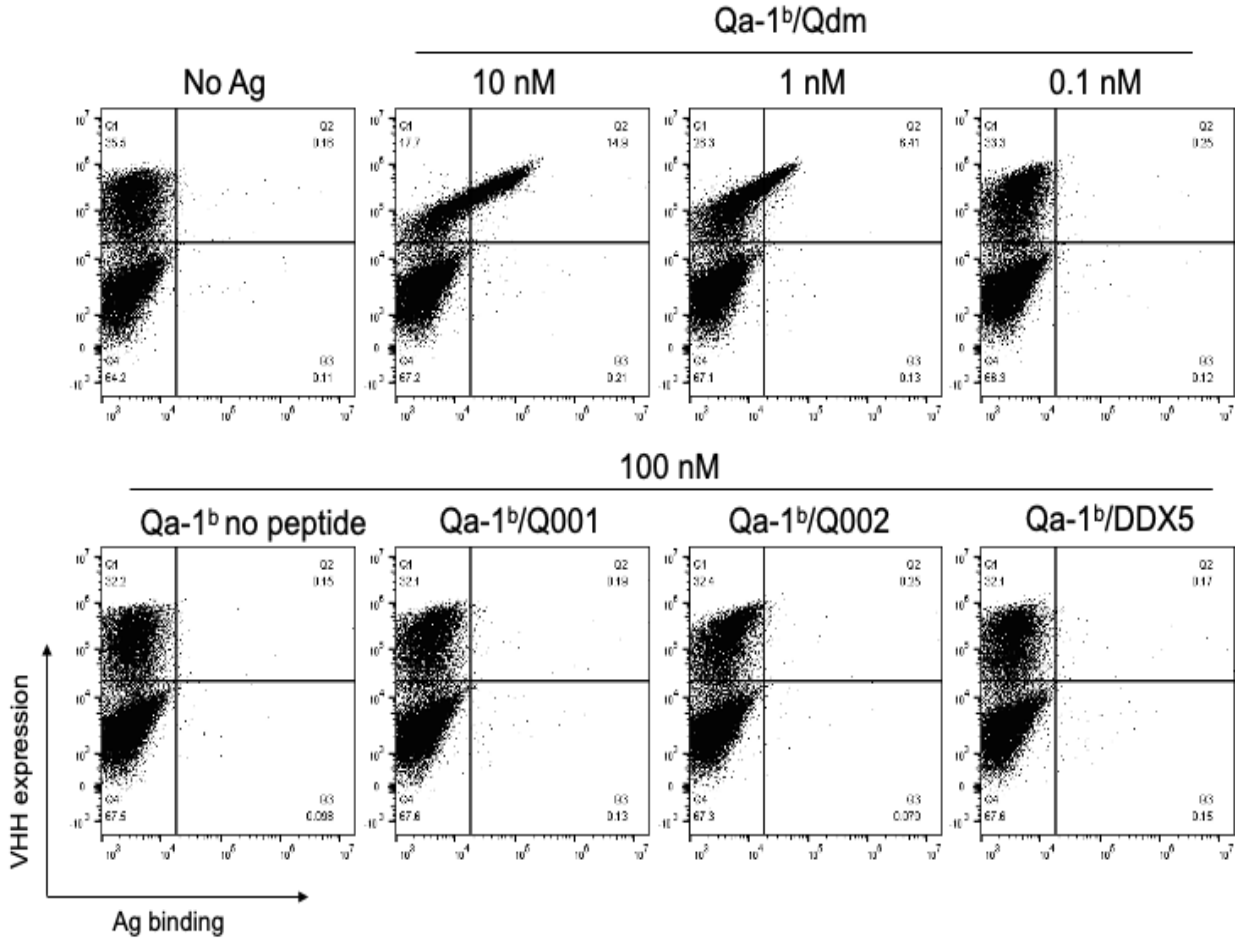

Chapter 2 1: Yeast display of clone EXX-1.

Staining of the single clones EXX-1 in yeast. Antigen (Ag) binding is indicated in Q2, with staining for both VHH expression and Ag binding. VHH expression was detected with an anti-Flag epitope tag. Ag binding of biotinylated antigens was
detected with SA-PE.

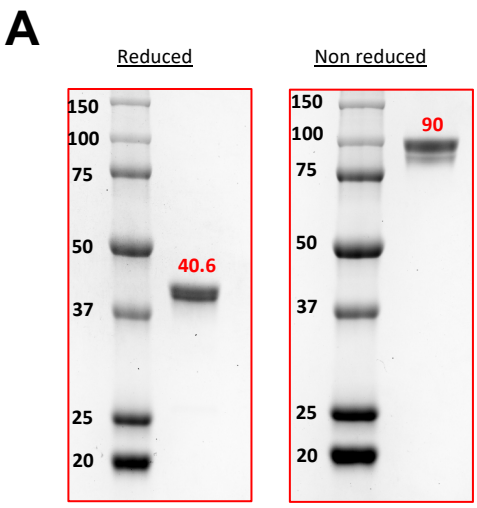
A
Reduced
Non reduced
150
100
75
50
37
25
20
40.6
90

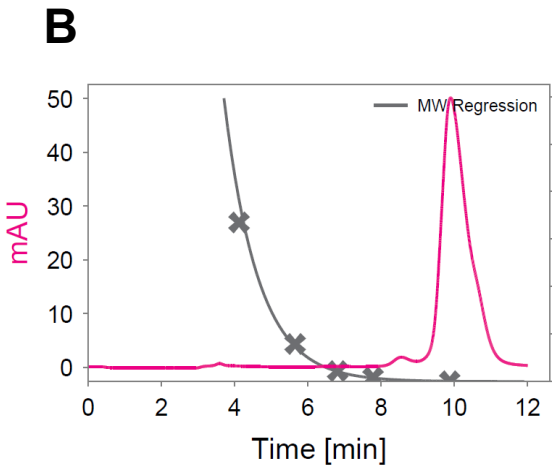
B
MW Regression
mAU
Time [min]

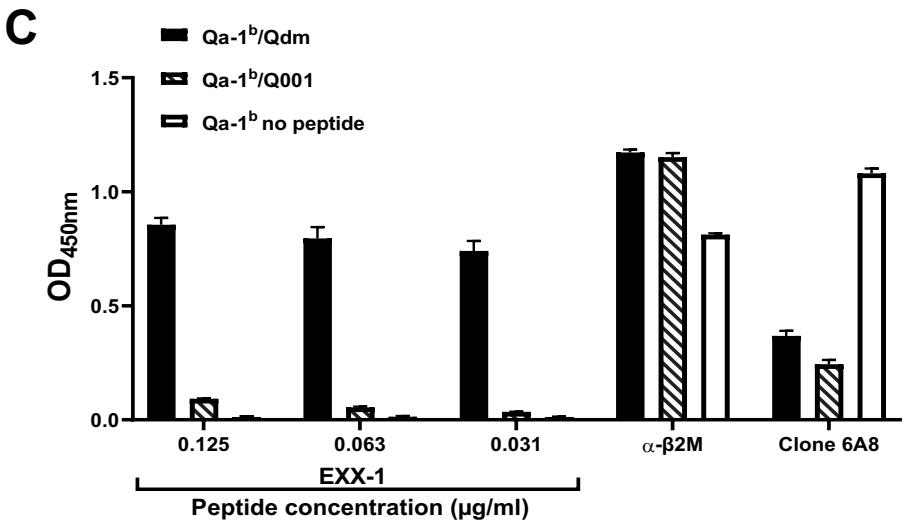
C
Qa-1b/Qdm
Qa-1b/Q001
Qa-1b no peptide
OD450nm
0.125
0.063
0.031
α-β2M
Clone 6A8
EXX-1
Peptide concentration (µg/ml)

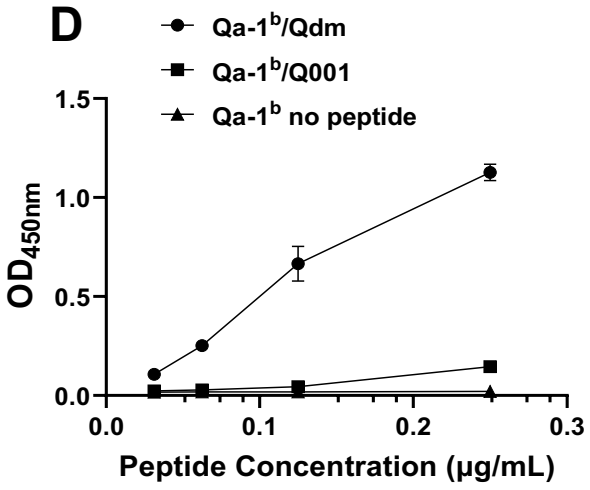
D
Qa-1b/Qdm
Qa-1b/Q001
Qa-1b no peptide
OD450nm
Peptide Concentration (µg/mL)

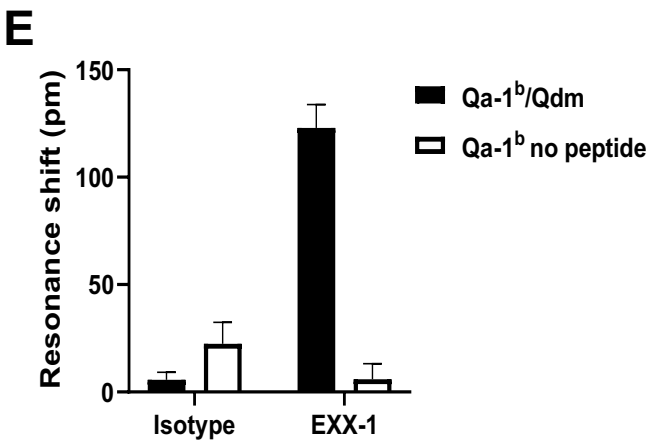
E
Resonance shift (pm)
Qa-1b/Qdm
Qa-1b no peptide
Isotype
EXX-1

Chapter 2 2: EXX-1 binds to recombinant Qa-1^{b}/Qdm complexes.

Characterization of purified EXX-1 mFc by (A) SDS-PAGE under reduced and non-reduced conditions (A) and by size exclusion chromatography (B). (C) Assessment of EXX-1 hFc specificity by ELISA. Plates were coated with EXX-1 hFc (0.125, 0.0625 and 0.03201 μg), anti-β2m (0.5 μg) or anti-Qa-1^{b} (clone 6A8, 0.5μg). Complexes of biotinylated Qa-1^{b} monomers (Qa-1$_{b}$/Qdm, Qa-1^{b} /Q001 or Qa-1^{b} no peptide) were added at 0.25 μg/mL. (D)Assessment of EXX-1 (1μg/ml) detection sensitivity by ELISA to Qa-1^{b} complexes (Qdm, Q001, no peptide) immobilized at 0.25, 0.125, 0.0625, and 0.0312 μg/ well. (E) Assessment of EXX-1 mFc (1μg/mL) binding to immobilized Qa-1^{b}/Qdm
or Qa-1^{b} no peptide using the ResoSens label-free bioassay system. (C-D) Absorbance data are shown as mean ± SD in triplicate and are representative of at least three independent experiments.

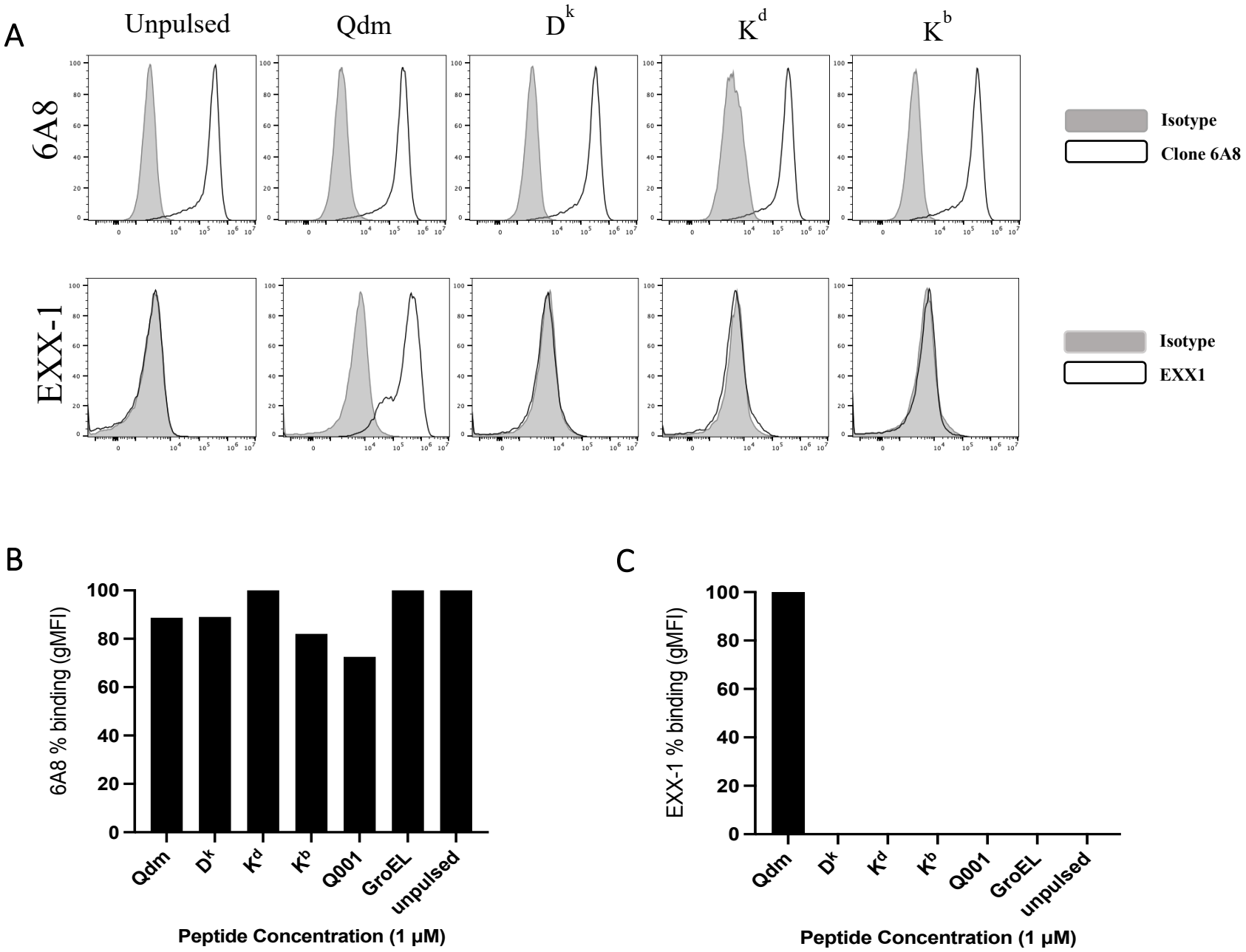
A
Unpulsed
Qdm
D^k
K^d
K^b
6A8
EXX-1
Isotype
Clone 6A8
Isotype
EXX1
B
6A8 % binding (gMFI)
Qdm
D^k
K^d
K^b
Q001
GroEL
unpulsed
Peptide Concentration (1 μM)
C
EXX-1 % binding (gMFI)
Qdm
D^k
K^d
K^b
Q001
GroEL
unpulsed
Peptide Concentration (1 μM)

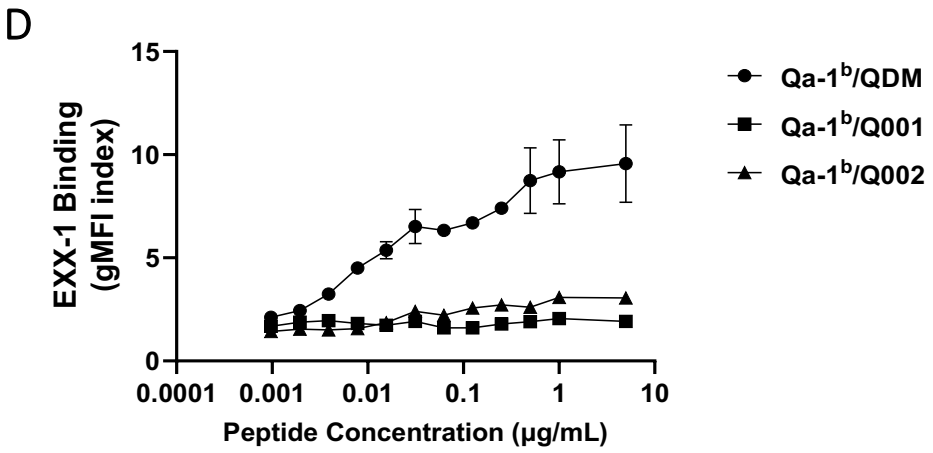

Chapter 2 3: EXX-1 antibody recognizes Qdm on peptide-pulsed 293T Qa-1^{b+} cells.

Qa-1^{b} transfected 293T cells (293T Qa-1^{b+}) were left unpulsed or pulsed for 3 hours at 37°C with 1mM of Qdm, Q001, Q002, GroEL, D^{k}, K^{d} or K^{b} as indicated. Unpulsed 293T Qa-1^{b+}, and peptide pulsed-cells were stained with (A, top panel and B)1 µg/mL of 6A8-biotin (1◦ Ab) and SA-PE (2◦ Ab) or (A, bottom panel and C) 1 µg/mL EXX-1 hFc (1◦ Ab) and GAM/PE (2◦ Ab). Filled gray denote isotype and black solid line denotes staining with indicated antibody.
(D) 293T Qa-1^{b+} cells were pulsed with a titration (5 to 0.00097 µM) of peptides (Qdm, Q001, or Q002) and stained with EXX-1 hFc at 1µg/mL. All data are representative of at least three independent experiments. Mean fluorescence intensity (MFI) = [(MFI of cells stained with 1◦ Ab + 2◦ Ab) − (MFI of cells stained only with 2◦ Ab)]. GeoMFI (gMFI) index = [(MFI of cells stained with 1◦ Ab + 2◦ Ab) ÷ (MFI of cells stained only with 2◦ Ab)]. Error bars represent mean ± SEM of each data set's group (triplicates samples).

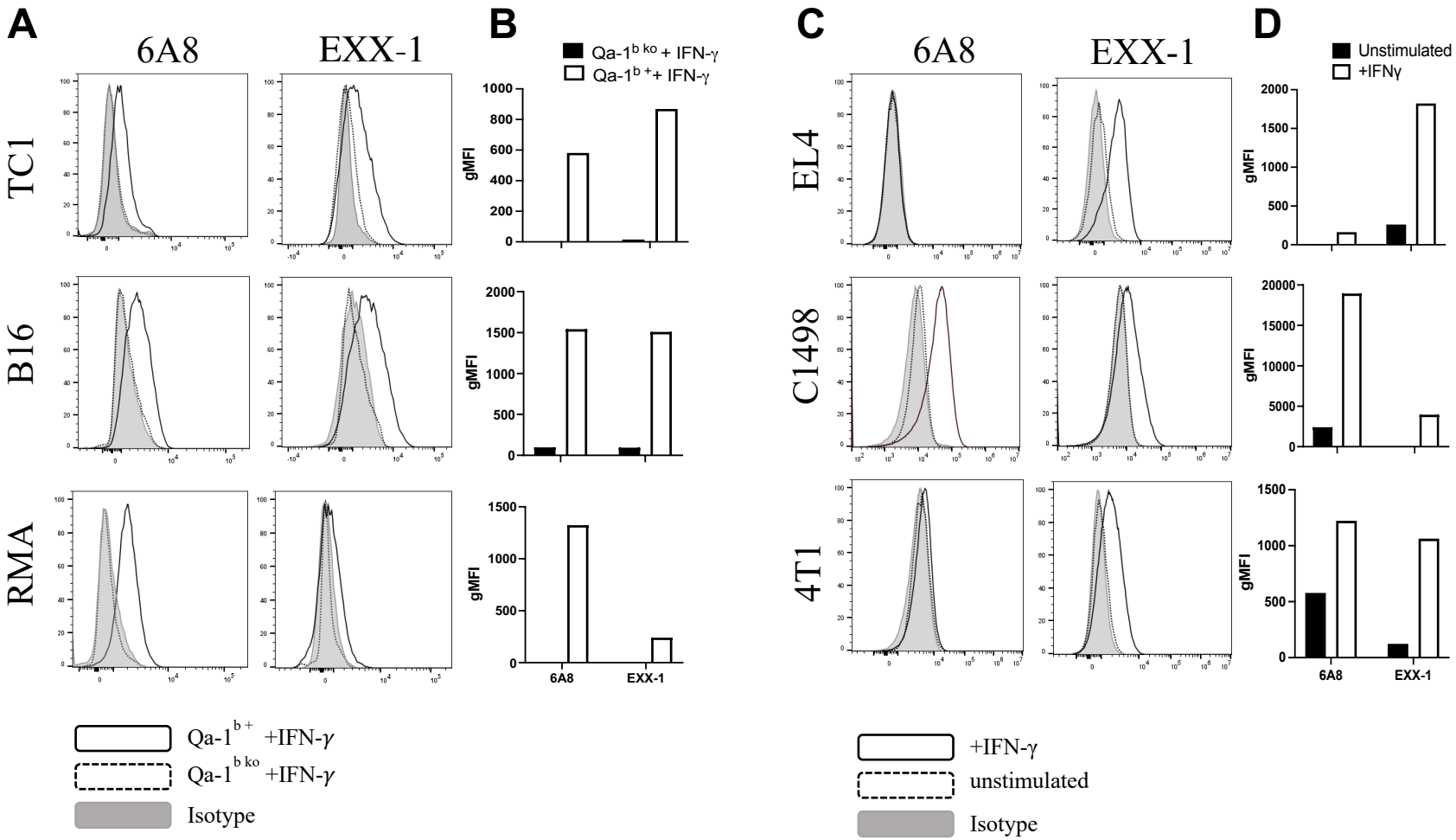
A
6A8
EXX-1
TC1
B16
RMA
B
Qa-1b ko + IFN-γ
Qa-1b + IFN-γ
gMFI
6A8
EXX-1
Qa-1b + +IFN-γ
Qa-1b ko +IFN-γ
Isotype
C
6A8
EXX-1
EL4
C1498
4T1
D
Unstimulated
+IFNγ
gMFI
6A8
EXX-1
+IFN-γ
unstimulated
Isotype

Chapter 2 4: Assessment of EXX-1 binding to mouse tumor cells in vitro.

(A) anti-Qa-1^{b} clone 6A8 (left panel) and EXX-1 (right panel) with (B) summarized data in in IFN-γ stimulated TC1, B16 and RMA parent cells (Qa-1^{b+}) and Qa-$1^{b\ ko}$ cells. Cells were stimulated with recombinant mIFN-γ (20 ng/mL) for 48 hours before staining. (C) anti-Qa-1^{b} clone 6A8 (left panel) and EXX-1 (right panel) with (D) summarized data in EL4, C1498, and 4T1 cells. Cells were stained with and without incubation with r-mIFN-γ (20 ng/mL) for 48 hours. The data presented are the pooled results of three independent experiments. GeoMean fluorescence intensity (gMFI) = [(MFI of cells stained with 1◦Ab + 2◦ Ab) - (MFI of cells stained only with 2◦ Ab)]. (A and C) Filled gray represents isotype, dashed black line represents (A) staining in Qa-$1^{b\ ko}$ or (C) unstimulated cells, solid black line represents staining in IFN-γ stimulated cells.

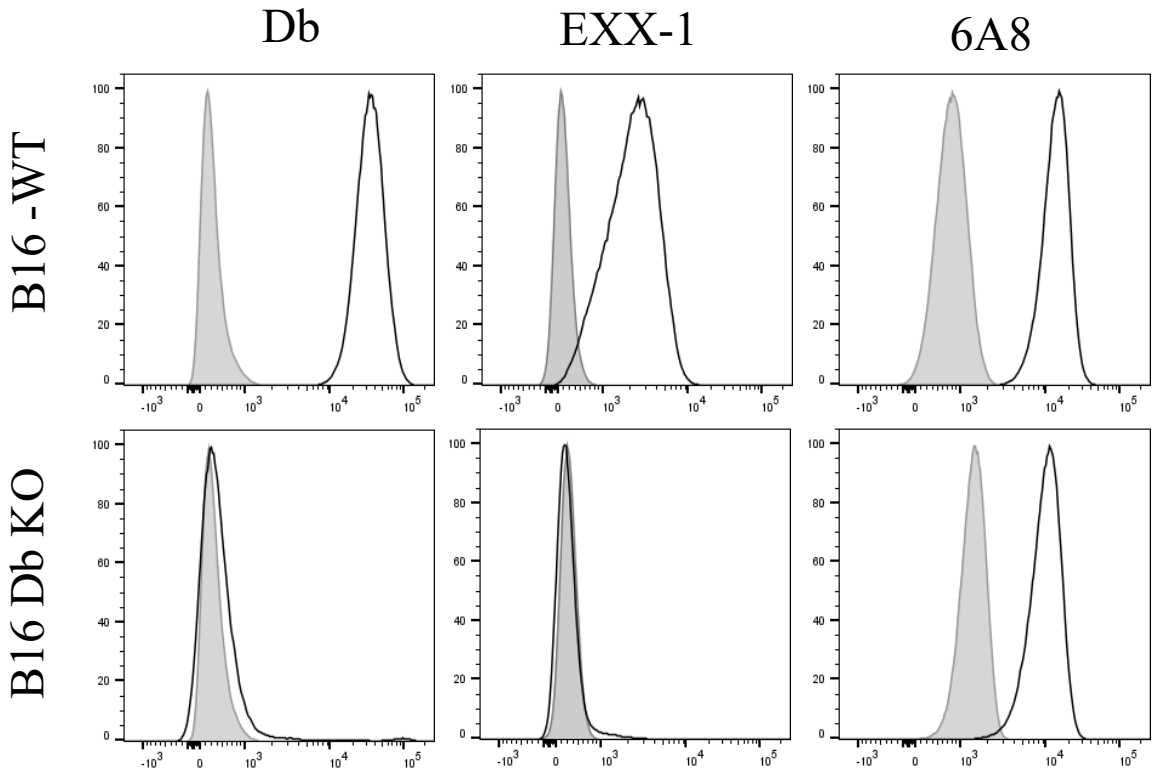

Chapter 2 5: EXX-1 binding is selective for Qdm peptide in Qa-1^{b}.

Staining 1 with anti-Db, EXX-1, or 6A8 in B16F10 wildtype (Top panel) or B16F10.Db knockout cells (Bottom panel). Control reagent is plotted in grey. Indicated antibody is plotted with a black line Cells were pre-treated with IFNγ for 24 hr before staining with antibodies.

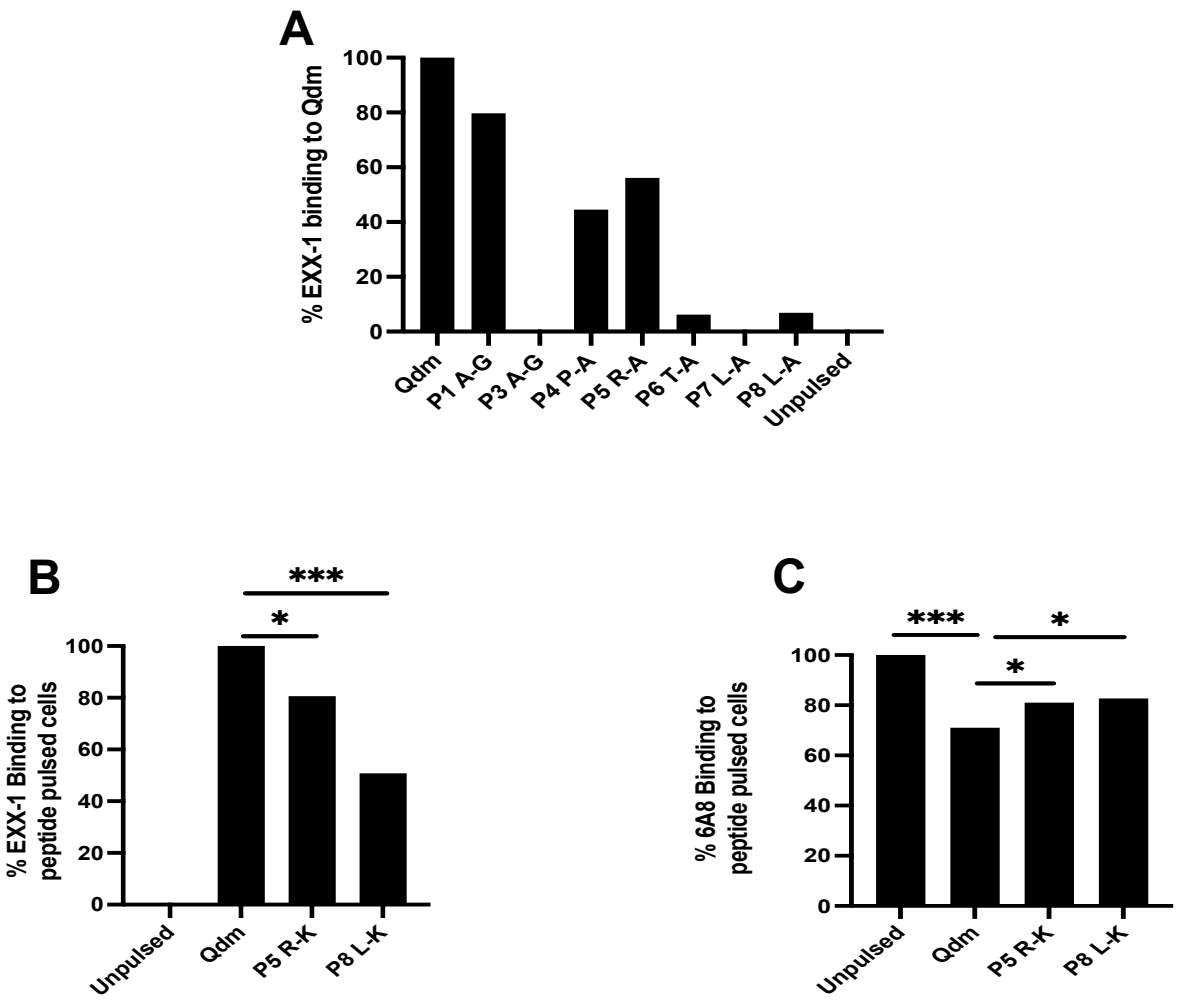

Chapter 2 6: Alanine scan analysis reveals EXX-1 has broad interactions across the peptide.

Qdm variant peptides were synthesized with (A) a single glycine or alanine residue substitution at p1, p3, p4, p5, p6, p7, or p8 or with (B and C) substitution at p5 and p8 with lysine and stained with (A) 1 µg/mL of EXX-1 and (B) 1 µg/mL of anti Qa-1^{b} clone 6A8. 293T Qa-1^{b+} cells were left unpulsed or pulsed with Qdm, p1A→G, p3A→G, p4P→A, p5R→A, p6T→A, p7L→A, p8L→A, p5R→K, or p8L→L as indicated. (A and B) EXX-1 was detected with GAM/PE (2◦ Ab) and (C) clone 6A8 was detected with SA-PE (2◦ Ab). % of binding to Qdm is calculated as [(MFI of EXX-1 in cells pulsed with the indicated peptide) ÷ (MFI of EXX-1 with Qdm) ×100]. GeoMFI (gMFI) index is calculated as [(MFI of cells stained with 1◦ Ab + 2◦ Ab) ÷ (MFI of cells stained only with 2◦ Ab)]. Data are representative of at two independent experiments. Error bars represent mean ± SD of triplicates assays. The p values were determined with unpaired Student t test. ****$p<0.0001$, ***$p<0.001$, *$p<0.05$.

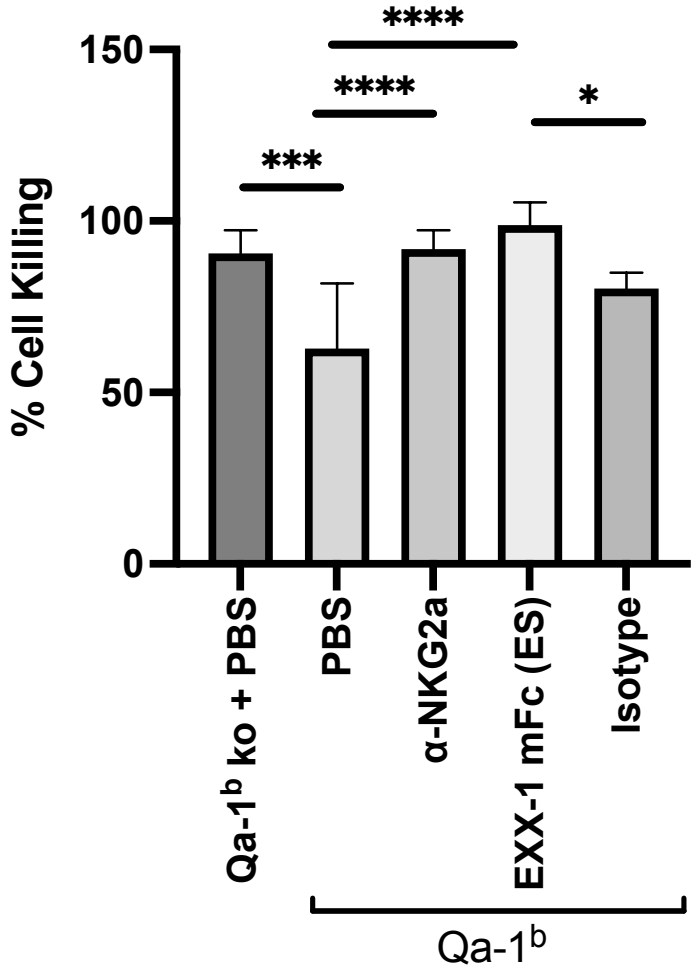

Chapter 2 7: EXX-1 enhances NK cell cytolytic activity in vitro.

Enriched NK cells isolated from spleens of na.ve C57Bl/6 mice were incubated with rmIL-2 (20 ng/mL) for 24 hr. NK cells were then co-cultured with m-IFN-γ -stimulated and calcein AM-labeled B16 Qa-1^{b+} or B16 Qa-$1^{b\,ko}$ tumor cells at a ratio of 3:1 (E:T) with or without antibodies as indicated for 24 hr. Percent cell killing was assessed by measuring calcein-AM release. All data are representative of at least three independent experiments (n= 3). Error bars represent mean±SEM within each group. The p values were determined with one-way ANOVA test. ****$p<0.0001$, ***$p\leq0.0001$, *$p\leq0.01$.

TABELS

Table 1 . Primers used for yeast display library construction.

Primer	Sequence (5’ to 3’)
Lla_04	ATAGCTCGACGATTGAAGGTAGAGCGGCCGCTTACCCATACGACGTTCCAGACT ACGCT**CAGGTGCAGCTGGTGCAGTCTG**G
Lla_05	ATAGCTCGACGATTGAAGGTAGAGCGGCCGCTTACCCATACGACGTTCCAGACT ACGCT**CAGGTCACCTTGAAGGAGTCTGG**
Lla_06	ATAGCTCGACGATTGAAGGTAGAGCGGCCGCTTACCCATACGACGTTCCAGACT ACGCT**CAGGTGCAGCTGCAGGAGTCGGG**
Lla_07	GATGCGGCCCTCTAGGATCAGCGGGTTTAAACTCACTTGTCGTCATCGTCTTTGT AGTC**TGAGGAGACRGTGACCTGGGTCC**

*Bold represents sequence complementary to the V-gene segments.

REFERENCES

1. Borst, L., S. H. van der Burg, and T. van Hall. 2020. The NKG2A-HLA-E Axis as a Novel Checkpoint in the Tumor Microenvironment. Clin Cancer Res 26: 5549-5556.
2. van Hall, T., P. Andre, A. Horowitz, D. F. Ruan, L. Borst, R. Zerbib, E. Narni-Mancinelli, S. H. van der Burg, and E. Vivier. 2019. Monalizumab: inhibiting the novel immune checkpoint NKG2A. J Immunother Cancer 7: 263.
3. Andre, P., C. Denis, C. Soulas, C. Bourbon-Caillet, J. Lopez, T. Arnoux, M. Blery, C. Bonnafous, L. Gauthier, A. Morel, B. Rossi, R. Remark, V. Breso, E. Bonnet, G. Habif, S. Guia, A. I. Lalanne, C. Hoffmann, O. Lantz, J. Fayette, A. Boyer-Chammard, R. Zerbib, P. Dodion, H. Ghadially, M. Jure-Kunkel, Y. Morel, R. Herbst, E. Narni-Mancinelli, R. B. Cohen, and E. Vivier. 2018. Anti-NKG2A mAb Is a Checkpoint Inhibitor that Promotes Anti-tumor Immunity by Unleashing Both T and NK Cells. Cell 175: 1731-1743 e1713.
4. van Montfoort, N., L. Borst, M. J. Korrer, M. Sluijter, K. A. Marijt, S. J. Santegoets, V. J. van Ham, I. Ehsan, P. Charoentong, P. Andre, N. Wagtmann, M. J. P. Welters, Y. J. Kim, S. J. Piersma, S. H. van der Burg, and T. van Hall. 2018. NKG2A Blockade Potentiates CD8 T Cell Immunity Induced by Cancer Vaccines. Cell 175: 1744-1755 e1715.
5. Imani, F., and M. J. Soloski. 1991. Heat shock proteins can regulate expression of the Tla region-encoded class Ib molecule Qa-1. Proc Natl Acad Sci U S A 88: 10475-10479.
6. Ohtsuka, M., H. Inoko, J. K. Kulski, and S. Yoshimura. 2008. Major histocompatibility complex (Mhc) class Ib gene duplications, organization and expression patterns in mouse strain C57BL/6. BMC Genomics 9: 178.
7. DeCloux, A., A. S. Woods, R. J. Cotter, M. J. Soloski, and J. Forman. 1997. Dominance of a single peptide bound to the class I(B) molecule, Qa-1b. J Immunol 158: 2183-2191.

8. Bai, A., J. Broen, and J. Forman. 1998. The pathway for processing leader-derived peptides that regulate the maturation and expression of Qa-1b. Immunity 9: 413-421.
9. Oliveira, C. C., P. A. van Veelen, B. Querido, A. de Ru, M. Sluijter, S. Laban, J. W. Drijfhout, S. H. van der Burg, R. Offringa, and T. van Hall. 2010. The nonpolymorphic MHC Qa-1b mediates CD8+ T cell surveillance of antigen-processing defects. J Exp Med 207: 207-221.
10. Kurepa, Z., and J. Forman. 1997. Peptide binding to the class Ib molecule, Qa-1b. J Immunol 158: 3244-3251.
11. Davies, A., S. Kalb, B. Liang, C. J. Aldrich, F. A. Lemonnier, H. Jiang, R. Cotter, and M. J. Soloski. 2003. A peptide from heat shock protein 60 is the dominant peptide bound to Qa-1 in the absence of the MHC class Ia leader sequence peptide Qdm. J Immunol 170: 5027-5033.
12. van Hall, T., C. C. Oliveira, S. A. Joosten, and T. H. Ottenhoff. 2010. The other Janus face of Qa-1 and HLA-E: diverse peptide repertoires in times of stress. Microbes Infect 12: 910-918.
13. Soloski, M. J., W. F. Lo, and E. S. Metcalf. 2000. Gram-negative pathogens and molecular mimicry: is there a case for mistaken identity? Response. Trends Microbiol 8: 446-447.
14. Bouwer, H. G., M. S. Seaman, J. Forman, and D. J. Hinrichs. 1997. MHC class Ib-restricted cells contribute to antilisterial immunity: evidence for Qa-1b as a key restricting element for Listeria-specific CTLs. J Immunol 159: 2795-2801.
15. van Hall, T., S. Laban, D. Koppers-Lalic, J. Koch, C. Precup, P. Asmawidjaja, R. Offringa, and E. J. Wiertz. 2007. The varicellovirus-encoded TAP inhibitor UL49.5 regulates the presentation of CTL epitopes by Qa-1b1. J Immunol 178: 657-662.

16. Kambayashi, T., J. R. Kraft-Leavy, J. G. Dauner, B. A. Sullivan, 1 O. Laur, and P. E. Jensen 2004. The nonclassical MHC class I molecule Qa-1 forms unstable peptide complexes. J Immunol 172: 1661-1669.

17. Salcedo, M., P. Bousso, H. G. Ljunggren, P. Kourilsky, and J. P. Abastado. 1998. The Qa-1b molecule binds to a large subpopulation of murine NK cells. Eur J Immunol 28: 4356- 4361.

18. Braud, V. M., D. S. Allan, C. A. O'Callaghan, K. Soderstrom, A. D'Andrea, G. S. Ogg, S. Lazetic, N. T. Young, J. I. Bell, J. H. Phillips, L. L. Lanier, and A. J. McMichael. 1998. HLA-E binds to natural killer cell receptors CD94/NKG2A, B and C. Nature 391: 795-10 799.

19. Zeng, L., L. C. Sullivan, J. P. Vivian, N. G. Walpole, C. M. Harpur, J. Rossjohn, C. S. Clements, and A. G. Brooks. 2012. A structural basis for antigen presentation by the MHC class Ib molecule, Qa-1b. J Immunol 188: 302-310.

20. Lee, N., D. R. Goodlett, A. Ishitani, H. Marquardt, and D. E. Geraghty. 1998. HLA-E surface expression depends on binding of TAP-dependent peptides derived from certain HLA class I signal sequences. J Immunol 160: 4951-4960.

21. Aldrich, C. J., A. DeCloux, A. S. Woods, R. J. Cotter, M. J. Soloski, and J. Forman. 1994. Identification of a Tap-dependent leader peptide recognized by alloreactive T cells specific for a class Ib antigen. Cell 79: 649-658.

22. Doorduijn, E. M., M. Sluijter, B. J. Querido, U. J. E. Seidel, C. C. Oliveira, S. H. van der Burg, and T. van Hall. 2018. T Cells Engaging the Conserved MHC Class Ib Molecule Qa-1(b) with TAP-Independent Peptides Are Semi-Invariant Lymphocytes. Front Immunol 9: 60.

23. Chen, Y., Z. Xin, L. Huang, L. Zhao, S. Wang, J. Cheng, P. Wu, and Y. Chai. 2019. CD8(+) T Cells Form the Predominant Subset of NKG2A(+) Cells in Human Lung Cancer. Front Immunol 10: 3002.

24. Abd Hamid, M., R. Z. Wang, X. Yao, P. Fan, X. Li, X. M. Chang, Y. Feng, S. Jones, D. Maldonado-Perez, C. Waugh, C. Verrill, A. Simmons, V. Cerundolo, A. McMichael, C. Conlon, X. Wang, Y. Peng, and T. Dong. 2019. Enriched HLA-E and CD94/NKG2A Interaction Limits Antitumor CD8(+) Tumor-Infiltrating T Lymphocyte Responses. Cancer Immunol Res 7: 1293-1306.

25. Zhou, J., M. Matsuoka, H. Cantor, R. Homer, and R. I. Enelow. 2008. Cutting edge: engagement of NKG2A on CD8+ effector T cells limits immunopathology in influenza pneumonia. J Immunol 180: 25-29.

26. Sivakumar, P. V., A. Gunturi, M. Salcedo, J. D. Schatzle, W. C. Lai, Z. Kurepa, L. Pitcher, M. S. Seaman, F. A. Lemonnier, M. Bennett, J. Forman, and V. Kumar. 1999. Cutting edge: expression of functional CD94/NKG2A inhibitory receptors on fetal NK1.1+Ly-49- cells: a possible mechanism of tolerance during NK cell development. J Immunol 162: 6976-6980.

27. Seaman, M. S., B. Perarnau, K. F. Lindahl, F. A. Lemonnier, and J. Forman. 1999. Response to Listeria monocytogenes in mice lacking MHC class Ia molecules. J Immunol 162: 5429-5436.

28. Lo, W. F., H. Ong, E. S. Metcalf, and M. J. Soloski. 1999. T cell responses to Gram44 negative intracellular bacterial pathogens: a role for CD8+ T cells in immunity to Salmonella infection and the involvement of MHC class Ib molecules. J Immunol 162: 5398-5406.

29. Weidanz, J. A., O. Hawkins, B. Verma, and 1 W. H. Hildebrand. 2011. TCR-like biomolecules target peptide/MHC Class I complexes on the surface of infected and cancerous cells. Int Rev Immunol 30: 328-340.

30. Dahan, R., and Y. Reiter. 2012. T-cell-receptor-like antibodies - generation, function and applications. Expert Rev Mol Med 14: e6.

31. Chang, A. Y., R. S. Gejman, E. J. Brea, C. Y. Oh, M. D. Mathias, D. Pankov, E. Casey, T. Dao, and D. A. Scheinberg. 2016. Opportunities and challenges for TCR mimic antibodies in cancer therapy. Expert Opin Biol Ther 16: 979-987.

32. Pardon, E., T. Laeremans, S. Triest, S. G. Rasmussen, A. Wohlkonig, A. Ruf, S. Muyldermans, W. G. Hol, B. K. Kobilka, and J. Steyaert. 2014. A general protocol for the generation of Nanobodies for structural biology. Nat Protoc 9: 674-693.

33. Van Deventer, J. A., and K. D. Wittrup. 2014. Yeast surface display for antibody isolation: library construction, library screening, and affinity maturation. Methods Mol Biol 1131: 151-181.

34. Kuball, J., B. Hauptrock, V. Malina, E. Antunes, R. H. Voss, M. Wolfl, R. Strong, M. Theobald, and P. D. Greenberg. 2009. Increasing functional avidity of TCR-redirected T cells by removing defined N-glycosylation sites in the TCR constant domain. J Exp Med 206: 463-475.

35. Kraft, J. R., R. E. Vance, J. Pohl, A. M. Martin, D. H. Raulet, and P. E. Jensen. 2000. Analysis of Qa-1(b) peptide binding specificity and the capacity of CD94/NKG2A to discriminate between Qa-1-peptide complexes. J Exp Med 192: 613-624.

36. Miller, J. D., D. A. Weber, C. Ibegbu, J. Pohl, J. D. Altman, and P. E. Jensen. 2003. Analysis of HLA-E peptide-binding specificity and contact residues in bound peptide required for recognition by CD94/NKG2. J Immunol 171: 1369-1375.

37. Braud, V., E. Y. Jones, and A. McMichael. 1997. The human major histocompatibility complex class Ib molecule HLA-E binds signal sequence-derived peptides with primary anchor residues at positions 2 and 9. Eur J Immunol 27: 1164-1169.

38. Neethling, F. A., V. Ramakrishna, T. Keler, R. Buchli, T. Woodburn, and J. A. Weidanz. 2008. Assessing vaccine potency using TCRmimic antibodies. Vaccine 26: 3092-3102.

39. Kaabinejadian, S., C. P. McMurtrey, S. Kim, R. Jain, W. Bardet, F. B. Schafer, J. L. Davenport, A. D. Martin, M. S. Diamond, J. A. Weidanz, T. H. Hansen, and W. H. Hildebrand. 2016. Immunodominant West Nile Virus T Cell Epitopes Are Fewer in Number and Fashionably Late. J Immunol 196: 4263-4273.

40. Patterson, A. M., S. Kaabinejadian, C. P. McMurtrey, W. Bardet, K. W. Jackson, R. E. Zuna, S. Husain, G. P. Adams, G. MacDonald, R. L. Dillon, H. Ames, R. Buchli, O. E. Hawkins, J. A. Weidanz, and W. H. Hildebrand. 2016. Human Leukocyte Antigen Presented Macrophage Migration Inhibitory Factor Is a Surface Biomarker and Potential Therapeutic Target for Ovarian Cancer. Mol Cancer Ther 15: 313-322.

41. Weidanz, J. A., T. Nguyen, T. Woodburn, F. A. Neethling, M. Chiriva-Internati, W. H. Hildebrand, and J. Lustgarten. 2006. Levels of specific peptide-HLA class I complex predicts tumor cell susceptibility to CTL killing. J Immunol 177: 5088-5097.

42. Zehn, D., C. J. Cohen, Y. Reiter, and P. Walden. 2004. Extended presentation of specific MHC-peptide complexes by mature dendritic cells compared to other types of antigen presenting cells. Eur J Immunol 34: 1551-1560.

43. Weidanz, J. A., P. Piazza, H. Hickman-Miller, D. Woodburn, T. Nguyen, A. Wahl, F. Neethling, M. Chiriva-Internati, C. R. Rinaldo, and W. H. Hildebrand. 2007. Development and implementation of a direct detection, quantitation and validation 1 system for class I MHC self-peptide epitopes. J Immunol Methods 318: 47-58.

44. Dass, S. A., M. N. Norazmi, A. A. Dominguez, M. Miguel, and G. J. Tye. 2018. Generation of a T cell receptor (TCR)-like single domain antibody (sDAb) against a Mycobacterium Tuberculosis (Mtb) heat shock protein (HSP) 16kDa antigen presented by Human Leukocyte Antigen (HLA)-A*02. Mol Immunol 101: 189-196.

45. Zhang, G., R. Liu, X. Zhu, L. Wang, J. Ma, H. Han, X. Wang, G. Zhang, W. He, W. Wang, C. Liu, S. Li, M. Sun, and B. Gao. 2013. Retargeting NK-92 for anti-melanoma activity by a TCR-like single-domain antibody. Immunol Cell Biol 91: 615-624.

46. Holland, C. J., R. M. Crean, J. M. Pentier, B. de Wet, A. Lloyd, V. Srikannathasan, N. Lissin, K. A. Lloyd, T. H. Blicher, P. J. Conroy, M. Hock, R. J. Pengelly, T. E. Spinner, B. Cameron, E. A. Potter, A. Jeyanthan, P. E. Molloy, M. Sami, M. Aleksic, N. Liddy, R. A. Robinson, S. Harper, M. Lepore, C. R. Pudney, M. W. van der Kamp, P. J. Rizkallah, B. K. Jakobsen, A. Vuidepot, and D. K. Cole. 2020. Specificity of bispecific T cell receptors and antibodies targeting peptide-HLA. J Clin Invest 130: 2673-2688.

47. Muyldermans, S. 2013. Nanobodies: natural single-domain antibodies. Annu Rev Biochem 82: 775-797.

48. Graham, C. M., J. R. Christensen, and D. B. Thomas. 2007. Differential induction of CD94 and NKG2 in CD4 helper T cells. A consequence of influenza virus infection and interferon-gamma? Immunology 121: 238-247.

49. van Stijn, A., A. T. Rowshani, S. L. Yong, F. Baas, E. Roosnek, I. J. ten Berge, and R. A. van Lier. 2008. Human cytomegalovirus infection induces a rapid and sustained change in the expression of NK cell receptors on CD8+ T cells. J Immunol 180: 4550-4560.

50. Lee, N., M. Llano, M. Carretero, A. Ishitani, F. Navarro, M. Lopez-Botet, and D. E. Geraghty. 1998. HLA-E is a major ligand for the natural killer inhibitory receptor CD94/NKG2A. Proc Natl Acad Sci U S A 95: 5199-5204.

51. Walters, L. C., K. Harlos, S. Brackenridge, D. Rozbesky, J. R. Barrett, V. Jain, T. S. Walter, C. A. O'Callaghan, P. Borrow, M. Toebes, S. G. Hansen, J. B. Sacha, S. Abdulhaqq, J. M. Greene, K. Fruh, E. Marshall, L. J. Picker, E. Y. Jones, A. J. McMichael, and G. M. Gillespie. 2018. Pathogen-derived HLA-E bound epitopes reveal broad primary anchor pocket tolerability and conformationally malleable peptide binding. Nat Commun 9: 3137.

52. Chun, T., C. J. Aldrich, M. E. Baldeon, L. V. Kawczynski, M. J. Soloski, and H. R. Gaskins. 1998. Constitutive and regulated expression of the class IB molecule Qa-1 in pancreatic beta cells. Immunology 94: 64-71.

53. Xu, H. C., J. Huang, A. A. Pandyra, E. Lang, Y. Zhuang, C. Thons, J. Timm, D. Haussinger, M. Colonna, H. Cantor, K. S. Lang, and P. A. Lang. 2017. Lymphocytes Negatively Regulate NK Cell Activity via Qa-1b following Viral Infection. Cell Rep 21: 2528-2540. Ferez, M., C. J. Knudson, A. Lev, E. B. Wong, P. Alves-Peixoto, L. Tang, C. Stotesbury, and L. J. Sigal. 2021. Viral infection modulates Qa-1b in infected and bystander cells to properly direct NK cell killing. J Exp Med 218.

CHAPTER 3

The NKG2A ligand Qdm/Qa-1^{b} is selectively displayed under inflammatory conditions and not in homeostasis.

Authors: Soroush Ghaffari[a], Susanne Gimlin[b], and Jon Weidanz[b,d,+]

Affiliations:

[a]Department of Biology, College of Science
The University of Texas at Arlington, TX, USA.

[b]Abexxa Biologics Inc. 500 S Cooper St, Arlington, TX, USA.

[d]College of Nursing and Health Innovation
The University of Texas at Arlington, Arlington, TX, USA

[+]Contact: Jon Weidanz
Email: weidanz @uta.edu,
College of Nursing and Health Innovation,
The University of Texas at Arlington, Arlington, TX, USA

ABSTRACT

The importance of the immune checkpoint inhibitors in the field of immuno-oncology implied a new era in cancer therapy. CD94/NKG2A is a heterodimer inhibitory complex that expressed on NK cells, in addition to and sub population of the T cells. Mouse CD94/NKG2A receptors specifically recognize Qa-1^b bound to the MHC class I-a leader sequence-derived peptide Qdm. Qdm is the dominant peptide loaded onto Qa-1^b under physiological conditions. Upon this interaction NKG2A positive cell will debilitate and won't be able to fight the malignancy. Therefore, inhibition of this immune checkpoints, which are the source of immune escape for various cancers, is one such immunotherapeutic dimension. Here, we have undertaken a comprehensive review to better understand the mode of action of our single domain antibody (EXX-1) as a checkpoint blockade for Qa-1^b/Qdm complex. Our results indicate that our antibody EXX-1 can recognized properly folded Qa-1^b complex only in the presence of the Qdm peptide.

INTRODUCTION

Field of cancer therapy has been revolutionized by the discovery of the immune checkpoint agents. These agents give the physicians, ability, and power to control the rapid growth of cancerous tissue. These agents known as immune checkpoint blockade (ICB).

Some of the examples of this therapeutic agents are monoclonal antibodies (mAbs) directed against the PD-1 (programmed-cell death protein 1)/PD-L1 (programmed-cell death ligand 1) that got FDA' approved for use in some tumor (1- 6). However, only proportion of the patient treated with them develop a strong response against their tumor. Therefore, identification of other potential biomarkers for development of new therapies is become many researcher goals now a day. Emerging lines of evidence also suggest that in many tumors' downregulation of the classical HLA class I molecules (7), are among many other reasons that tumor specific cytotoxic $CD8^+$ T lymphocytes are not able to attack the tumors. In the other word, loss of HLA class I expression on tumors is associated with poor outcomes of the malignancies (7- 16).

While majority of study conducted in the field of ICB focus on how to activate and stimulate $CD8^+$ T cells and thus marsh the strongest anti-tumor response, we realized that this narrative potentially underestimates the antitumor roles mediated by NK cells in response to 'immuno-edited' tumors.

Some research recently reported that by targeting on blocking NKG2A, we can unleash the suppressed naïve immunity and eventually recruits $CD8^+$ T cell to the tumor microenvironment (TME) (17, 18). NKG2A is an inhibiting receptor expressed on subsets of cytotoxic lymphocytes and engages the non-classical molecule HLAE (human) or Qa-1^b (mouse) (19, 20). Quick review of the human proteomic revealed that majority of human cells normally keep low level of HLAE expression. Although trophoblast cells in the placenta and ductal epithelial cells

in the testis and epididymis are considers as exception since they display high levels of HLAE expression. This will suggest that HLA-E might have a role in immune tolerance.

One the key factors in stabilization of the HLA-E protein on the cell surface are the availability of peptide ligands which is related to proper function of the antigen processing machinery of cells (12, 21). Moreover, these peptides are rather monomorphic and normally derive from the leader sequences of non-classical MHC class I proteins (named 'Qdm' in the mouse and 'VMAL' in humans).

Lee N and his team in 1998 showed that maximal expression of the HLA-E expression on the tumor cells through provision of Qdm or VMAL peptides (11), resulting inhibition of NKG2A-expressing cells and causes to cancer cells skip and evade immune system. Therefore, to better understand the mode of action of our antibody (EXX-1) we assessed the binding affinity in different conditions.

MATERIALS AND METHODS

Peptide Qdm (AMAPRTLLL), Q001 (AQAERTPEL, DENN domain containing protein 3), VMAL (VMAPRTLLL) and CMV (VMTPRTLVL) were synthesized by Genscript, USA.

Antibody specific for mouse Qa-1^b (6A8.6F10.1A6; cat#559828) was purchased from BD Pharmingen. Anti β_2M (B2M-0; cat#MA1-19141) was purchased from Invitrogen.

Purified anti-human HLAE antibody (3D12; cat#342602) was purchased from Biolegend.

Binding specificity of EXX-1 was also determined by ResoSens label-free bioassay system using Integrated ResoVu software was used for data acquisition and statistical analysis (Resonant Sensors Incorporated).

Production of Qa-1^b peptide monomers:

The extracellular domain of mouse Qa-1^b containing a C-terminus BirA peptide sequence for biotinylation and human β2M genes were cloned in pET21(+) vector purchased from Sigma-Aldrich and transformed into BL21(DE3) Escherichia coli (New England Biolabs). Proteins were produced, purified from inclusion bodies, and used in refolding reactions with synthesized peptides to produce Qa-1^b/peptide complex as described previously (22). The Qa-1^b/peptide mixture was concentrated, and correctly folded complex was isolated from impurities using size exclusion chromatography (SEC) and a Superdex 75 (S75) column (GE Healthcare Bio-Sciences AB). A portion of the purified refolded complex, designated as active monomer, was biotinylated using the BirA biotin ligase enzyme (Avidity) and purified a second time on the S75 column. Purified material (unbiotinylated and biotinylated) was analyzed by mass spectrometry to detect Qa-1^b heavy chain, β2M, peptide (indicating peptide loading) and the percentage of material that was biotinylated (for biotin-labeled molecules). All mass spectrometry work was performed at the Proteomics Core Lab at the University of Texas Southwestern Medical Center.

Affinity and binding specificity determined using label-free bioassay system:

The binding specificity of EXX-1 was determined using label-free technology (ResoSens instrument, Resonant Sensors, Incorporated).

Biotin label monomers with HLAE or Qa-1^b peptide complexes including: HLAE with VMAL, CMV, HLAE with no peptide and HLAE alone with no β2 microglobulin (β2M), Qa-1^b with

Qdm, Q-001, Qa-1^b with no peptide and Qa-1^b alone with no β2M diluted in dilution/wash buffer (0.1% BSA, 0.05% Tween-20) was immobilized on neutravidin coated Bionetic label-free microarray plate at 5 μg/mL until binding reached equilibrium. The plate was subsequently washed 2x with dilution/wash buffer (0.1% BSA, 0.05% Tween-20) in PBS). EXX-1, anti β2M, anti Qa-1^b clone 6A8 and anti HLAE antibody (2.5 μg/mL in dilution/wash buffer) and was loaded on immobilized biotinylated monomers until binding reached equilibrium. The plate was subsequently washed 2x in dilution/wash buffer followed by immediately incubated on reader for approximately 30 minutes. Binding specificity calculated using Tracedrawer kinetic analysis software.

RESULTS

EXX-1 specifically recognizes the Qa-1^b/Qdm complex

To understand the interaction mode between our antibody EXX-1 and its target antigen, we used label-free technology. First, we assess the binding specificity of the EXX-1 to recombinant mouse Qa-1^b (peptide MHC) loaded with its specific peptide Qdm, control peptide Q001, Qa-1^b with no peptide, and Qa-1^b heavy chain with no β2M. Based on the obtained data, EXX-1 is shown to be selective for the Qa-1^b /Qdm complex (Fig. 1C). In contrast, EXX-1 displayed little to no binding to control antigens, including Qa-1^b/Q001 and Qa-1^b no peptide and Qa-1^b heavy chain. On the other hand, anti-b2M antibody bound to Qa-1^b /Qdm, Qa-1^b /Q001, and Qa-1^b no peptide indicating the presence of b2M associated with Qa-1^b heavy chain. We used anti-Qa-1^b antibody (clone 6A8) as a positive control to demonstrate the presence of a Qa-1^b heavy chain in all complexes (Fig. 1A, 1B). However, we observed that clone 6A8 only shows binding to Qa-1^b with no peptide and Qa-1^b heavy chain while not showing any affinity for the other two antigens.

Next, to better dissect and compare the mode of action of EXX-1 and clone 6A8, we denatured the Qa-1^b/Qdm complex. For this purpose, we incubate the biotinylated monomer for 10 minutes at 60 ℃ and 37 ℃. Bionetic plates were then coated with 5 μg/mL of the denatured Qa-1^b /Qdm (60 ℃ and 37 ℃). Then the affinity of the anti-β2 M, EXX-1, and clone 6A8 antibody against immobilized denatured monomers were measured. We observed anti β2M shows binding to Qa-1^b/Qdm sample heated at 37 ℃ while losing its affinity for the sample heated to 60 ℃ (Fig. 2C). Lack of binding indicates, β2M and Qdm peptides were separated from the complex, and our protein is completely denatured.

On the other hand, we observed EXX-1 recognize its target antigen at 37 ℃ while losing its affinity for the samples heated at 60 ℃ (Fig. 2A). In contrast, clone 6A8 antibodies only recognized the fully denatured protein (60 ℃ heated samples- Fig. 2B). Taken together, our findings demonstrate that EXX-1 antibody binding is highly specific for folded Qa-1^b/Qdm monomer while clone 6A8 has an opposite mode of action and only recognizes the denatured peptide MHC complex and Qa-1^b heavy chain samples.

Anti-human HLAE clone 3D12 shows the same pattern as clone 6A8 and binds to HLAE protein regardless of the presence or absence of the peptide (Fig. 3B).

DISCUSSION

Multiple reports, including research published previously by our team, have described TCRm like antibodies and their potential as novel research tools or therapeutic modules (23- 27). TCRm like antibodies are generally known for their high affinity and target selectivity. Due to this characteristic, these antibodies have been widely used to detect peptide-loaded Major Histocompatibility Complexes (pMHC) on the cell surface. Also, they have the potential to be

used to further our understanding of antigen presentation and regulation of pMHC complex expression (28- 30). However, one of the major challenges of these antibodies is their tendency to exhibit binding modes focused towards hot spots on the HLA surface that can lead to a greater degree of cross-reactivity (31).This short report unveiled the novel characteristics of our newly discovered single domain antibody EXX-1 and its mode of action against target antigen Qa-1^b/Qdm peptide MHC complex.

Earlier research conducted by Drs. Forman, Soloski, and his team indicate that Qdm peptide (AMAPRTLLL) is a dominant peptide expressed by the Qa-1^b heavy chain in mouse tumor cells. Therefore, to understand the roles of Qa-1^b, they develop a CTL clone specific for Qa-1^b/Qdm complex known as anti-mouse Qa-1^b clone 6A8 (7, 12). They reported that their antibody is specific for Qa-1^b/Qdm complex and able to recognize Qa-1^{b+} /H-$2d^+$ target cells but not Qa-1^{b+}/H-$2k^+$ target cells (12).

We used clone 6A8 to detect the presence or absence of the Qa1^b heavy chain in our assays. Moreover, we used it to have a positive control for our newly discovered EXX-1.

Based on the data presented in this report regarding EXX-1 and its mode of action, we realized that our antibody is specific for Qdm peptide presented by Qa-1^b complex and has selectivity to correctly folded protein. At the same time, clone 6A8 only binds to denatured protein and most likely the Qa-1^b heavy chain. This newly discovered feature makes EXX-1 a uniquely selective research tool for pursuing studies into the biology and function of mouse non classical HLA (Qa-1^b/Qdm) complex.

The human ortholog of Qa-1^b, known as HLAE, presents VL9 peptides (VMALPTRLLL) that serve as the ligand for the NKG2A/CD94 inhibitory receptor. Like Qa-1^b/Qdm complex, HLA-E/VL9 peptide expression in healthy cells is speculated and hypothesized to protect against lysis

from NK cells and a subset of CD8+ T-cells (9, 32, 33). Thus, to compare this common checkpoint pathway between humans and mice, we evaluated the binding affinity of the commercially available anti human HLAE (clone 3D12). Obtained data shows that 3D12 exhibits binding modes focused towards hot spots on the HLAE surface that can lead to a greater degree of cross-reactivity. In other word, 3D12 antibody has an affinity for HLAE independent of the presence or absence of the peptide in the complex. Therefore, our exciting discovery about EXX-1 and its mode of action can potentially have a translational application in human HLAE and the benefit that HLAE checkpoint blockade antibodies could bring to treat human cancers.

FIGURES

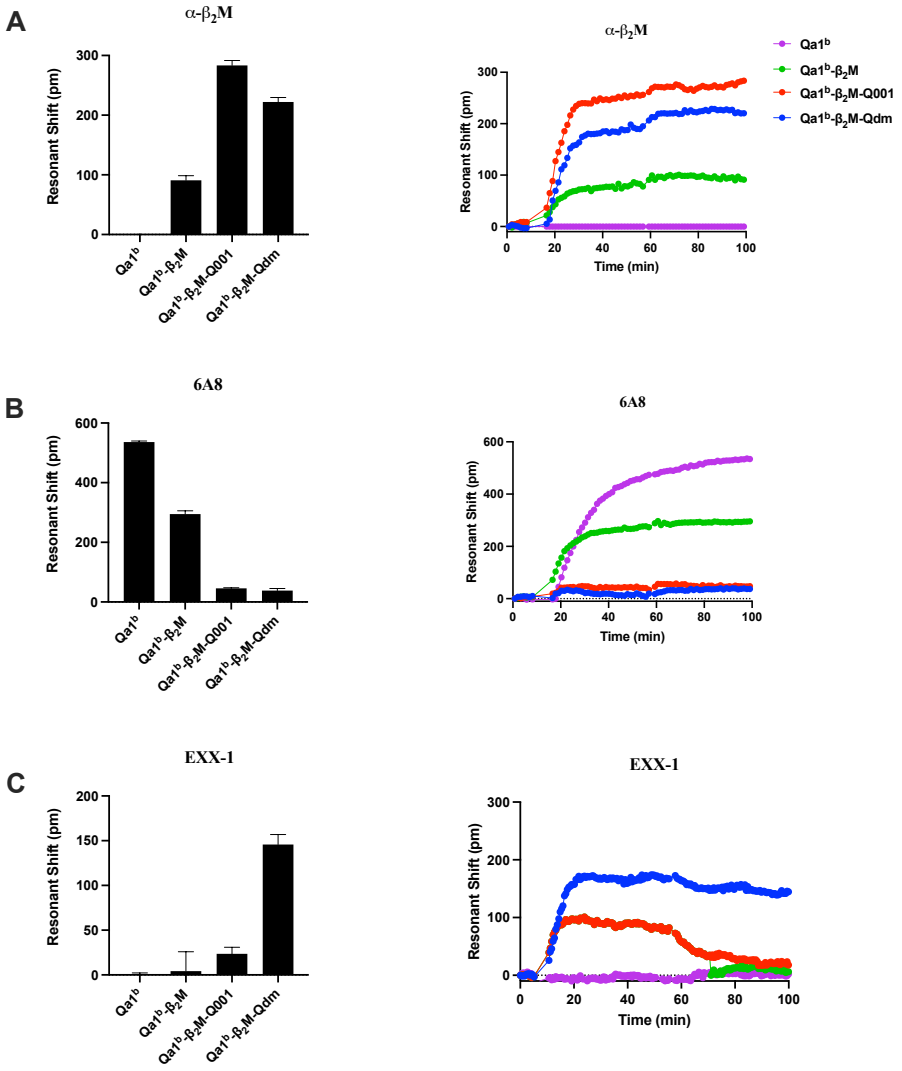

Chapter 3 1: EXX-1 specifically recognizes the Qdm peptide present by the Qa-1^b complex.

EXX-1 mAb affinity tested against immobilized Qa-1^b loaded with specific peptide Qdm, negative control peptide Q001, Qa-1^b with no peptide, and Qa-1^b heavy chain. Anti-β2M and anti-Qa-1^b were used for the detection of the β2M and Qa-1^b associated with monomers, respectively. Graphs shows (A) anti-β2M, (B) anti-Qa-1^b, and (C) EXX-1 mAb affinity to immobilized monomers. Each sample ran as triplicated. The data presented are the pooled results of three independent experiments.

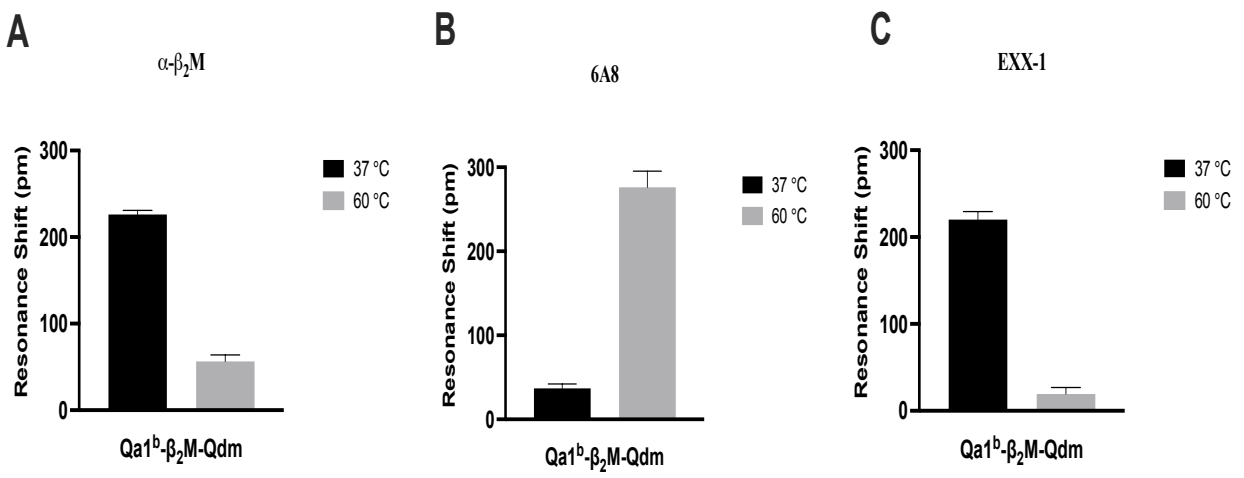

Chapter 3 2: Comparison of the EXX-1 vs. anti-Qa-1^b affinity to Qa-1^b/Qdm complex.

EXX-1 binding affinity was measured against the Qa-1^b/Qdm protein complex incubated at 60℃ (denatured) and 37℃ for 10 minutes. Anti-β2M and anti-Qa-1^b were used for the detection of the β2M and Qa-1^b associated with monomers, respectively. Graphs show the binding affinity of (A) anti β2M, (b) anti-Qa-1^b clone 6A8, and (C) EXX-1 to the 37 ℃ and 60 ℃ heated Qa1^b/Qdm complexes.

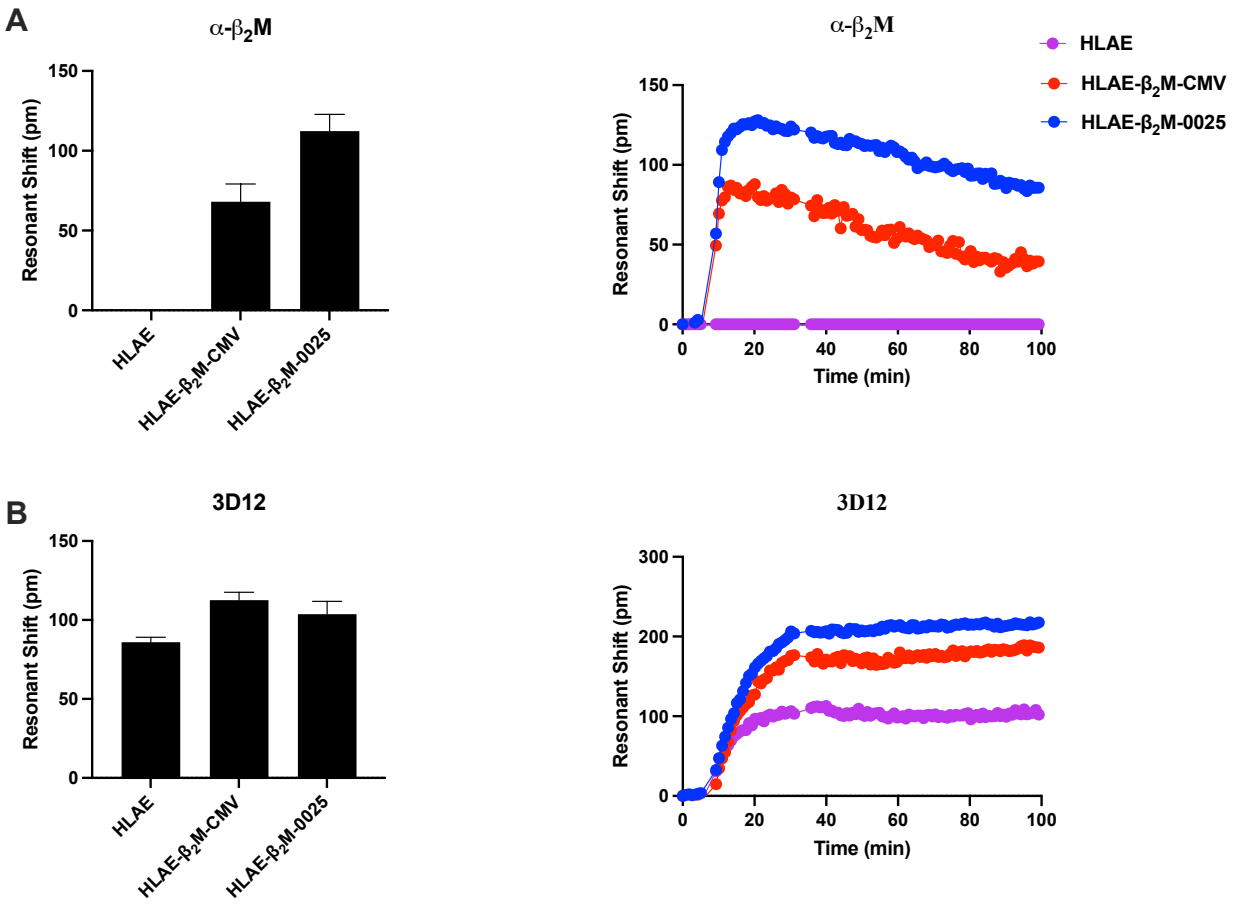

Chapter 3 3: Anti Human HLAE (clone 3D12) affinity to the peptide loaded HLAE.

3D12 mAb affinity tested against immobilized HLAE loaded with specific peptide V9, negative control peptide CMV and HLAE heavy chain. Anti-β2M were used for the detection of the β2M associated with monomers. Graphs shows (A) anti-β2M and (B) 3D12 mAb affinity to immobilized monomers. Each sample ran as triplicated.

REFERENCES

1. Borst, L., S. H. van der Burg, and T. van Hall. 2020. The NKG2A-HLA-E Axis as a Novel Checkpoint in the Tumor Microenvironment. Clin Cancer Res 26: 5549-5556.
2. van Hall, T., P. Andre, A. Horowitz, D. F. Ruan, L. Borst, R. Zerbib, E. Narni-Mancinelli, S. H. van der Burg, and E. Vivier. 2019. Monalizumab: inhibiting the novel immune checkpoint NKG2A. J Immunother Cancer 7: 263.
3. Andre, P., C. Denis, C. Soulas, C. Bourbon-Caillet, J. Lopez, T. Arnoux, M. Blery, C. Bonnafous, L. Gauthier, A. Morel, B. Rossi, R. Remark, V. Breso, E. Bonnet, G. Habif, S. Guia, A. I. Lalanne, C. Hoffmann, O. Lantz, J. Fayette, A. Boyer-Chammard, R. Zerbib, P. Dodion, H. Ghadially, M. Jure-Kunkel, Y. Morel, R. Herbst, E. Narni-Mancinelli, R. B. Cohen, and E. Vivier. 2018. Anti-NKG2A mAb Is a Checkpoint Inhibitor that Promotes Anti-tumor Immunity by Unleashing Both T and NK Cells. Cell 175: 1731-1743 e1713.
4. Van Montfoort, N., L. Borst, M. J. Korrer, M. Sluijter, K. A. Marijt, S. J. Santegoets, V. J. van Ham, I. Ehsan, P. Charoentong, P. Andre, N. Wagtmann, M. J. P. Welters, Y. J. Kim, S. J. Piersma, S. H. van der Burg, and T. van Hall. 2018. NKG2A Blockade Potentiates CD8 T Cell Immunity Induced by Cancer Vaccines. Cell 175: 1744-1755 e1715.
5. Imani, F., and M. J. Soloski. 1991. Heat shock proteins can regulate expression of the Tla region-encoded class Ib molecule Qa-1. Proc Natl Acad Sci U S A 88: 10475-10479.
6. Ohtsuka, M., H. Inoko, J. K. Kulski, and S. Yoshimura. 2008. Major histocompatibility complex (Mhc) class Ib gene duplications, organization and expression patterns in mouse strain C57BL/6. BMC Genomics 9: 178.

7. Kambayashi, T., J. R. Kraft-Leavy, J. G. Dauner, B. A. Sullivan, 1 O. Laur, and P. E. Jensen. 2004. The nonclassical MHC class I molecule Qa-1 forms unstable peptide complexes. J Immunol 172: 1661-1669.
8. Salcedo, M., P. Bousso, H. G. Ljunggren, P. Kourilsky, and J. P. Abastado. 1998. The Qa-1b molecule binds to a large subpopulation of murine NK cells. Eur J Immunol 28: 4356-4361.
9. Braud, V. M., D. S. Allan, C. A. O'Callaghan, K. Soderstrom, A. D'Andrea, G. S. Ogg, S. Lazetic, N. T. Young, J. I. Bell, J. H. Phillips, L. L. Lanier, and A. J. McMichael. 1998. HLA-E binds to natural killer cell receptors CD94/NKG2A, B and C. Nature 391: 795- 799.
10. Zeng, L., L. C. Sullivan, J. P. Vivian, N. G. Walpole, C. M. Harpur, J. Rossjohn, C. S. Clements, and A. G. Brooks. 2012. A structural basis for antigen presentation by the MHC class Ib molecule, Qa-1b. J Immunol 188: 302-310.
11. Lee, N., D. R. Goodlett, A. Ishitani, H. Marquardt, and D. E. Geraghty. 1998. HLA-E surface expression depends on binding of TAP-dependent peptides derived from certain HLA class I signal sequences. J Immunol 160: 4951-4960.
12. Aldrich, C. J., A. DeCloux, A. S. Woods, R. J. Cotter, M. J. Soloski, and J. Forman. 1994. Identification of a Tap-dependent leader peptide recognized by alloreactive T cells specific for a class Ib antigen. Cell 79: 649-658
13. Doorduijn, E. M., M. Sluijter, B. J. Querido, U. J. E. Seidel, C. C. Oliveira, S. H. van der Burg, and T. van Hall. 2018. T Cells Engaging the Conserved MHC Class Ib Molecule Qa-1(b) with TAP-Independent Peptides Are Semi-Invariant Lymphocytes. Front Immunol 9: 60.

14. Chen, Y., Z. Xin, L. Huang, L. Zhao, S. Wang, J. Cheng, P. Wu, and Y. Chai. 2019. CD8(+) T Cells Form the Predominant Subset of NKG2A(+) Cells in Human Lung Cancer. Front Immunol 10: 3002.

15. Abd Hamid, M., R. Z. Wang, X. Yao, P. Fan, X. Li, X. M. Chang, Y. Feng, S. Jones, D. Maldonado-Perez, C. Waugh, C. Verrill, A. Simmons, V. Cerundolo, A. McMichael, C. Conlon, X. Wang, Y. Peng, and T. Dong. 2019. Enriched HLA-E and CD94/NKG2A Interaction Limits Antitumor CD8(+) Tumor-Infiltrating T Lymphocyte Responses. Cancer Immunol Res 7: 1293-1306.

16. Zhou, J., M. Matsuoka, H. Cantor, R. Homer, and R. I. Enelow. 2008. Cutting edge: engagement of NKG2A on CD8+ effector T cells limits immunopathology in influenza pneumonia. J Immunol 180: 25-29.

17. Andre P, Denis C, Soulas C, Bourbon-Caillet C, Lopez J, Arnoux T, Blery M, Bonnafous C, Gauthier L, Morel A, et al. Anti-NKG2A mAb is a checkpoint inhibitor that promotes anti-tumor immunity by unleashing both T and NK cells. Cell. 2018;175(7):1731–1743. doi: 10.1016/j.cell.2018.10.014.

18. Braud VM, Allan DS, O'Callaghan CA, Soderstrom K, D'Andrea A, Ogg GS, Lazetic S, Young NT, Bell JI, Phillips JH, et al. HLA-E binds to natural killer cell receptors CD94/NKG2A, B and C. Nature. 1998;391:795–799. doi: 10.1038/35869.

19. Braud VM, Allan DS, O'Callaghan CA, Soderstrom K, D'Andrea A, Ogg GS, Lazetic S, Young NT, Bell JI, Phillips JH, et al. HLA-E binds to natural killer cell receptors CD94/NKG2A, B and C. Nature. 1998;391:795–799. doi: 10.1038/35869

20. Le Drean E, Vely F, Olcese L, Cambiaggi A, Guia S, Krystal G, Gervois N, Moretta A, Jotereau F, Vivier E. Inhibition of antigen-induced T cell response and antibody-induced NK

cell cytotoxicity by NKG2A: association of NKG2A with SHP-1 and SHP-2 protein-tyrosine phosphatases. Eur J Immunol. 1998;28(1):264–276. doi: 10.1002/(SICI)1521-4141(199801)28:01<264::AID-IMMU264>3.0.CO;2-O

21. van Hall T, Oliveira CC, Joosten SA, Ottenhoff TH. The other Janus face of Qa-1 and HLA-E: diverse peptide repertoires in times of stress. Microbes Infect. 2010;12(12–13):910–918. doi: 10.1016/j.micinf.2010.07.011
22. Kuball, J., B. Hauptrock, V. Malina, E. Antunes, R. H. Voss, M. Wolfl, R. Strong, M. Theobald, and P. D. Greenberg. 2009. Increasing functional avidity of TCR-redirected T cells by removing defined N-glycosylation sites in the TCR constant domain. J Exp Med 18 206: 463-475.
23. Dahan, R., and Y. Reiter. 2012. T-cell-receptor-like antibodies - generation, function and applications. Expert Rev Mol Med 14: e6.
24. Neethling, F. A., V. Ramakrishna, T. Keler, R. Buchli, T. Woodburn, and J. A. Weidanz. 2008. Assessing vaccine potency using TCRmimic antibodies. Vaccine 26: 3092-3102.
25. Kaabinejadian, S., C. P. McMurtrey, S. Kim, R. Jain, W. Bardet, F. B. Schafer, J. L. Davenport, A. D. Martin, M. S. Diamond, J. A. Weidanz, T. H. Hansen, and W. H. Hildebrand. 2016. Immunodominant West Nile Virus T Cell Epitopes Are Fewer in Number and Fashionably Late. J Immunol 196: 4263-4273.
26. Patterson, A. M., S. Kaabinejadian, C. P. McMurtrey, W. Bardet, K. W. Jackson, R. E. Zuna, S. Husain, G. P. Adams, G. MacDonald, R. L. Dillon, H. Ames, R. Buchli, O. E. Hawkins, J. A. Weidanz, and W. H. Hildebrand. 2016. Human Leukocyte Antigen- Presented Macrophage Migration Inhibitory Factor Is a Surface Biomarker and Potential Therapeutic Target for Ovarian Cancer. Mol Cancer Ther 15: 313-322.

27. Weidanz, J. A., T. Nguyen, T. Woodburn, F. A. Neethling, M. Chiriva-Internati, W. H. Hildebrand, and J. Lustgarten. 2006. Levels of specific peptide-HLA class I complex

28. Zehn, D., C. J. Cohen, Y. Reiter, and P. Walden. 2004. Extended presentation of specific MHC-peptide complexes by mature dendritic cells compared to other types of antigen presenting cells. Eur J Immunol 34: 1551-1560.

29. Weidanz, J. A., P. Piazza, H. Hickman-Miller, D. Woodburn, T. Nguyen, A. Wahl, F. Neethling, M. Chiriva-Internati, C. R. Rinaldo, and W. H. Hildebrand. 2007. Development and implementation of a direct detection, quantitation and validation 1 system for class I MHC self-peptide epitopes. J Immunol Methods 318: 47

30. Kaabinejadian, S., C. P. McMurtrey, S. Kim, R. Jain, W. Bardet, F. B. Schafer, J. L. Davenport, A. D. Martin, M. S. Diamond, J. A. Weidanz, T. H. Hansen, and W. H. Hildebrand. 2016. Immunodominant West Nile Virus T Cell Epitopes Are Fewer in Number and Fashionably Late. J Immunol 196: 4263-4273.

31. Holland, C. J., R. M. Crean, J. M. Pentier, B. de Wet, A. Lloyd, V. Srikannathasan, N. Lissin, K. A. Lloyd, T. H. Blicher, P. J. Conroy, M. Hock, R. J. Pengelly, T. E. Spinner, B. Cameron, E. A. Potter, A. Jeyanthan, P. E. Molloy, M. Sami, M. Aleksic, N. Liddy, R. A. Robinson, S. Harper, M. Lepore, C. R. Pudney, M. W. van der Kamp, P. J. Rizkallah, B. K. Jakobsen, A. Vuidepot, and D. K. Cole. 2020. Specificity of bispecific T cell receptors and antibodies targeting peptide-HLA. J Clin Invest 130: 2673-2688.

32. Lee, N., M. Llano, M. Carretero, A. Ishitani, F. Navarro, M. Lopez-Botet, and D. E. Geraghty. 1998. HLA-E is a major ligand for the natural killer inhibitory receptor CD94/NKG2A. Proc Natl Acad Sci U S A 95: 5199-5204.

33. Walters, L. C., K. Harlos, S. Brackenridge, D. Rozbesky, J. R. Barrett, V. Jain, T. S. Walter, C. A. O'Callaghan, P. Borrow, M. Toebes, S. G. Hansen, J. B. Sacha, S. Abdulhaqq, J. M. Greene, K. Fruh, E. Marshall, L. J. Picker, E. Y. Jones, A. J. McMichael, and G. M. Gillespie. 2018. Pathogen-derived HLA-E bound epitopes reveal broad primary anchor pocket tolerability and conformationally malleable peptide binding. Nat Commun 9: 3137.

CHAPTER 4

Cancer vaccines used in combination with TCR-like antibody blockade of the Qa-1^{b}/Qdm complex, the ligand for the immune checkpoint NKG2A, induce anti-tumor immunity

Authors: Soroush Ghaffari[1], Katherine Upchurch-Ange[2], Gizem Oter[2] and Jon Weidanz[2,3,*]

Affiliations:

[1]Department of Biology, College of Science

The University of Texas at Arlington, TX, USA.

[2]Abexxa Biologics Inc. 500 S Cooper St, Arlington, TX, USA.

[3]College of Nursing and Health Innovation

The University of Texas at Arlington, Arlington, TX, USA

*** Correspondence:**
Jon Weidanz
Email: weidanz @uta.edu

College of Nursing and Health Innovation,

The University of Texas at Arlington, Arlington, TX, USA

ABSTRACT

Immune checkpoint blockade antibodies have revolutionized the field of immuno-oncology for the last decade. Anti CTLA-4 and anti-PD-1 are among the first cancer checkpoint immunotherapies that got FDA approval to treat certain malignancies. However, not everyone can benefit from them due to the insufficient expression of the checkpoint marker on their cells. Thus, the response generated against them is not enough, and cancer can skip the immune system.

Since then, scientists have tried to identify new checkpoints modules that can be used by themselves or in combination with other therapeutic regimens. CD94/NKG2A receptor is another inhibitory marker expressed naturally by natural killer cells (NK) and sub-population of CD8+ T cells (NKT). NKG2A will recognize and bind to specific peptide-loaded by Qa-1^b (mouse) or HLAE (human). On the other hand, Qa-1^b can be expressed on the surface of tumor cells, immune infiltrating lymphocytes, and myeloid cells. Interaction between NKG2A/Qa-1^b or HLAE will lead to suppression of the immune cells.

EXX-1 is a single domain TCR-like antibody designed by our team to be specific for Qdm peptide-loaded in the Qa-1^b complex. In this study, we used EXX-1 antibody fused with engineered silenced Fc-fragment (LALA mutation). We evaluated its anti-tumor properties as a single-agent therapy in A20 tumor models. Our findings show that treatment of A20 tumor-bearing mice with EXX-1 Fc silenced (ES) antibody causes suppression in tumor growth while didn't lead to tumor regression.

To enhance the efficacy of our therapy, we combine cancer vaccine with EXX-1 in A20 and TC-1 tumor models. Our results show that the vaccine combination with EXX-1 (ES) antibody in A20 tumor-bearing mice reinvigorate tumor rejection response and eventually leads to tumor-

free survival in 35% of mice. In contrast, isotype control-treated mice had 0% tumor-free survival. These findings indicate that cancer vaccines might improve clinical responses to therapeutic HLAE/Qa-1^b blocking antibodies.

Key Words: Cancer vaccine, checkpoint blockade, TCR like antibody, Qa-1^b/HLAE blockade.

Highlights:

- Qa-1^b/HLAE interaction with NKG2A, suppress both NK and T cell effector function.
- Combined blocking of Qa-1^b/HLAE with cancer vaccine promote anti-tumor immunity.

INTRODUCTION

The idea to deploy the immune system to eliminate tumor cells was first proposed in the 19th century by Friedrich Fehleisen, Wilhelm Busch, and William B Coley (1). These three scientists described a potential link between the host immune system and control of malignant cells and in the case of Coley, used bacteria to induce inflammation to fight cancer (2). Since those early days, remarkable advances have ensued using antibodies to block inhibitory immune checkpoint pathways used by tumor cells to suppress immune cells. Best known and clinically relevant inhibitory molecules targeted with blocking antibodies are Cytotoxic T lymphocyte antigen-4 (CTLA-4) and Programmed cell death protein 1 (PD-1) immune checkpoints. Use of blocking antibodies to disrupt these inhibitory pathways have led to T-cell mediated anti-tumor responses and to objective responses in some patients with certain types of malignancies including metastatic melanoma, non-small-cell lung cancer, kidney cancer, bladder cancer, Hodgkin lymphoma (3-7). However, widespread application of immune checkpoint blockade (ICB) therapy for cancer patients has been limited and there is enormous need to understand the mechanisms of acquired resistance (8, 9), optimal strategies for combination uses of ICBs (9) and identifying additional inhibitory immune checkpoints that might be blocked to yield clinical benefit (10).

A recently described new immune checkpoint is the CD94/NK group 2 member A (NKG2A) axis. The ligand for the NKG2A axis is the non-classical Major Histocompatibility Complex (MHC) class I molecule Qa-1^b loaded with a leader sequence peptide, AMAPRTLLL derived from MHC class I Db and Kb. The peptide is also known as Qa-1 determinant modifier (Qdm). Several recent studies have shown blockade of the NKG2A axis using monoclonal antibodies to either mouse or human NKG2A receptor resulted in tumor growth inhibition and survival benefit

(12). Our team previously reported discovery of a single-domain T-cell receptor-like (TCR-L) antibody, EXX-1 that displayed high selectivity for the Qa-1^b/Qdm peptide complex (12). Additionally, our group showed EXX-1 antibody blockade of the NKG2A axis in vitro enhanced NK lysis of cancer cells (12).

Therapeutic cancer vaccines represent another modality for immunotherapy (13, 14). The rationale behind this modality is to boost the immune system via actively priming T-cells to respond to tumor neo-antigens to mediate tumor clearance. Developing a therapeutic cancer vaccine has faced many challenges with encouraging results observed in preclinical studies that did not translate into the clinic (15). To date the Food and Drug Administration (FDA) has only approved one therapeutic vaccine, sipuleucel-T, that is used to treat metastatic castration-resistant prostate cancer in a limited group of nearly asymptomatic patients (16). The disappointing results from vaccine trials has led to evaluating therapeutic vaccines in combination with ICB's to attempt induction of potent anti-tumor immune response (17). Recently, van Montfoort et al., showed therapeutic benefit in murine tumor models of cancer vaccines when used in combination with an anti-NKG2A blocking antibody. In contrast, the cancer vaccine alone had little effect on tumor growth inhibition or improving survival time (18). These findings suggest therapeutic cancer vaccines could potentially be made efficacious for cancer patients when used in combination with an ICB and more specifically, blockade of the NKG2A axis.

In the current study, we tested the hypothesis that blocking the NKG2A ligand, Qa-1^b/Qdm peptide complex using a TCR-like antibody would convert an ineffective therapeutic cancer vaccine into one that is effective at inducing anti-tumor responses. We show therapeutic cancer vaccine candidates are only efficacious when combined with EXX-1 antibody, or blockade of the

NKG2A axis, in two different murine tumor models. Our results are consistent with previous findings demonstrating antibody blockade of the NKG2A receptor resulted in converting ineffective therapeutic cancer vaccine candidates into potent induces of anti-tumor immunity in mouse tumor models (18).

METHOD AND MATERAILS

Antibodies and reagents

Antibodies specific for anti-mouse CD4-AF700 (RMA4-5 cat#100528), CD8-APC Cy7(53-6.7-cat#110714), NKp46-PE Cy7 (29A1.4; cat#137617), SA-APC (405204), CD44-BV421(IM7-103040), F4/80- PE Cy5 (BM8-cat#123112), CD62L- FITC (MEL-14,cat#104406), IL10-APC (JES5-16E3- cat# 505009), TNF-α-APC Cy7 (MP6-XT22- cat# 560658), granzyme B-PE Cy7 (QA16A02- cat# 372214), IFN-γ- PE Dazzle^{TM} 594 (XMG1.2- cat# 505846), Aqua Fixable Viability Kit (cat#423101/423102), TrueStain FcX plus (cat#156604), FluoroFix buffer (cat#422101) and RBC lysis buffer (cat#420302) were purchased from BioLegend. Anti-mouse CD3-PerCP Cy5.5, (17A2, cat 65002) was purchased from Tonbo Bioscience. SA-PE (cat#12-4317-87) was purchased from eBioscience. Anti-mouse Fc gamma RI/CD64 (cat#29741), mouse recombinant M-CSF (cat# 416-ML-050/CF), mouse recombinant IL-4 (cat# 404-ML-050/CF), recombinant mouse IFN-γ (cat# 485-MI-100/CF) and mouse recombinant GM-CSF (cat# 415-ML-020/CF) were purchased from R&D Systems. CpG ODN 1826 (cat#. tlrl-1826) was purchased from Invivogen. Pre-separation filter,70 μm (cat#130-095-823) and anti-mouse NKG2A/C/E-PE (20d5; cat#130-105-620) were purchased from Miltenyi Biotec. Antibodies specific for anti-mouse CD3-BV421 (17A2; cat#555276), biotin-labeled anti-mouse Qa-1^{b} (6A8.6F10.1A6; cat#559829), anti-mouse Qa-1^{b}-PE (6A8.6F10.1A6; cat#566640) ,GlogiPlug^{TM}

(cat#555029), Incomplete Freunds Adjuvant (cat#263910), Perm/Wash buffer (Cat#554723) and Perm/Fix buffer (cat#554714) were purchased from BD Pharmingen. AffiniPure Goat Anti-Human (GAH) IgG, Fcγ fragment specific-PE (cat#109-115-098) , AffiniPure Goat Anti-Mouse (GAM) IgG (subclasses 1+2a+2b+3)-PE (cat#115-115-164), AffiniPure Goat Anti-Human (GAH) IgG, Fcγ fragment specific-APC (cat#115-135-164) and AffiniPure Goat Anti-Mouse (GAM) IgG (subclasses 1+2a+2b+3)-APC (cat#115-135-164) were purchased from Jackson Immuno Research. CellTrace CFSE Cell Proliferation kit (cat#C34554) was purchased from Thermofisher. Matrigel matrix was purchased from Corning (cat#354248). Peptides Fluc1 (GFQSMYTFV), Fluc2 (VALPHRTAC), Fluc3 (VPFHHGFGM) were synthesized by GenScript USA. Peptide HPV16 E743–77 (GQAEPDRAHYNIVTFCCKCDSTLRLCVQSTHVDIR) was synthesized by IHB facility at the LUMC university.

Software and algorithms

GraphPad Prisem V9 (graphpad, http://www.graphpad.com/ scientific-software/prism;RRID: SCR_002798), FlowJo v10.8.1(https://www.flowjo.com/solutions/ flowjo; RRID: SCR_008520) were used for the analysis of data presented in this manuscript.

Mice

BALB/c mice were purchased from Jackson Laboratories. 57BL/6 mice were purchased from Charles River Laboratories (L'Arbresle, France). All mice were purchased under specific pathogen-free conditions. Female mice were used at 6 to 18 weeks of age and were allowed to acclimate to the housing facility for at least one week prior to experiments. All animal

experiments were performed in accordance with the rules of the UTA or LUMC ethics and animal welfare committees (IACUC).

Mouse tumor Cell lines

A20 murine lymphoma cell line was purchased from the Imanis Life Science Collection (Imanis-CL152-STAN). Parental A20 cells were transduced with 1) LV-Fluc-P2A-Neo (Imanis #LV067) encoding the enhanced green fluorescent (eGFP) cDNA under the spleen focus-forming virus (SFFV) promoter and linked to the neomycin resistance gene (Neo) via a P2A cleavage peptide and 2) LV-Fluc-P2A-Puro (Imanis #LV012) encoding the firefly luciferase (Fluc) cDNA under the SFFV promoter and linked to the puromycin resistance gene (Puro) via a P2A cleavage peptide.

A20 cells cultured in RPMI-1640 medium (RPMI-hyclone; GE biosience) supplemented with 10% heat inactivated FBS (GE-bioscience), 2% glutamine and penicillin/streptomycin (gibco), and 50 μM β- mercaptoethanol (sigma) (complete medium) at 37℃ in a humidified atmosphere containing 5% CO_2. To maintain the expression of the Fluc and GFP genes, 1 mg/mL geneticin (G418) and 1 μg/mL puromycin were added to the culturing media one week after cell line growth was stabilized.

The tumor cell line TC-1 expresses the HPV16-derived oncogenes E6 and E7 and activated Ras oncogene and were a gift from T.C. Wu (John Hopkins University, Baltimore, USA). Cells were culture in Iscove's modified Dulbecco's medium (IMDM; Invitrogen) supplemented with 8% FBS (gibco), 2% glutamine and penicillin/streptomycin (gibco) (complete medium) at 37℃ in a humidified atmosphere containing 5% CO_2.

All cell lines were assured to be free of rodent viruses and Mycoplasma by regular PCR analysis. TC-1 authentication was done by antigen-specific T cell recognition and cells of low passage number were used for all experiments.

Generation of bone marrow derived DCs (BMDCs) and bone marrow derived macrophage (BMDM)

Bone marrow derived DCs (BMDC) were generated from tibias and femurs of the mice under the sterile conditions. Red blood cells were lysed after 5 min of incubation of harvested cells on ice with RBC Lysis Buffer and then washed with RPMI 1640 medium. Cells were then cultured in presence of recombinant mouse cytokine GM-CSF (20 ng/ml) in RPMI-Hyclone supplemented with 10% heat-inactivated FBS, 2% glutamine and penicillin/streptomycin at 37°C in a humidified atmosphere containing 5% CO_2. Half of the culture medium was replaced every other day (day 2, 4, 6) to remove the unattached cells and cell debris, then replaced with the fresh medium supplemented with 20 ng/ml GM-CSF. On day 6, culture medium was additionally supplemented with 20 ng/mL of CpG ODN 1826 (InvivoGen). On day 7, CpG matured BMDCs were pulsed with 50 μg of each fluc peptide (Fluc1: GFQSMYTFV, Fluc2: VALPHRTAC, Fluc3: VPFHHGFGM) (19) for 3 hours at 37°C in humidified atmosphere containing 5% CO_2. After 3 hours, all peptide-pulsed BMDC were harvested, washed, and resuspended in PBS+0.1%BSA to be injected in mice or used for in-vitro assays.

For generation of the BMDM, mice bone marrow harvested as explained before. Harvested monocytes were then cultured in presence of recombinant mouse cytokine M-CSF (50 ng/ml) in DMEM-F12 (gibco) supplemented with 10% heat-inactivated FBS, 2% glutamine and penicillin/streptomycin at 37°C in a humidified atmosphere containing 5% CO_2. Half of the

culture medium was replaced every other day (day 2, 4, 6) to remove the unattached cells and cell debris, then replaced with the fresh medium supplemented with 50 ng/ml M-CSF. On day 6, culture medium was additionally supplemented with 20 ng/mL of IFN-γ and 100 ng/mL of LPS (sigma) for generation of M1 or 20 ng/mL of IL-4 for generation of M2. On day 7 matured Mϕ, M1, and M2 cells were harvested, washed, and resuspended in PBS+0.1% BSA prior to FACS staining.

Mouse tumor models

For tumor inoculation, $1x10^5$ TC-1 and $5x10^6$ A20, tumor cells were injected subcutaneous (s.c.) in the flank of C57BL6 and BalbC mice respectively. Tumor cells were resuspended in 100 µL PBS+0.1% BSA mixed with 100 µL Matrigel® matrix prior to inoculation. Tumors were measured three times a week with a digital caliper and the size is expressed as a volume ((length x $width^2$)/2). When a palpable tumor was present, mice were split (randomized) into groups and were treated with immunotherapy. Mice were sacrificed when tumors reached a volume of 1500 mm^3. For the purposes of Kaplan-Meier curves, mice were considered dead when tumor volume exceeded 1000 mm^3.

EXX-1 blocking antibody and isotype control was produced by ATUM (Newark, California) and is engineered with mouse IgG2a LALA mutation. Treatments with checkpoint blockade antibodies in A20 model were initiated when tumor volumes were between 150 and 200 mm^3. Antibodies were administered intraperitoneal (i.p.) at a dose of 200 µg/mice (diluted in 1X PBS) on days 9, 11, 13, 15, 17 and 19 post-transplantations.

For the DC vaccination studies, mice bearing A20 tumors were treated with two vaccinations on days 9 and 18 post-transplantations with peptide pulsed CpG matured BMDC. BMDCs were

injected intravenous (i.v). and peritumoral (p.t.) in 200 µL per mice (100 µL i.v. and 100 µL i.p.). Antibodies administered i.p. at 200 µg/mice (diluted in 1X PBS) on days 11, 13, 15, 17, 19 and 21 post-transplantations.

For TC-1 model, tumors bearing mice were treated by peptide vaccine on day 8 after tumor inoculation. 150 mg of the HPV16 E743–77 peptide, emulsified at a 1:1 ratio with Incomplete Freunds Adjuvant (IFA; Difco), injected s.c. in the contralateral flank (13). Antibodies were administered at a dose of 200 µg/ mice (diluted in 1X PBS) i.p. on days 11, 14 ,18, 21, 24 and 29 post tumoral injection. Vaccine-induced T cell responses were measured by intracellular cytokine staining (ICS) and flow cytometry. Peripheral blood lymphocyte (PBL) samples were collected 6 days after vaccination and incubated overnight with the short HPV16 E749–57 peptide in the presence of 1 mg/ml GolgiPlug^{TM}.

Flow cytometry analysis of tumor-infiltrating mouse lymphocytes (TILs) & Tumor associated macrophages (TAM)

Tumors were dissected into small pieces and digested with enzymes A and D from the Mouse Tumor Dissociation Kit (Miltenyi Biotec) and program: m_implant_tumor_2 of the GentleMACS Dissociator (Miltenyi Biotec). Tumors were incubated at 37 °C for 30 minutes to achieved enzymatic digestion. Digested tumors were then filtered through a 70 mm-pore size MACS Smart Strainer (Miltenyi Biotec) and washed with RPMI 1640+10% FBS medium. For A20 tumors, this step was followed by another purification using Dead Cell Removal Kit (Miltenyi Biotec). 1x10^6 cells/well were used for staining and blocked with 2.5 µg mouse Fc gamma RI/CD64 antibody and 5 µg anti-mouse CD16/CD32 antibody at 4°C for 15 min. 1µg/ml EXX-1 or isotype control antibody added to each well at 4°C for 30 min. Cells were washed

twice with FACS staining buffer (0.2% BSA 2 mM EDTA 0.02% NaN3 in PBS) before addition of secondary antibody cocktail.

Goat anti human-APC was added to wells at 1:100 dilution in FACS buffer. For detection of biotin-labeled antibodies (anti Qa-1^b clone 6A8 or isotype control), SA-PE was added at a 1:50 dilution in FACS buffer. All samples were stained using zombie aqua viability stain, anti-mouse CD3-PerCP Cy5.5, CD4-AF700, CD8-V450, F4/80-PE Cy5, NKp46-PE Cy7 at 4℃ for 30 mins. Cells then washed 2x with FACS buffer.

Spleens were mechanically dissociated, in RPMI 1640 medium supplemented with 10% FBS. Dissociated spleens were passed through 70 mm-pore size-separation filters (Miltenyi Biotec) and washed with RPMI 1640 medium. Red blood cells were lysed after 5 min of incubation on ice with RBC Lysis Buffer and then washed with RPMI 1640 medium. $1x10^6$ cells/well of splenocyte were used for staining and blocked with 2.5 µg mouse Fc gamma RI/CD64 antibody and 5 µg anti-mouse CD16/CD32 antibody at 4℃ for 15 min. Splenocyte then stained with zombie aqua viability stain, anti-mouse CD3-PerCP Cy5.5, CD4-AF700, CD8-V450, F4/80-PE Cy5, NKp46-PE Cy7, NKG2A/E/C (clone 20D5), CD44-BV421, CD62L-FITC at 4℃ for 30 mins. Stained cells were then washed 2x with FACS buffer (0.2% BSA 2 mM EDTA 0.02% NaN3 in PBS).

Isolated matured Mϕ, M1 and M2 blocked with 2.5 µg mouse Fc gamma RI/CD64 antibody and 5 µg anti-mouse CD16/CD32 antibody at 4℃ for 15 min. Macrophages then stained with zombie aqua viability stain, anti-mouse F4/80-PE, anti-mouse Qa-1^b-PE, F4/80-PE Cy5 and EXX-1-AF647. Stained cells were then washed 2x with FACS buffer (0.2% BSA 2 mM EDTA 0.02% NaN3 in PBS).

All samples were then analyzed on Beckman Coulter CytoFLEX S V4-B2-Y4-R3 flow cytometer (Beckman coulter). Flowcytometry data were analyzed using FlowJo software version 10. For gating, cells were first selected based on FSC and SSC, followed by selection of singlets and live cells.

Functional assays with BALB/c splenocytes and A20 TILs

Splenocyte from A20 bearing mice were isolated as previously described and labeled with CFSE cell proliferation kit. Labeled splenocytes were co-cultured with matured CpG stimulated BMDCs, pulsed with luciferase peptides (as described before). Unpulsed BMDC cells were used as a negative control. All cells ($1x10^6$/well) were blocked with 2.5 µg and 5 µg (per well) of mouse Fc gamma RI/CD64 and anti-mouse CD16/CD32 antibodies respectively at room temperature for 15 minutes. Cells were stained with antibody cocktails including zombie aqua viability stain, CD3-PerCP Cy5.5, CD4-AF700 and CD8-V450 at 4℃ for 30 min. Cells were then fixed and permeabilized by Perm/Fix buffer for 10 min at room temperature. Antibody cocktail for intra-cellular cytokine detection (ICS): IFN-γ-PE Dazzle™ 594, TNF-α-APC Cy7, granzyme-B-PE Cy7 added to the ICS' antibody cocktail at room temperature for 15 min. Samples were then analyzed on Beckman Coulter CytoFLEX S V4-B2-Y4-R3 flow cytometer (Beckman coulter). Flowcytometry data were analyzed using FlowJo software version 10. For gating, cells were first selected based on FSC and SSC, followed by selection of singlets and live cells.

CONTACT FOR REAGENT AND RESOURCE SHARING

Further information and requests for resources and reagents should be addressed to the Lead Contact Jon Weidanz (Weidanz@uta.edu).

RESULTS

EXX-1 immunotherapy used as a single-agent therapy

Several earlier studies reported single-agent blockade of the NKG2A axis with an antibody to the NKG2A receptor revealed modest anti-tumor responses in mice (11, 18). Here, we evaluated the anti-tumor activity of a novel TCR-like antibody, EXX-1 produced with a mutated mouse Fc domain (Effector Silent; ES) in a therapeutic setting using the A20 murine lymphoma model. BALB/c mice were treated with 10mg/kg of either EXX-1 (ES) or isotype control antibody via intraperitoneal (i.p.) injection every other day starting on Day 9 until Day 21 post tumoral injection. A modest effect on tumor growth inhibition was observed in A20-bearing mice treated with EXX-1 (ES) compared to mice that received control antibody. Figure 1A shows size of individual mouse tumors treated with EXX-1 (ES) (panel, left) or control antibody (panel, right). Additionally, a significant difference ($p > 0.001$) in mean tumor size was observed by Day 17 post tumoral injection between tumor-bearing mice treated with EXX-1 (ES) compared to control antibody (Fig. 1B) suggesting EXX-1 (ES) mediated anti-tumor responses via blockade of the NKG2A axis. Furthermore, EXX-1 (ES) therapy significantly improved survival time ($p>0.05$) compared to control antibody (Fig. 1C). Although none of the mice treated with EXX-1 (ES) displayed complete tumor regression, our findings show that blockade of the NKG2A axis

by targeting tumor cells via the Qa-1^b/Qdm peptide complex is effective and resulted in 40% of mice surviving beyond 27 days compared to 0% of mice in the control group.

EXX-1 Fc (ES) treatment reverts ineffective DC cancer vaccine into potent inducer of anti-tumor immunity

Next, we determined whether using EXX-1 (ES) antibody in combination with a dendric cell (DC) peptide vaccine could lead to tumor-regression. Mice bearing A20-luciferase positive tumors received, via tail vein injection, an initial DC peptide vaccine on day 9 post tumoral injection and a boaster at day 16 (Fig. 2A). To prepare the vaccine, DC cells were pulsed with three different synthetic peptides, each 9 amino acids in length, that were derived from the firefly luciferase protein and previously shown to be immunogenic in BALB/c mice (19). Vaccinated mice were then treated with isotype control or EXX-1 (ES) antibody on days 11, 13, 15, 17, 19 and 21 post tumoral injection. Tumor growth was monitored 3x weekly using digital calipers and tumor sizes plotted for individual mice revealed a pattern of tumor growth inhibition and tumor regression in the cohort of mice that received EXX-1 (ES) + DC peptide vaccine compared to the control antibody + DC peptide vaccine cohort which was not able to inhibit growth or regress tumors (Fig. 2B). Moreover, we observed 8/23 or 35% of mice that received EXX-1 (ES) + DC peptide vaccine were tumor-free at 60 days post tumoral injection, whereas none of the mice from the cohort treated with control antibody + DC peptide vaccine were alive after day 53 post tumoral injection (Fig. 2C) indicating EXX-1 (ES) antibody blockade converted the DC peptide vaccine into a potent inducer of anti-tumor immunity. Additionally, mice treated with EXX-1 (ES) + DC peptide vaccine displayed significantly better progression-free survival and duration

of response compared to control group with 50% of mice treated with EXX-1 (ES) + DC vaccine showing complete or partial responses (Fig. 2D & E).

Figure 2F shows a significantly greater percentage of infiltrated NKG2A+ CD8 T cells and NKG2A+ NK cells in A20 tumor tissue from mice treated with EXX-1 (ES) + DC vaccine compared to control mice suggesting that blocking NKG2A interaction with its ligand is necessary for generation of prolonged anti-tumor immunity in mice, which is in line with literature showing that TCR triggering is required for the induction of NKG2A on CD8 T cells (20).

EXX-1 (ES) in combination with DC peptide vaccine promotes durable anti-tumor immunity

To better understand the mechanism behind the tumor regression in EXX-1 treated mice, tumor-free mice were divided into two groups and rechallenged with either the same tumor (A20) or breast and mammary gland tumor (4T1). In addition, same tumors were engrafted in naïve mice as a control for our experiment. Tumor growth was monitored 3x weekly and tumor sizes plotted for individual mice revealed a pattern of tumor rejection in the cohort of mice previously treated with EXX-1 (ES) + DC peptide vaccine (Fig. 3A). However, unchecked tumor growth and pre-mature dead were observed in control groups including naïve mice bearing A20 lymphoma (Fig. 3B), rechallenged mice with 4T1 tumor (Fig. 3C) or naïve mice with 4T1 tumor (Fig. 3D). Additionally, EXX-1 (ES) treated mice, rechallenged with A20 significantly improved survival time ($p>0.05$) compared to control groups (Fig. 3E) indicating EXX-1 (ES) antibody therapy converted the DC peptide vaccine into a potent inducer of anti-tumor immunity. Furthermore, staining results of the rechallenged mice splenocyte shows a significantly greater percentage of

infiltrated CD8 T cells in splenocyte from mice treated with EXX-1 (ES) + DC vaccine compared to control mice while the ratio of infiltered CD4 T cells were same among different groups of study (Fig. 3F).

Figure 3G show upregulation of effector memory CD8+ T cells (TEM, $CD62L^{-}$ $CD44^{+}$) in the spleen of the A20 rechallenged mice compare to control groups. Additionally, TEM in A20 rechallenged mice demonstrate lower NKG2A expression on their surface in compared to control groups (Fig. 3H), suggesting that NKG2A expression on CD8 T cells is predominantly present in immune-reactive tumors and by blocking its interaction with Qa-1^{b}/Qdm via EXX-1 (ES) we promote long lasting immunity against different malignancy.

Finally, quantitative analysis of the tumor infiltrating CD8+ T cell in A20 rechallenged mice revealed a significant difference ($p < 0.05$) in the production level of the cytolytic chemokine including IFN-γ (Fig. S1-A) TNF-α (Fig. S1-B) Granzyme B (Fig. S1-C) and perforin (Fig. S1-D) produced by CpG stimulated mature dendritic cell (DC) + peptide in compared to naïve DC. These data suggest that Qa-1^{b}/Qdm blockade in combination with another ICI can promote durable protective anti-tumor response in a preclinical mouse model.

Flow cytometry characterization of harvested A20 tumors

We then monitor the expression level of the Qa-1^{b}/Qdm in ex vivo harvested A20 tumors. Figure 4A show upregulation of the Qa-1^{b}/Qdm on the surface of the tumor while anti Qa-1^{b} (clone 6A8) shows modest binding (Fig. 4B) indicating association of the Qdm peptide with Qa-1^{b} complex is a crucial factor for the suppression of the immune system and thus uncontrolled tumor growth in mice.

Previous reports have suggested that murine or human tumor associated macrophage (TAM) can acquire the check point molecule like PD-1 to drive the tumor growth inhibitor (21). Therefore, we assessed the expression level of the Qa-1^b/Qdm, ligand for NKG2A on the surface of the tumor associated macrophages (TAM). Figure 4E show that 10-20 % of tumor infiltrating cells are consists of macrophages (F4/80+, CD68+). Further we observe that EXX-1 (ES) stained TAMs at higher rate in compared to clone 6A8 suggesting that Qdm peptide is associate with Qa-1^b complex. Overall data suggest that macrophages can arm the NK cells thus by blocking the Qa-1^b/Qdm on the surface of the tumor associated macrophages we can promote the anti-tumor immunity and enhance the efficacy of our therapy in cancer patients (22, 24).

In vitro characterization of the bone marrow derived Macrophage (BMDM)

Tumor associated macrophages (TAMs) are often thought to polarized toward either an inflammatory macrophage-M or tumor promotion-M2 (27-29). Therefore, naïve (M0), inflammatory (M1) and pro-tumor (M2) macrophages stained with EXX-1 (top panel) or anti Qa-1^b-clone 6A8 (bottom panel). Staining results reveled EXX-1has higher staining intensity to M1 macrophage (Fig. 5B, bottom panel) compared to M0 and M2 (Fig. 5A and 5C, bottom panel). On the other hand, clone 6A8 demonstrate modest staining only to M1 and M2 macrophages (Fig. 5B and 5C, top panel). These data revealed that virtually majority of Qa-1^b/Qdm^+ TAMs expressed an M1-like surface profile. Therefore, specific inhibition of the NKG2A: Qa-1^b axis in TAMs is responsible for the anti-tumor efficacy that we observed in A20 tumor mice treated with EXX-1.

Therapeutic Vaccination in TC-1 model, induces the Qa-1^b/Qdm expression in tumor cells and enhances the effect immunotherapy

Finally, we tried to investigate the efficacy of EXX-1 as check point blockade in C57BL6 mice and we choose TC-1 as tumor model. Previously Van Montfoort et al. (13) and later our team demonstrate that these tumor cells do not constitutively express Qa-1^b/Qdm on their surface and they need external stimuli such as exposure of cells to recombinant IFN−γ. Van Hall et al. shown that vaccination of TC-1 tumor bearing mice with HPV derived long peptide will result in up regulation of Qa-1^b complex in this tumor (13). Therefore, we exploited the possibility of the combination of therapeutic vaccine as a mean to induce Qa-1^b/Qdm prior to treatment with checkpoint blockade. Tumor bearing mice were vaccinated with two doses of the HPV derived peptide in combination with isotype control or EXX-1 mAb as a check points blockade (Fig. 6 A). Tumor growths were monitored for up to 40 days post tumoral injection.

Taken together, these data imply an important restraining role of the NKG2A/Qa-1^b axis for therapeutic cancer vaccines, mediated via an increased NKG2A expression on CD8 T cells in the tumor and induction of Qa-1^b on tumor cells. Thus, blockade of this axis can potently improve efficacy of therapeutic cancer vaccines. (Fig. 6B). Obtained results revealed that HPV vaccination leading to a surge of T cell in TME which results a temporary regressions of tumor size. Then we observed that EXX-1 checkpoint therapy inhibit the tumor growth in vaccinated mice while tumor in isotype control treated mice exponentially grew. Furthermore, we realized the huge difference in the vaccinated and unvaccinated mice treated with EXX-1 therapy. These data suggesting that activation of tumor-specific T cells in the local environment can induce expression of the inhibitory ligand for CD94/NKG2A receptor (Fig. 6 C, 6D).

DISCUSSION

Immune checkpoint inhibitors have revolutionized the field of cancer immuno-oncology and proved to be effective against several types of cancers. However, the main drawback of the current available immunotherapies is that not everyone can benefit from them. In other words, many cancer patients do not respond to their therapy as their tumor expresses insufficient amount of immune checkpoint marker. Moreover, sometimes the response generated by the immune system is not enough for tumor regression. Thus, the scientific community realized that the efficacy of these treatments needs to be further improved, as does the ability to control their toxicity. One way of achieving this goal is to discover new immune modulatory targets other than PD-1 and CTLA-4 and develop a new therapy for them to promote effective immune responses against cancer. CD94/NKG2A and its interaction with peptides loaded by non-classical MHC Ia, Qa-1^b (mouse), and HALE (human) are the centers of attention as a new checkpoint for the past decade. One of the advantages of targeting the HLAE or Qa-1^b-NKG2A axis is the safety of this approach compared to the other checkpoint pathways. Orr et al. reported that the lack of CD94 protein receptors in mice was associated with no abnormality in genetically modified mice (32). Therefore, many groups tried to develop an antibody to interrupt this axis by blocking the NKG2A molecule. Research published by many groups, including andré, showed that mouse anti NKG2A (clone 20D5) by itself doesn't implement any therapeutic effect as none of the mice treated with it showed tumor regression.

We realized targeting Qa-1^b/Qdm or HLAE/V9 could be another approach to interrupt the NKG2A axis while still taking advantage of enhancing T and NK cell responses. Our team developed a specific antibody to Qa-1^b/Qdm known as EXX-1. In the proposed research, the efficacy of EXX-1 in an invivo setup was evaluated. The study revealed that EXX-1(ES) as an

immune checkpoint blockade by itself could initiate a growth inhibition in tumor bearing mice. However, the efficacy of these treatments needs to be further improved as it did not lead to tumor regression.

André et al. have shown that NK and T cells in TME express the NKG2A receptor while HLAE is frequently overexpressed in some tumors (11). Though our results indicate mouse tumor cells need to be stimulated by some cytokine such as IFN-γ to express the Qa-1^b/Qdm. Braud et al. research showed that the low expression level of the NKG2A+CD8+ T cells could be induced at the surface of CD8+ T cells (33).

To enhance the efficacy of our checkpoint therapy, we used the vaccine approach to stimulate and traffic the immune cells to TME. In our experiment tumor bearing mice received two doses of tumor vaccine while they were treated with isotype control or EXX-1 mAb. Our results revealed that vaccination has a synergistic effect for EXX-1 as a checkpoints blockade. We observed that the vaccine changed the balance of the immune cells in the TME via the induction of the inhibitory receptor NKG2A. Plus, our data revealed that vaccine caused an increase in the expression of Qa-1^b/Qdm on the surface of tumor cells. On the other note, our staining results of the tumor infiltrating immune cells in A20 bearing mice indicate a surge in NKG2A+ CD8+ T cells in vaccinated mice. Also, 35% tumor regression in vaccinated mice treated with EXX-1 was observed. This result confirms that combination of cancer vaccine with EXX-1, potentiate the efficacy of the therapy in mice.

In addition, combination therapy approach is activating the T cell immunity which leads to tumor rejection in rechallenged mice. Staining results of tumor free mice splenocyte revealed the presence of the effector memory CD8+ T cells in these mice, suggesting that our finding is in line with previously published literature (34, 35).

Although the NKG2A/Qa-1^b interaction was initially described to impact NK cell function, we argue that NK cells are the only immune cells involved in the tumor regression process. Vander sulis et al. reported that cancer vaccination could induce cytokine-producing T cells that cause strong macrophage-skewing capacity, essential for tumor shrinkage (13). Staining results of tumor infiltration immune cells shows that those macrophages (F4/80+ cells) have an up-regulation in the Qa-1^b/Qdm as well. To better understand this phenomenon, we stained the bone marrow derived macrophages. Results demonstrate a strong binding shift in the Qa-1^b/Qdm expression level in the M1 population. These studies together illustrate that the intratumoral myeloid cells can play a significant role in the upregulation of the Qa-1^b/Qdm. Therefore, an immune-based treatment can polarize the tumor-promoting function of macrophages into tumor-rejection responses. Indeed, Felix Klug and Yuting Ma were able to show a comparable strong binding shift by preforming intratumoral macrophage staining (31, 36).

Accordingly, cancer therapy leading to tumor regressions mostly coincides with strong changes in myeloid cells in the tumor. We observed CD8 + T cell induced by cancer vaccination can produce cytokines like IFN-γ, TNF-α, Granzyme B, or perforin, which are likely involved in the immune modulation process. These chemokines are known to mediate the recruitment of (inflammatory) macrophages to the tumor.

Taken together, these data imply an important role of the NKG2A/Qa-1^b axis in the field of immuno-oncology and cancer therapies. The combination of Qa-1^b/Qdm blockade with cancer vaccines increased NKG2A expression on tumor-associated CD8 T cells and eventually Qa-1^b/Qdm on tumor cells. Thus, the cancer vaccine can help to improve the therapeutic efficacy of the checkpoints blockade.

FIGURES

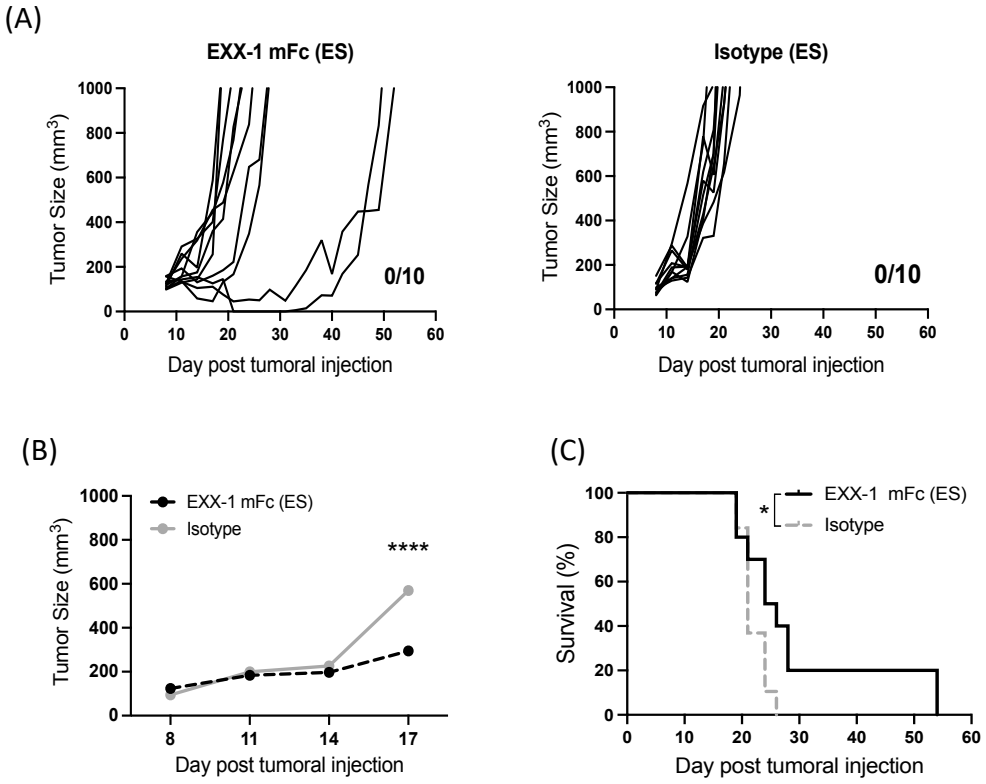

Chapter 4 1: EXX-1 immunotherapy relapses tumor progression.

A20 tumor cells were engrafted in BALB/c mice. Tumor bearing mice were then treated on day 9 through 21 in every other day intervals (total of 7 doses) with an isotype control or EXX-1 mFc (ES) mAb. Graphs show (A) individual mouse tumor growth in each treatment groups (B) comparison of the average tumor growth in each treatment group and (C) combined survival curves. Error bars represent mean ± SE (n=10 in each group). (B) Unpaired Student T- test ****$p<0.0001$; (C) Log rank test *$p = 0.0142$.

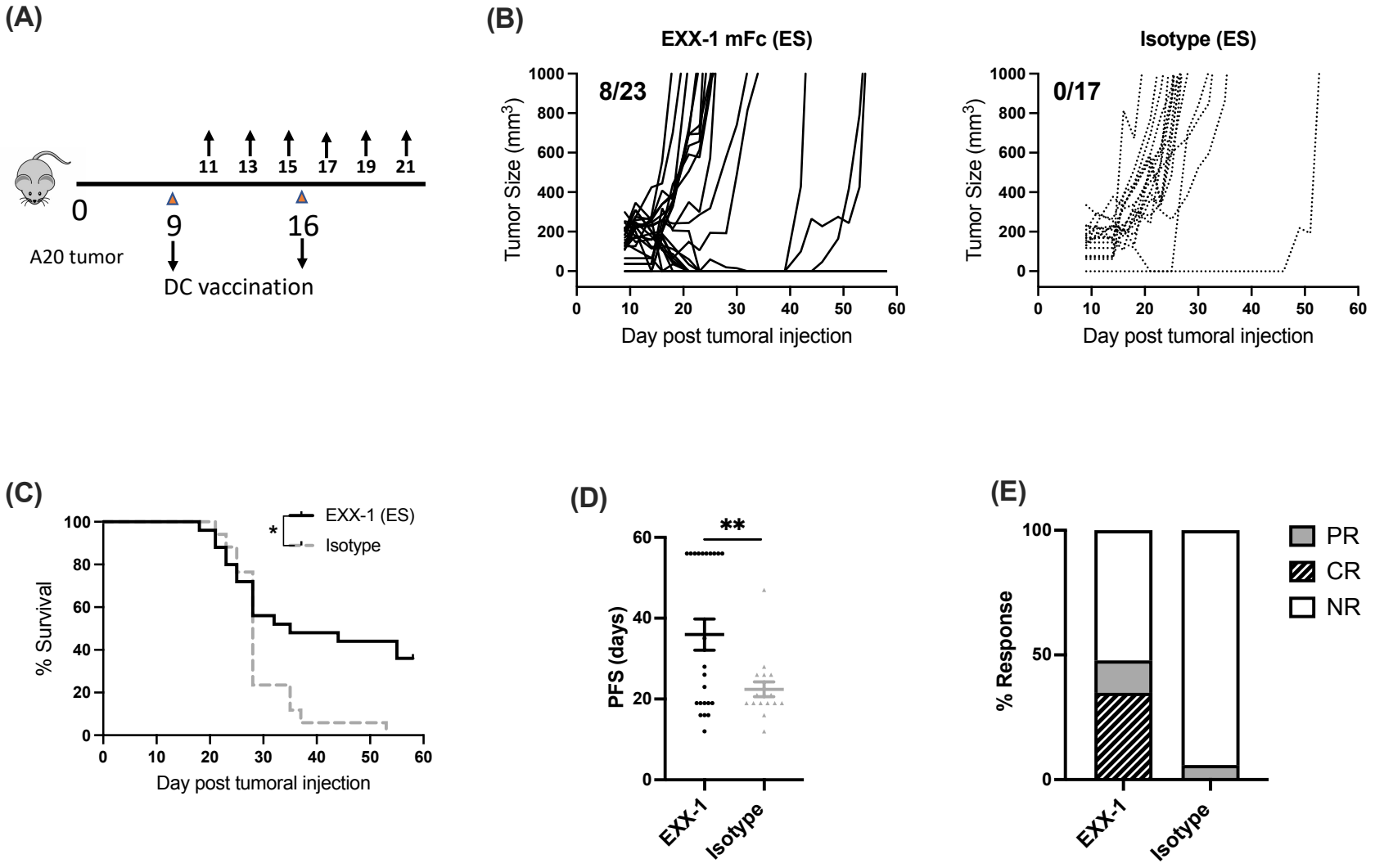
(A)
11
13
15
17
19
21
0
9
16
A20 tumor
DC vaccination
(B)
EXX-1 mFc (ES)
8/23
Tumor Size (mm3)
Day post tumoral injection
Isotype (ES)
0/17
Tumor Size (mm3)
Day post tumoral injection
(C)
EXX-1 (ES)
Isotype
*
% Survival
Day post tumoral injection
(D)
**
PFS (days)
EXX-1
Isotype
(E)
PR
CR
NR
% Response
EXX-1
Isotype

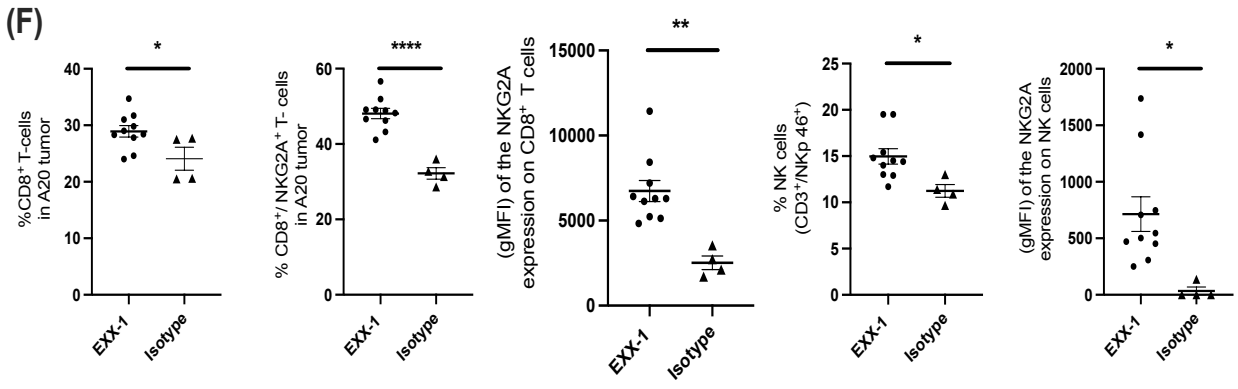

Chapter 4 2: DC Vaccination enhances the effect of EXX-1.

A20 tumor cells were engrafted in BALB/c mice. Tumor bearing mice were vaccinated with mature primed dendritic cells (DCs) on day 9 and 16. Vaccinated mice were then treated on day 9 through 21 in every other day intervals (totals of 7 doses) with an isotype control (n=17) or EXX-1 mFc (ES) mAb (n=23). (A) experimental layout of the vaccination in the A20 model. (B) individual mouse tumor growth in each treatment groups. (C) combined survival curves of pooled results of two independent experiments. Log rank test *p = 0.0142. (D) Progress free survival (PFS) of duration of the time (days) after completion of therapy that mice survival without progression of tumor size (n=25).
(E) Response rate in different treatment groups. Means ± SEM during the relapse phase and therapy response rates according to RECIST criteria. NR, no response; PR, partial response; CR, complete response.
(F) Tumor infiltrating $CD8^+$ T-cells and NK cells were analyzed for the expression of Qa-1^b/Qdm complex in the mice treated with either EXX-1 (ES) (n=10) or Isotype (n=4). Error bars represent mean ± SE. The data presented are the pooled results of two independent experiments. (D, F) Unpaired student T test, *p = 0.043, **p = 0.0014, ***p = 0.0005.

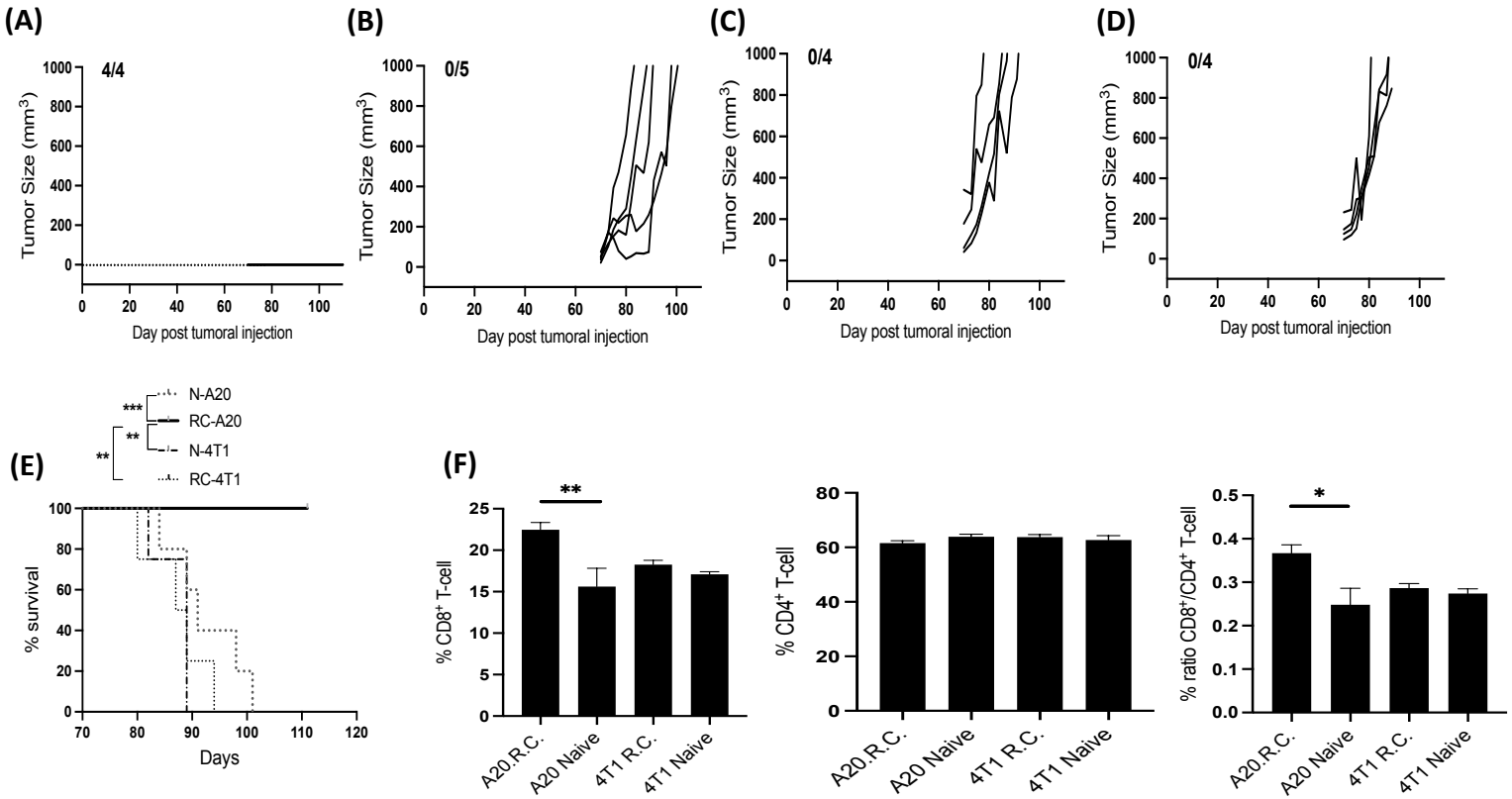
(A)
4/4
Tumor Size (mm3)
Day post tumoral injection
(B)
0/5
Tumor Size (mm3)
Day post tumoral injection
(C)
0/4
Tumor Size (mm3)
Day post tumoral injection
(D)
0/4
Tumor Size (mm3)
Day post tumoral injection
(E)
N-A20
RC-A20
N-4T1
RC-4T1
***
**
**
% survival
Days
(F)
**
% CD8+ T-cell
*
% CD4+ T-cell
% ratio CD8+/CD4+ T-cell
A20.R.C.
A20 Naive
4T1 R.C.
4T1 Naive

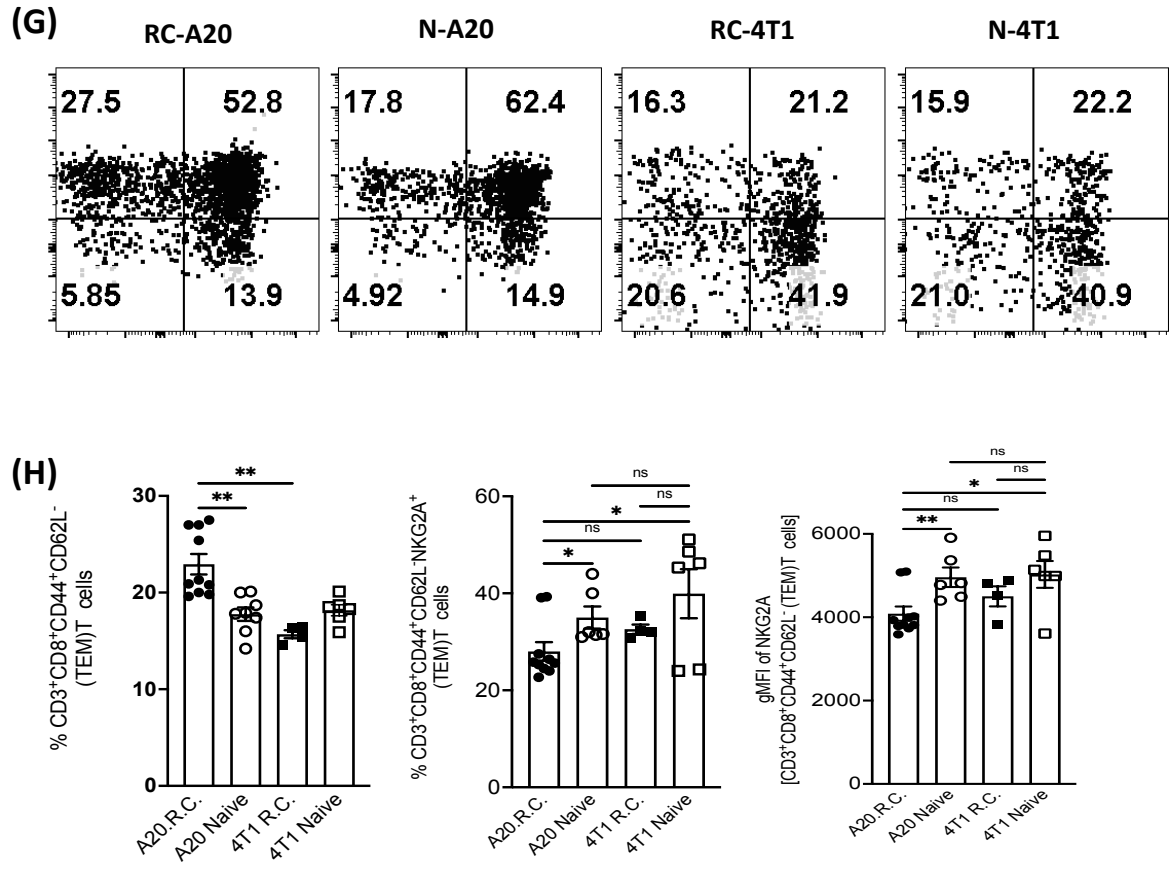

Chapter 4 3: A combination of DC vaccination with EXX-1 promotes anti-tumor immunity in A20 tumor-bearing BALB/c mice.

Graphs shows tumor growth in (A) rechallenged mice with A20 tumor, (B) Naïve mice engrafted with A20 tumor, (C) rechallenge mice with 4T1 tumor, (D) Naïve mice engrafted with 4T1 tumor. Triangular marks on the graphs indicate the day of tumor engraftment. (E) combined survival curves. Percentage of the tumor infiltrating (F) $CD8^+$ T cells and (G) $CD4^+$ T cells. (H) The $CD8^+/CD4^+$ T cell ratio in rechallenged mouse splenocytes. (I) Representative dot plots of expression levels of CD44 and CD62L in naive or rechallenged mice splenocytes and(J) compiled data of the frequency of effector memory (TEM) $CD8^+$ T cells and their expression of NKG2A in naïve compared with rechallenged mice. Error bars represent Mean ± SEM. (D) Log rank test, **P=0.0011 ***p = 0.0007 (F, H, I) one-way ANOVA *p = 0.0043, **p = 0.0014.

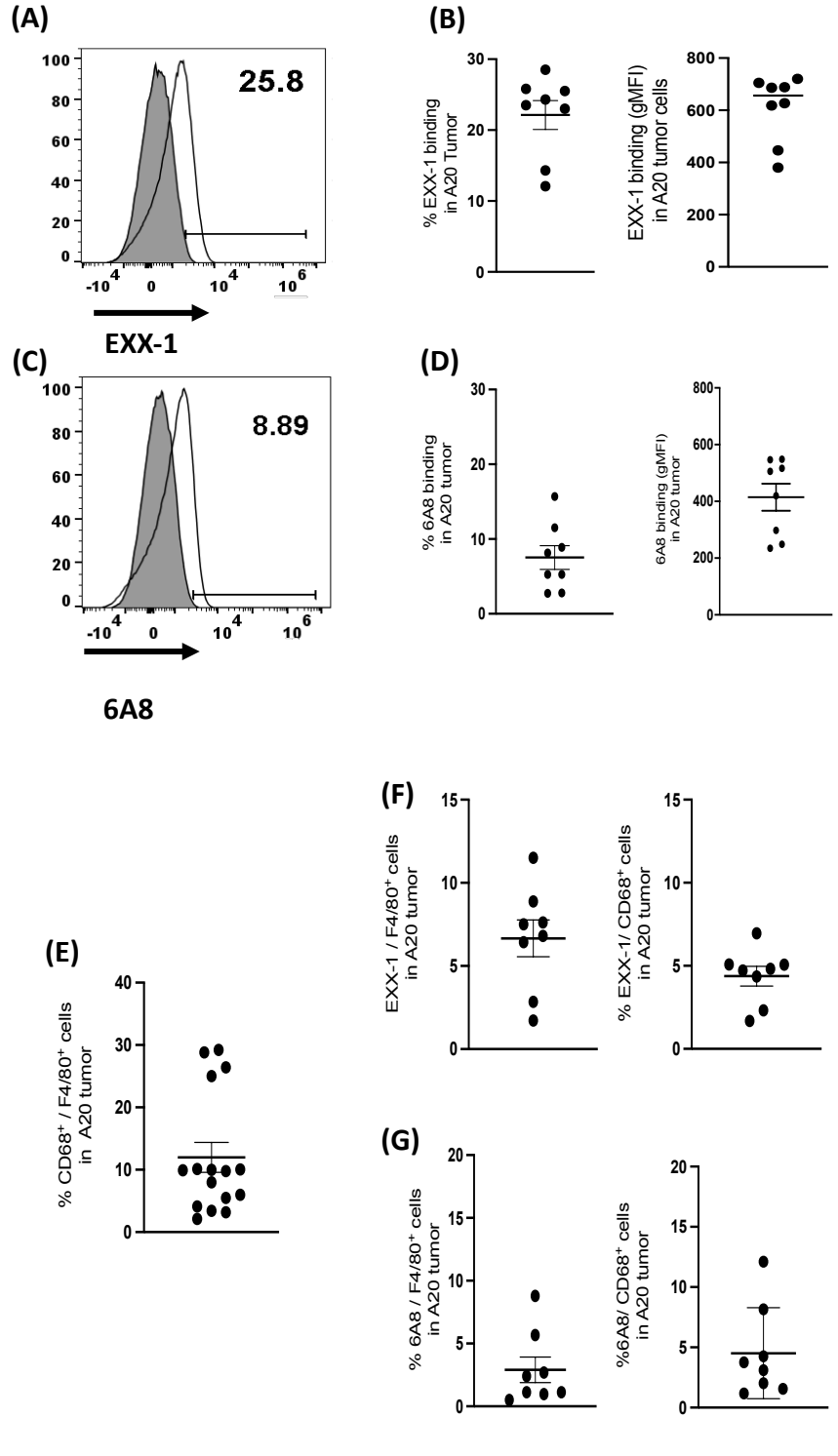
(A)
25.8
EXX-1
(B)
% EXX-1 binding in A20 Tumor
EXX-1 binding (gMFI) in A20 tumor cells
(C)
8.89
6A8
(D)
% 6A8 binding in A20 tumor
6A8 binding (gMFI) in A20 tumor
(E)
% CD68+ / F4/80+ cells in A20 tumor
(F)
EXX-1 / F4/80+ cells in A20 tumor
% EXX-1/ CD68+ cells in A20 tumor
(G)
% 6A8 / F4/80+ cells in A20 tumor
%6A8/ CD68+ cells in A20 tumor

Chapter 4 4: Flow cytometry characterization of harvested A20 tumors.

Staining in isotype treated A20 tumor bearing mice. (A) FACS histogram of EXX-1 binding and (B) compilation of percentage and gMFI of EXX-1 binding. (C) FACS histogram of 6A8 binding and (D) compilation of percentage and gMFI of 6A8 binding. Grey histograms: isotype control; white histograms: EXX-1 or 6A8 mAbs. Numbers are indicative of fluorescence intensity. Graph (E) represent tumor infiltrating (E) frequency of tumor infiltrating macrophages (TIM). TIM populations were evaluated for the expression of (F) the Qa-1^b/Qdm complex (EXX-1) or (G) Qa-1^b (6A8) Error bars represent mean ± SE within each group (n=8).

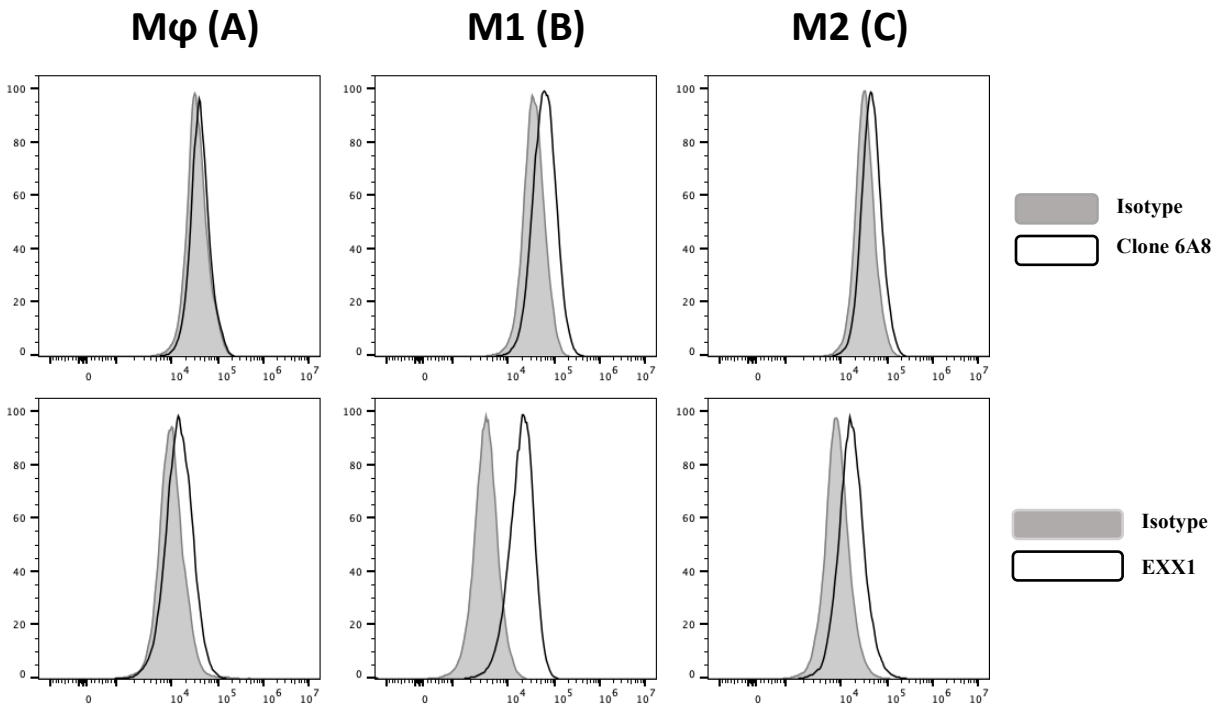

Chapter 4 5: In vitro characterization of the bone marrow derived Macrophage (BMDM).

Graphs show staining of (A) Mϕ **,** (b) M1 and (C) M2 with EXX-1 (Top panel) or 6A8 (Bottom panel). Control reagent is plotted in grey. Indicated antibody is plotted with a black line.

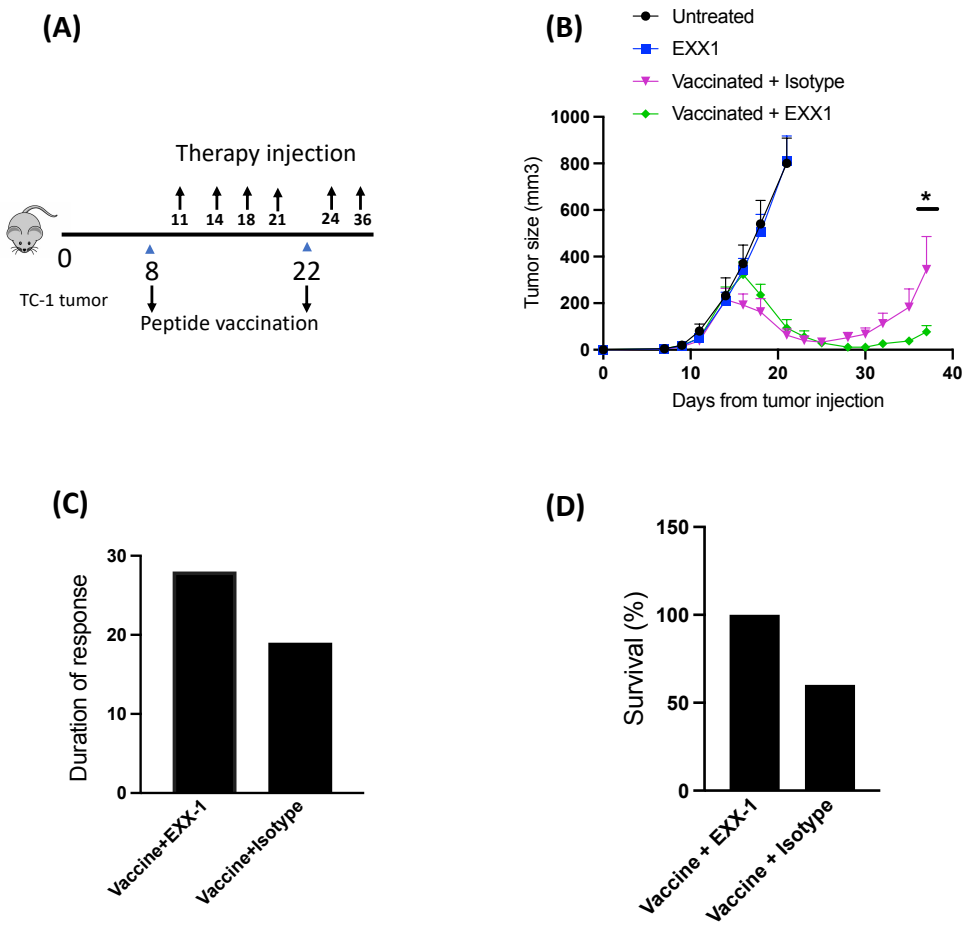

Chapter 4 6: Therapeutic Vaccination in TC-1 model, induces the Qa-1^b/Qdm expression in tumor cells and enhances the effect immunotherapy.

(A) experimental layout of the vaccination protocol in the TC-1 models. (B) Average tumor growth in each treatment group. Error bars represent mean ± SD. One-way ANOVA **p = 0.026. n = 10. Duration of the response (C) survival days and (D) survival rate (survival %) in TC-1 tumors bearing mice, treated with vaccine and an isotype control or vaccine and EXX-1 mFc (ES) mAb.

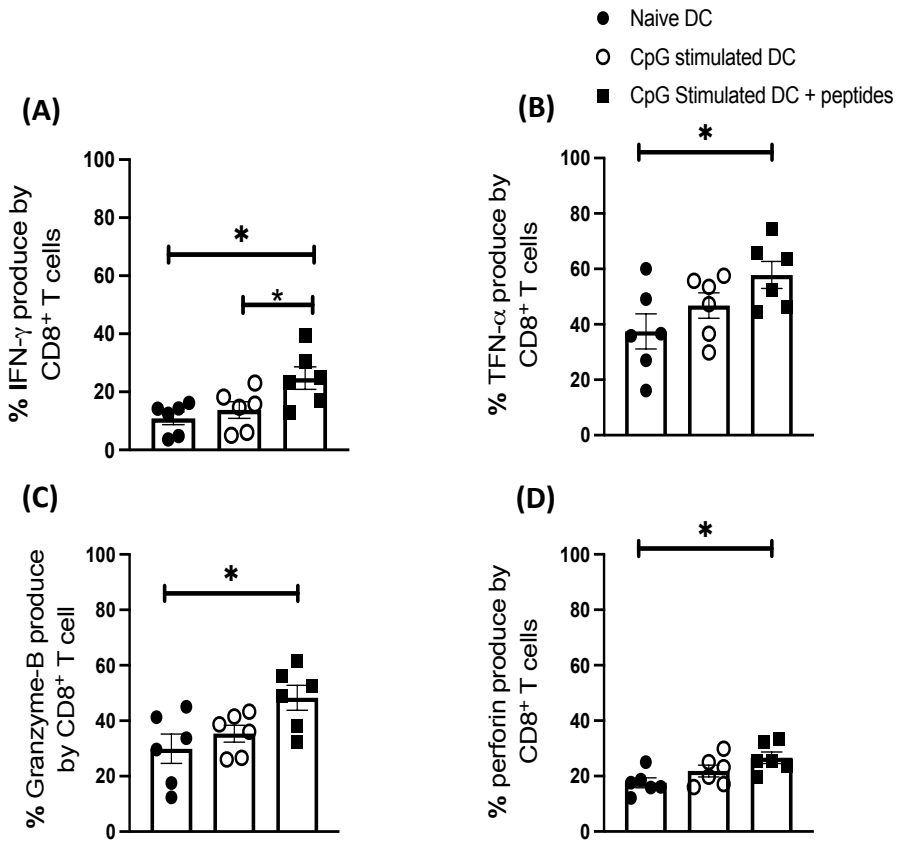

Supplement figure 4 1: DC vaccination induces tumor specific CD8+ T cells

The Production frequency of the (A) IFN-γ, (B) TNF-α, (C) Granyzme B and (D) perforin in tumor infiltrating $CD8^+$ T cells. Error bars represent mean ± SEM (n=6). One-way ANOVA test, *p <0.05, **p = 0.0088, ***p = 0.0003, ****p<0.0001.

REFRENCES

1. Waldman, Alex D et al. “A guide to cancer immunotherapy: from T cell basic science to clinical practice.” Nature reviews. Immunologyvol. 20,11 (2020): 651-668. doi:10.1038/s41577-020-0306-5
2. DeVita, Vincent T Jr, and Edward Chu. “A history of cancer chemotherapy.” Cancer research vol. 68,21 (2008): 8643-53. doi:10.1158/0008-5472.CAN-07-6611
3. Okazaki, Taku, and Tasuku Honjo. “PD-1 and PD-1 ligands: from discovery to clinical application.” International immunology vol. 19,7 (2007): 813-24. doi:10.1093/intimm/dxm057
4. Okazaki, Taku et al. “A rheostat for immune responses: the unique properties of PD-1 and their advantages for clinical application.” Nature immunology vol. 14,12 (2013): 1212-8. doi:10.1038/ni.2762
5. Schumacher, Ton N, and Robert D Schreiber. “Neoantigens in cancer immunotherapy.” Science (New York, N.Y.) vol. 348,6230 (2015): 69-74. doi:10.1126/science.aaa4971
6. Sharma, Padmanee, and James P Allison. “The future of immune checkpoint therapy.” Science (New York, N.Y.) vol. 348,6230 (2015): 56-61. doi:10.1126/science.aaa8172
7. Sharma, Padmanee, and James P Allison. “Immune checkpoint targeting in cancer therapy: toward combination strategies with curative potential.” Cell vol. 161,2 (2015): 205-14. doi:10.1016/j.cell.2015.03.030

8. van der Burg, Sjoerd H et al. “Vaccines for established cancer: overcoming the challenges posed by immune evasion.” Nature reviews. Cancer vol. 16,4 (2016): 219-33. doi:10.1038/nrc.2016.16
9. Schmidt, Emmett V. “Developing combination strategies using PD-1 checkpoint inhibitors to treat cancer.” Seminars in immunopathology vol. 41,1 (2019): 21-30. doi:10.1007/s00281-018-0714-9
10. Khair, Duaa O et al. “Combining Immune Checkpoint Inhibitors: Established and Emerging Targets and Strategies to Improve Outcomes in Melanoma.” Frontiers in immunology vol. 10 453. 19 Mar. 2019, doi:10.3389/fimmu.2019.00453
11. André, Pascale et al. “Anti-NKG2A mAb Is a Checkpoint Inhibitor that Promotes Anti-tumor Immunity by Unleashing Both T and NK Cells.” Cell vol. 175,7 (2018): 1731-1743.e13. doi:10.1016/j.cell.2018.10.014
12. Ghaffari, Soroush et al. “A single-domain TCR-like antibody selective for the Qa-1^b/Qdm peptide complex enhances tumoricidal activity of NK cells via the NKG2A immune checkpoint”. Journal of immunology. Under review.
13. van der Sluis, Tetje C et al. “Therapeutic Peptide Vaccine-Induced CD8 T Cells Strongly Modulate Intratumoral Macrophages Required for Tumor Regression.” Cancer immunology research vol. 3,9 (2015): 1042-51. doi:10.1158/2326-6066.CIR-15-0052
14. Ossendorp, F et al. “Specific T helper cell requirement for optimal induction of cytotoxic T lymphocytes against major histocompatibility complex class II negative tumors.” The Journal of experimental medicine vol. 187,5 (1998): 693-702. doi:10.1084/jem.187.5.693

15. Bowen, William S et al. “Current challenges for cancer vaccine adjuvant development.” Expert review of vaccines vol. 17,3 (2018): 207-215. doi:10.1080/14760584.2018.1434000
16. Kantoff, Philip W et al. “Sipuleucel-T immunotherapy for castration-resistant prostate cancer.” The New England journal of medicine vol. 363,5 (2010): 411-22. doi:10.1056/NEJMoa1001294
17. Vo, Manh-Cuong et al. “Lenalidomide and Programmed Death-1 Blockade Synergistically Enhances the Effects of Dendritic Cell Vaccination in a Model of Murine Myeloma.” Frontiers in immunology vol. 9 1370. 18 Jun. 2018, doi:10.3389/fimmu.2018.01370
18. van Montfoort, N., L. Borst, M. J. Korrer, M. Sluijter, K. A. Marijt, S. J. Santegoets, V. J. van Ham, I. Ehsan, P. Charoentong, P. Andre, N. Wagtmann, M. J. P. Welters, Y. J. Kim, S. J. Piersma, S. H. van der Burg, and T. van Hall. 2018. NKG2A Blockade Potentiates CD8 T Cell Immunity Induced by Cancer Vaccines. Cell 175: 1744-1755 e1715.
19. Limberis, M P et al. “Identification of the murine firefly luciferase-specific CD8 T-cell epitopes.” Gene therapy vol. 16,3 (2009): 441-7. doi:10.1038/gt.2008.17
20. Gunturi, Anasuya et al. “The role of TCR stimulation and TGF-beta in controlling the expression of CD94/NKG2A receptors on CD8 T cells.” European journal of immunology vol. 35,3 (2005): 766-75. doi:10.1002/eji.200425735
21. Klezovich-Bénard, Maria et al. “Mechanisms of NK cell-macrophage Bacillus anthracis crosstalk: a balance between stimulation by spores and differential disruption by toxins.” PLoS pathogens vol. 8,1 (2012): e1002481. doi:10.1371/journal.ppat.1002481

22. Nedvetzki, Shlomo et al. “Reciprocal regulation of human natural killer cells and macrophages associated with distinct immune synapses.” Blood vol. 109,9 (2007): 3776-85. doi:10.1182/blood-2006-10-052977

23. Lapaque, Nicolas et al. “Interactions between human NK cells and macrophages in response to Salmonella infection.” Journal of immunology (Baltimore, Md. : 1950) vol. 182,7 (2009): 4339-48. doi:10.4049/jimmunol.0803329

24. Gordon SR, Maute RL, Dulken BW, Hutter G, George BM, McCracken MN, Gupta R, Tsai JM, Sinha R, Corey D, Ring AM, Connolly AJ, Weissman IL. PD-1 expression by tumour-associated macrophages inhibits phagocytosis and tumour immunity. Nature. 2017 May 25;545(7655):495-499. doi: 10.1038/nature22396. Epub 2017 May 17. PMID: 28514441; PMCID: PMC5931375

25. Tjwa, Eric T T L et al. “Restoration of TLR3-activated myeloid dendritic cell activity leads to improved natural killer cell function in chronic hepatitis B virus infection.” Journal of virology vol. 86,8 (2012): 4102-9. doi:10.1128/JVI.07000-11

26. Michel, Tatiana. “Consequences of the Crosstalk Between Monocytes/macrophages and Natural Killer Cells.” Frontiers in immunology. 3 (2013): n. pag. Web

27. Biswas, S. K., Allavena, P. & Mantovani, A. Tumor-associated macrophages: functional diversity, clinical significance, and open questions. Semin. Immunopathol. **35**, 585–600. https://doi.org/10.1007/s00281-013-0367-7 (2013).

28. Coussens, L. M. & Werb, Z. Inflammation and cancer. Nature **420**, 860 867. https://doi.org/10.1038/nature01322 (2002).

29. Parisi, L. et al. Macrophage polarization in chronic inflammatory diseases: Killers or builders?. J. Immunol. Res. **2018**,8917804. https://doi.org/10.1155/2018/8917804 (2018).

30. Oshi, M., Tokumaru, Y., Asaoka, M. et al. M1 Macrophage and M1/M2 ratio defined by transcriptomic signatures resemble only part of their conventional clinical characteristics in breast cancer. Sci Rep **10,** 16554 (2020). https://doi.org/10.1038/s41598-020-73624-w
31. Klug, Felix et al. “Low-dose irradiation programs macrophage differentiation to an iNOS^{+}/M1 phenotype that orchestrates effective T cell immunotherapy.” Cancer cellvol. 24,5 (2013): 589-602. doi:10.1016/j.ccr.2013.09.014.
32. Vance, R E et al. “Recognition of the class Ib molecule Qa-1(b) by putative activating receptors CD94/NKG2C and CD94/NKG2E on mouse natural killer cells.” The Journal of experimental medicine vol. 190,12 (1999): 1801-12. doi:10.1084/jem.190.12.1801
33. Braud, Veronique M et al. “Expression of CD94-NKG2A inhibitory receptor is restricted to a subset of CD8+ T cells.” Trends in immunology vol. 24,4 (2003): 162-4. doi:10.1016/s1471-4906(03)00064-4
34. Sharma, Padmanee et al. “Primary, Adaptive, and Acquired Resistance to Cancer Immunotherapy.” Cell vol. 168,4 (2017): 707-723. doi:10.1016/j.cell.2017.01.017
35. Ma, Yuting et al. “Anticancer chemotherapy-induced intratumoral recruitment and differentiation of antigen-presenting cells.” Immunity vol. 38,4 (2013): 729-41. doi:10.1016/j.immuni.2013.03.003.
36. Silva, Tarsia G et al. “Expression of the nonclassical HLA-G and HLA-E molecules in laryngeal lesions as biomarkers of tumor invasiveness.” Histology and histopathologyvol. 26,12 (2011): 1487-97. doi:10.14670/HH-26.1487
37. Wang, Tingting, et al. "A Cancer Vaccine-Mediated Postoperative Immunotherapy for Recurrent and Metastatic Tumors." Nature Communications, vol. 9, 2018, pp. 1-12.

38. Melief, Cornelis J M et al. “Therapeutic cancer vaccines.” The Journal of clinical investigation vol. 125,9 (2015): 3401-12. doi:10.1172/JCI80009

39. van Esch, E M G et al. “Alterations in classical and nonclassical HLA expression in recurrent and progressive HPV-induced usual vulvar intraepithelial neoplasia and implications for immunotherapy.” International journal of cancer vol. 135,4 (2014): 830-42. doi:10.1002/ijc.28713

40. Talebian Yazdi, Mehrdad et al. “The positive prognostic effect of stromal CD8+ tumor-infiltrating T cells is restrained by the expression of HLA-E in non-small cell lung carcinoma.” Oncotarget vol. 7,3 (2016): 3477-88. doi:10.18632/oncotarget.6506

41. Seliger, Barbara et al. “HLA-E expression and its clinical relevance in human renal cell carcinoma.” Oncotarget vol. 7,41 (2016): 67360-67372. doi:10.18632/oncotarget.11744

42. Gooden, Marloes et al. “HLA-E expression by gynecological cancers restrains tumor-infiltrating $CD8^+$ T lymphocytes.” Proceedings of the National Academy of Sciences of the United States of America vol. 108,26 (2011): 10656-61.doi:10.1073/pnas.1100354108.

43. Duluc, Dorothée et al. “Interferon-gamma reverses the immunosuppressive and protumoral properties and prevents the generation of human tumor-associated macrophages.” International journal of cancer vol. 125,2 (2009): 367-73. doi:10.1002/ijc.24401

44. Heusinkveld, Moniek et al. “M2 macrophages induced by prostaglandin E2 and IL-6 from cervical carcinoma are switched to activated M1 macrophages by CD4+ Th1 cells.” Journal of immunology (Baltimore, Md. : 1950) vol. 187,3 (2011): 1157-65. doi:10.4049/jimmunol.1100889

CHAPTER 5

Targeting the NKG2A ligand with a single-agent TCR-like antibody having an active Fc-domain induces tumor regression in murine models

Authors: Soroush Ghaffari[1], Katherine Upchurch-Ange[2] and Jon Weidanz[2,3,*]

Affiliations:

[1]Department of Biology, College of Science
The University of Texas at Arlington, TX, USA.

[2]Abexxa Biologics Inc. 500 S Cooper St, Arlington, TX, USA.

[3]College of Nursing and Health Innovation
The University of Texas at Arlington, Arlington, TX, USA

*** Correspondence:**
Jon Weidanz
Email: weidanz @uta.edu

College of Nursing and Health Innovation,
The University of Texas at Arlington, Arlington, TX, USA

ABSTRACT

Antagonizing antibodies against immune checkpoint inhibitory molecules (ICI) has gained an excellent reputation in immuno-oncology. NKG2A and its interaction with Qa-1^b/HLA-E ligand, known to have a significant role in modulating anti-tumor effector cell responses. Recent studies in mice and patients with Head & Neck cancer have shown modest benefit after treatment with single-agent anti-NKG2A blocking antibodies. On the other hand, clinical trials of the human anti-NKG2A antibody, monolizamab in combination with anti-PD-L1 blocking antibody have shown promises indicating that NKG2A blockade may synergize with anti-PD-L1 therapy.

Our group previously developed a single-domain T-cell receptor-like (TCR-like) antibody (EXX-1) with specificity for the Qa-1^b/Qdm peptide complex, the ligand for the murine NKG2A/CD94 receptor. We have shown EXX-1 (Effector Silent; ES) as a single agent blocking antibody, creating a modest delay in mice tumor growth and their overall survival time. Moreover, we have shown that cancer vaccine effectiveness can be markedly enhanced when combined with EXX-1 (ES) antibody.

In this study, we focused on utilizing the EXX-1 antibody containing an active Fc domain and evaluated its anti-tumor properties as a single-agent therapy in A20 and CT26 murine tumor models. Our findings show that treating A20 tumor-bearing mice with EXX-1 (Fc active) antibody causes tumor regression and leads to tumor-free survival in 35% of mice. In contrast, control antibody and anti-NKG2A treated mice had 0% and 11% tumor-free survival, respectively. Similar anti-tumor responses were observed in CT26 tumor bearing mice that received EXX-1 (Fc active) antibody compared to isotype control and anti-PD-1 therapy. Finally, the mode of action for EXX-1 (Fc active) blocking antibody revealed NK and effector CD8+ T-cells involvement with long-lived immunity provided by memory CD8+ T-cells.

Taken together, our results indicate targeting the NKG2A through Qa-1^b/Qdm peptide complex on tumor cells is an effective means of blocking the NKG2A axis. Also, using a blocking antibody containing an active Fc domain may have additional anti-tumor benefits by recruiting antibody-dependent cellular cytotoxicity (ADCC) mode of action.

INTRODUCTION

The immune system can recognize pathogens and is poised to eliminate them while at the same time held in check by inhibitory receptors to prevent its self-destruction. This inhibitory receptor or so-called immune checkpoints inhibitor refers to any protein marker expressed by our cells to help our body maintain its self-tolerance (1-3). Since the discovery of these novel proteins, scientists have tried to use them to unleash suppressed immunity to fight cancers. This is how the checkpoint blockade concept got introduced to the world of immuno-oncology. Anti CTLA-4 and anti PD-1 are among the first checkpoint blocking agent got approved by Food and Drug Administration (FDA) to be used in cancer therapy. Preliminary clinical findings of these therapies indicate broad and diverse opportunities to enhance anti-tumor immunity with the potential to produce durable clinical responses. However complex biology of immune checkpoint pathways caused that not all patients get cured by these antibodies. Thus, immunologists realized more still needs to be done to improve the rate of response to ICB therapy including understanding mechanisms of acquired resistance, finding optimal ways of combining ICB with other immune therapies and identifying additional immune checkpoint pathways and associated blocking antibodies.

CD94/NKG2A and its ligand Qa-1^b (in mouse) or HLAE (in human) are other checkpoints that being center of attention for the last decade. NKG2A is a member of the c-lectin-type receptor family and is expressed as a heterodimeric receptor with CD94 on NK and tumor-infiltrating CD8+ T cells. NKG2A expression is regulated by T cell activation via TCR engagement and by IL-15 and TGF-b cytokines. The NKG2A receptor contains two immunoreceptor tyrosine-based inhibitory motifs (ITIMs) and regulates effector cell cytolytic activity. Previously reported that 5% of CD8+ T cells in healthy individual expressing the NKG2A receptor on their surface while

others associate expression of the NKG2A may represent an exhausted phenotype in CD8+T cells (4-7). Interaction between NKG2A and its ligand relay inhibition signals to the NK cells and CD8+ T cells (8, 9). Many groups have put their effort into developing an agent that disrupts this axis through the blocking of NKG2A. Clone Z270 (Monalizumab) and clone 20D5 are monoclonal antibodies designed to block human and mouse NKG2A, respectively. Recent study conducted by andré et al. shows anti mouse NKG2A (20D5) as single therapy didn't create a significant outcome. At the same time, combination of other blocking agents such as anti-PD-1, enhanced the efficacy of anti-NKG2A (10).

Our group previously shown that TCR-like antibodies can also be raised to specifically bind a given peptide/HLA complex, much like a TCR engages the peptide/ HLA (14). Our team developed a single domain antibody named EXX-1 specific for Qdm peptide expressed by mouse Qa-1^b complex. We showed EXX-1 (ES) as a single therapy suppresses the tumor growth in mice bearing tumors by interrupting the NKG2A: Qa-1^b axis. Moreover, by combination of our checkpoint blockade with cancer vaccine, we were able convert an ineffective therapeutic cancer vaccine into one that is effective at inducing anti-tumor responses. We observed 35% tumor regression in mice bearing tumor, which leads to tumor immunity in tumor bearing mice.

Another way to enhance the efficacy of checkpoint antibody is through antibody-dependent cell-mediated cytotoxicity mechanism (ADCC). ADCC is a lytic mechanism mediated by mono nuclear cells that carries receptors for the Fc portion of IgG [11]. Fc receptor-bearing effector cells then can recognize the IgG portion of their target and kill antibody-coated target cells. Years of preclinical and clinical work have shown that in human monoclonal antibodies (mAbs) with immunoglobulin (Ig) G1 have the highest capability for ADCC compared with other isotypes (eg, IgG2). However, mice antibodies with immunoglobulin (Ig) G2 are associated with

the highest rates of ADCC (12, 13). Previously worked conducted in this field demonstrate that TCR-like antibodies with ADCC showed promising results in eliciting destruction of lymphoma and colorectal cancer (15, 16). To be more specific, TCR-like antibody and peptide/ HLA interactions can be used to modulated ADCC killing potential, indicating that, TCR-like antibody docking to defined regions of the peptide/HLA severely dampened ADCC. In the presented research, we fused EXX-1 with mouse IgG2A to test our hypothesis and evaluate the potential benefit that ADCC combination with the checkpoints blockade antibodies may bring for patient.

METHODS and MATERIALS

Antibodies and reagents

Antibodies specific for anti-mouse CD4-AF700 (RMA4-5; cat#100528), NKp46-PE Cy7 (29A1.4; cat#137617), SA-APC (405204), F4/80- PE Cy5 (BM8; cat#123112), Ultra-LEAF™ Purified anti-Asialo-GM1(Poly21460; cat#146002), Aqua Fixable Viability Kit (cat#423101/423102), TrueStain FcX plus (cat#156604), FluoroFix buffer (cat#422101) and RBC lysis buffer (cat#420302) were purchased from BioLegend. Anti-mouse CD3-PerCP Cy5.5 (17A2; cat 65002), CD8-V450 (2.43; cat#75-1886), CD16/32 (2.4G2; cat#70-0161), CD45-FITC (30-F11; cat# 35-0451), and CD11c-APC Cy7 (N418; cat#25-0114) were purchased from Tonbo Bioscience. SA-PE (cat#12-4317-87) was purchased from eBioscience. Anti-mouse Fc gamma RI/CD64 (cat#MAB20741) was purchased from R&D Systems. Pre-separation filter,70 μm (cat#130-095-823) and anti-mouse NKG2A/C/E-PE (20d5; cat#130-105-620) were purchased from Miltenyi Biotec. Biotin-labeled anti-mouse Qa-1^b (6A8.6F10.1A6; cat#559829) and anti-mouse Qa-1^b- PE (6A8.6F10.1A6; cat#566641) were purchased from BD Pharmingen. AffiniPure Goat Anti-Human (GAH) IgG, Fcγ fragment specific-PE (cat#109-115-098) ,

AffiniPure Goat Anti-Mouse (GAM) IgG (subclasses 1+2a+2b+3)-PE (cat#115-115-164), AffiniPure Goat Anti-Human (GAH) IgG, Fcγ fragment specific-APC (cat#115-135-164) and AffiniPure Goat Anti-Mouse (GAM) IgG (subclasses 1+2a+2b+3)-APC (cat#115-135-164) were purchased from Jackson Immuno Research. CellTrace CFSE Cell Proliferation kit (cat#C34554) and CountBright™ Plus Absolute Counting Beads (cat# 3036995) were purchased from Thermofisher. Matrigel matrix was purchased from Corning (cat#354248). Liberase TL Research Grade (cat# 5401020001) was purchased from Millipore Sigma. Normal rabbit serum (cat#7487) was purchased from Abcam. InvivoMAb anti mouse CD8α (YTS169.4; cat#BE0117), InvivoMAb rat IgG2b κ isotype control (LTF-2; cat#BE0090), InvivoMAb anti mouse PD-1 [CD279] (RMP1-14; cat#BE0146) and InvivoMAb rat IgG2a isotype control (2A3; cat#BE0089) were purchased from Bioxcell.

Software and algorithms

GraphPad Prisem V9 (graphpad, http://www.graphpad.com/ scientific-software/prism;RRID: SCR_002798), FlowJo v10.8.1(https://www.flowjo.com/solutions/ flowjo; RRID: SCR_008520) were used for the analysis of data presented in this manuscript.

Mice

BALB/c mice were purchased from Jackson Laboratories. All mice were purchased under specific pathogen-free conditions. Female mice were used at 6 to 18 weeks of age and were allowed to acclimate to the housing facility for at least one week prior to experiments. All animal experiments were performed in accordance with the rules of the UTA ethics and animal welfare committees (IACUC).

Mouse tumor Cell lines

A20 murine lymphoma cell line was purchased from the Imanis Life Science Collection (Imanis-CL152-STAN). Parental A20 cells were transduced with 1) LV-Fluc-P2A-Neo (Imanis #LV067) encoding the enhanced green fluorescent (eGFP) cDNA under the spleen focus-forming virus (SFFV) promoter and linked to the neomycin resistance gene (Neo) via a P2A cleavage peptide and 2) LV-Fluc-P2A-Puro (Imanis #LV012) encoding the firefly luciferase (Fluc) cDNA under the SFFV promoter and linked to the puromycin resistance gene (Puro) via a P2A cleavage peptide.

A20 cells cultured in RPMI-1640 medium (RPMI-Hyclone; GE biosience) supplemented with 10% heat inactivated FBS (GE-bioscience), 2% glutamine and penicillin/streptomycin (Gibco), and 50 µM β- mercaptoethanol (sigma) (complete medium) at 37℃ in a humidified atmosphere containing 5% CO_2. To maintain the expression of the Fluc and GFP genes, 1 mg/mL geneticin (G418) and 1 µg/mL puromycin were added to the culturing media one week after cell line growth was stabilized.

CT26 is colon carcinoma cell line developed by exposing BALB/c mice to N-nitroso-N-methylurethane (NMU), resulting in a grade IV carcinoma that is fast growing and easily implantable (21). CT26_WT cell line was purchased from the American type culture collection (CRL-2638). Cells were culture in RPMI-1640 medium (RPMI; Cytovia) supplemented with 10% FBS (GIBCO), 2% glutamine and penicillin/streptomycin (gibco) (complete medium) at 37℃ in a humidified atmosphere containing 5% CO_2.

All cell lines were assured to be free of rodent viruses and Mycoplasma by regular PCR analysis. Cells of low passage number were used for all experiments.

Mouse tumor models

For tumor inoculation, $2.5x10^5$ CT26_WT and $5x10^6$ A20, tumor cells were injected subcutaneous (s.c.) in the flank of the BalbC mice. Tumor cells were resuspended in 100 µL PBS+0.1% BSA mixed with 100 µL Matrigel® matrix prior to inoculation. Tumors were measured three times a week with a digital caliper and the size is expressed as a volume ((length x width^2)/2). When a palpable tumor was present, mice were split (randomized) into groups and were treated with immunotherapy. Mice were sacrificed when tumors reached a volume of 1500 mm^3. For the purposes of Kaplan-Meier curves, mice were considered dead when tumor volume exceeded 1000 mm^3.

EXX-1 blocking antibody and isotype control was produced by ATUM (Newark, California) and is engineered with mouse IgG2a. Treatments with checkpoint blockade antibodies in A20 model were initiated when tumor volumes were between 150 and 200 mm^3. Antibodies were administered intraperitoneal (i.p.) at a dose of 200 µg/mice (diluted in 1X PBS) on days 9, 11, 13, 15, 17 and 19 post-transplantations.

For NK cell depletion experiment, 100 µL of polyclonal anti-asialo-GM1 antibody were administered i.p. into BALB/c mice once weekly. Normal rabbit serum was injected as an isotype control.

For the CD8$^+$ T cells depletion experiment, each mouse was injected i.p. with 400 µg of depleting anti-CD8α mAb for the first dose and then 200 µg once weekly for two subsequent injections. A rat IgG2b κ was used as control. Immune cell depletions were initiated as indicated in the figure legends. Mice response to anti-asialo-GM1 antibody and anti-CD8α mAb were measured by flow cytometry (FACS analysis).

For CT26_WT model, tumor bearing BALB/c mice were treated by blocking antibodies including: EXX-1, anti PD-1 and their isotype controls at a dose of 200 µg/diluted in 1X PBS) i.p. on days 6, 8 ,10, 12, 14, 16 and 18 post tumoral injection.

Flow cytometry analysis of the ex-vivo harvested tumor cells and tumor-infiltrating mouse lymphocytes (TILs)

Tumors were dissected into small pieces and digested with enzymes A and D from the Mouse Tumor Dissociation Kit (Miltenyi Biotec) and program: m_implant_tumor_2 of the GentleMACS Dissociator (Miltenyi Biotec). Tumors were incubated at 37 ℃ for 30 minutes to achieved enzymatic digestion. Red blood cells in digested tumor were lysed after 5 min of incubation on ice with RBC Lysis Buffer and then washed with RPMI+ 1640 10% FBS medium medium. Tumor cells were then filtered through a 70 mm-pore size MACS Smart Strainer (Miltenyi Biotec). For A20 tumors, this step was followed by another purification using Dead Cell Removal Kit (Miltenyi Biotec). $1x10^6$ cells/well were used for staining and blocked with 2.5 µg mouse Fc gamma RI/CD64 antibody and 5 µg anti-mouse CD16/CD32 antibody at 4℃ for 15 min. Antibody staining cocktails containing 1µg/ml EXX-1 to or isotype control antibody, CD3-PerCP Cy5.5, CD4-AF700, CD8-V450, F4/80-PE Cy5, NKp46-PE Cy7, CD11c- APC Cy7, CD45-FITC, anti Qa-1^b (clone 6A8)-PE or isotype control, anti NKG2A-PE or isotype control and zombie aqua viability stain was added to each well at 4°C for 30 min. Cells were washed twice with FACS staining buffer (0.2% BSA 2 mM EDTA 0.02% NaN3 in PBS). Cells were resuspended in 50 µL/well FACS staining buffer and 50 µL/well absolute counting beads.

Evaluation of the mice response to anti-asialo-GM1 antibody and anti-CD8α mAb by flow cytometry

Peripheral blood samples were collected 14 days after first dose of injection of anti-asialo-GM1 and anti-CD8α antibodies (50 ul/ mice). Staining antibody cocktail containing NKp46-PE Cy7 and CD8-V450 were added to each well and incubate at room temperature for 15 minutes. Then 1 ml of the 1X FACS Lysin solution (diluted in water) were added to each well and incubated at room temperature for 10 minutes (in dark place). RBC lysed samples were then washed with 2 ml of the FACS staining buffer (0.2% BSA 2 mM EDTA 0.02% NaN3 in PBS).

All samples were then analyzed on Beckman Coulter CytoFLEX S V4-B2-Y4-R3 flow cytometer (Beckman coulter). Flowcytometry data were analyzed using FlowJo software version 10. For gating, cells were first selected based on FSC and SSC, followed by selection of singlets and live cells.

CONTACT FOR REAGENT AND RESOURCE SHARING:

Further information and requests for resources and reagents should be addressed to the Lead Contact Jon Weidanz (Weidanz@uta.edu).

RESULTS

EXX-1 with active Fc domain induces NK mediated tumor regression in A20 tumor bearing mice

It's been more than a decade that worlds come to know that our immune system is kept in check through molecules expressed by our cells known as checkpoint inhibitors. Since then, immunologists have aimed to understand their mode of action and develop them as therapeutic

tools for certain malignancies. Very soon they realized that only a minority of patients respond to these immunotherapies and thus they tried to improve their efficacy. Here we assessed whether EXX-1 with active Fc have a better therapeutic outcome in tumor-bearing mice in comparison to isotype control. At the same time, we were interested to know whether there is a benefit in targeting the Qa-1^b/Qdm side of the axis versus NKG2A. To address our inquiries, A20 (B-lymphoma) was engrafted s.q. into BALB/c mice. One week after tumor inoculation, A20 formed solid tumor, and mice treated with 10mg/kg of either isotype control, EXX-1 fused with mouse IgG2A or mouse anti NKG2A (clone 20D5) via intraperitoneal (i.p.) injection.

Figure 1A- 1C shows size of individual mouse tumors treated with EXX-1 Fc (active Fc), isotype control or mouse anti NKG2A antibodies respectively. Additionally, a difference in mean tumor size was observed by day 16 post tumoral injection between tumor-bearing mice treated with EXX-1 (active Fc) compared to control antibody (Fig. 1D) suggesting EXX-1 (active Fc) mediated anti-tumor responses via blockade of the NKG2A axis. Furthermore, EXX-1 (active Fc) therapy significantly improved survival time ($p>0.05$) compared to control antibody (Fig. 1E). Our data show 35% of the mice that received EXX-1 as a checkpoint blockade antibody were tumor-free while isotype control led to premature dead in mice.

Direct comparison of tumor regression caused by EXX-1 and anti-NKG2A (clone 20D5) suggesting a benefit in targeting Qa-1^b/Qdm compared to its counterpart NKG2A as only 11% of the mice treated NKG2A respond to therapy and become tumor free (Fig 1E). Our results were in line with previously published data by andré et al, pertaining to the efficacy of a-NKG2A blockaded as a single therapy (10).

EXX-1 mAb with active Fc promote durable anti-tumor immunity in A20 tumor-bearing mice

To better understand the mechanism behind the tumor regression in EXX-1 treated mice, tumor-free mice were rechallenged with the same tumor (A20). We engraft the A20 tumor in naïve mice as a control for our experiment. Following subcutaneous injection of tumor cells into syngeneic BALB/c mice, A20 (B cell lymphoma) cells progressively grew in all naïve mice (Fig. 1A). By contrast, none of the rechallenged mice display tumor growth (Fig. 1B). In addition, obtained results from Kaplan-Meier curves indicate a 100% survival rate in the rechallenged mice with A20, which was previously cured by immunotherapy (Fig 2C). Obtained results indicated that EXX-1 with active Fc domain have an active role in the recruitment of CD8+ T cells in the tumor microenvironment (TME) and promoting the memory response they these cells will create against their target. These results were in line with the study previously conducted by our group on the evaluation of EXX-1 efficacy as a therapy in combination with the cancer vaccine (17).

Qa-1^{b}/Qdm interaction with NKG2A suppress the anti-tumor activity of NK and CD8+ T cells

Although presence of the CD8+T cells in TME are essential for the tumor regression in mice treated with EXX-1 (active Fc domain), we argue that improved survival benefit in these mice is solely mediated by T cells. To prove our point and discover the roles of other immune cell responsible for tumor regression, we evaluated EXX-1 (active Fc) efficacy in presence and absence of NK or CD8+ T cells. Efficacy of EXX-1 were determined by tumor growth kinetic

among different groups of therapy. Obtained results indicate that Both NK cells (Fig 3A) and CD8+ T cells (Fig 3C) were required to control tumor growth, since administration of anti-asialo-GM1 and anti-CD8α mAbs, into tumor-bearing mice in combination with EXX-1 abolished the effect of our checkpoint blockade and led to premature death in animal from respective groups. In contrast, EXX-1 efficacy did not obliterate in control groups as Kaplan Meyer survival estimator still shown 40-45% survival rate in these groups (Figures 3B and 3D). These results suggest that NK cells in addition to cytotoxic T lymphocytes play an important role in tumor remission caused by EXX-1, especially in early stage of tumorogenesis. Moreover, indicate that TCR- like antibodies with active Fc has potential to recruit ADCC mechanism. Our finding is also corroborating the important roles of Qa-1^b/HLAE interaction with NKG2A positive cells in TME and potential benefit that patient may get from their blockade therapeutics. The depletion efficacy of NK and CD8+ T cell in our experiment was validated by flow cytometry detection of these. cells in peripheral blood mononuclear cells (PBMCs). Results indicated that we were able to successfully eliminate both NK or CD8+ T cells in their respective groups (Fig S1).

Boosting EXX-1 therapeutic potency in colorectal cancer via ADCC mechanism

We then investigated whether Qa-1^b/Qdm blockade through EXX-1 active Fc could promote anti-tumor immunity in other tumor models. We use colorectal carcinoma grade IV (CT26) in BALB/c mice. This model was previously characterized as a solid tumor with enriched infiltrating immune cells such as cytotoxic T-cell and NK cells in their TME (19, 20). Gang Shi et al., reported a therapeutic benefit utilizing a combination of anti PD-1 with other therapy created in CT26 bearing mice (21). Therefore, CT26 bearing mice treated one week after tumor

inculcation with 10mg/kg of either EXX-1 Fc active, anti- PD-1 or isotype control antibody. A modest effect on tumor growth inhibition was observed in CT26-bearing mice treated with EXX-1 compared to mice that received anti PD-1 or control antibodies. Figure 4A-4D shows size of individual mouse tumors treated with EXX, control antibody, anti PD-1 or its control antibody respectively.

Additionally, EXX-1 therapy significantly improved survival time compared to anti PD-1 or control antibody (Fig. 4E) suggesting EXX-1 with active Fc mediated anti-tumor responses via blockade of the NKG2A axis in CT26 models. Although none of the mice treated with EXX-1 active Fc displayed complete tumor regression, our findings show that blockade of the NKG2A axis by targeting tumor cells via the Qa-1^b/Qdm peptide complex is effective and resulted in 40% of mice surviving beyond 14 days compared to 0% of mice in the control groups including anti PD-1 treated mice.

Phenotypic characterization of ex-vivo harvested CT26_WT tumor.

Next, by ex-vivo analysis of the CT26 tumor we tried to uncover the reason behind significant differences of tumor sizes observed among different groups of therapy. Figure 5A-5C shows tumor size in mice treated with EXX-1 active Fc, anti PD-1 and isotype control respectively. Given the variation of response generate in different treatment groups, we sought to further characterize the immune cell phenotype in the tumor microenvironment. Staining results of CT26 tumor with EXX-1 antibody revealed a modest up-regulation in the Qa-1^b/Qdm on the surface of the tumor cells (Fig 5D-left panel). In addition, we observed that tumor-associated macrophages (TAM) show binding to EXX-1 antibody (Fig 5E-left pannel), meaning that they have an overexpression in Qa1/Qdm.

Taylor M et al, previously reported an increase in myeloid cells population, particularly M2 macrophages (MHCII+CD206+) in their CT26 tumor model. They assume detected surges in the M2 cells are associated with immune suppression, tumor growth, and metastasis of CT26 tumor (23). Taken together our data revealed that EXX-1 with active Fc is the main reason for tumor growth inhibition observed in our recent study. In other word, we can assume by blocking the Qa-1^b/Qdm on the surface of M2-like macrophages, we can suppress the M2 cells in TME and control the tumor growth in CT26 model.

DISCUSSION

Past decade has seen numerously breakthrough in the field of immune-oncology and become clear that modulation of the immune system can be used combatting the cancer. Despite the advances, immuno-oncology still contained many mysteries and the full spectrum of checkpoint-blocking therapies along with their mode of action, currently is the subject of many studies. Our team previously developed an immune checkpoint blockade antibody (mAb) for mouse Qa-1^b/Qdm complex (EXX-1). Preliminary data from In-vitro characterization of our antibody, confirmed that EXX-1 is highly selective to the Qdm peptide presented by the Qa-1b MHC complex. We also showed that blockade of Qa-1^b/Qdm through EXX-1 promoted the NK cells proliferation. On the other hand, our results from testing EXX-1 functionality in an in-vivo setting suggest that EXX-1 can reverts ineffective cancer vaccine into potent inducer of anti-tumor immunity.

In our current study, we demonstrate the potential benefit that antibody-dependent cellular cytotoxicity (ADCC) mechanism may have on the efficacy of the checkpoint blockade modules.

For this purpose, we conjugate EXX-1 to mouse IgG2A that previously reported by many scientists including Kipps, et al., for its capability in induction of the ADCC in mice (23). We observed that treating tumor bearing mice with EXX-1 (mouse IgG2A) leads to tumor regression and eventually complete tumor elimination in 40 % of the treated mice. On the other hand, our results revealed that treated mice developed and prolong anti-tumor immunity. By elimination of the NK and CD8+ T cells in A20 tumor bearing mice we tried to further investigate the cellular mechanism behind the EXX-1 mode of action. Interestingly we observed that tumor regression mediated by EXX-1 eliminated in the depleted NK or CD8 + T cell mice. Moreover, we found out that NK cells play a crucial role in tumor growth inhibition at the earlier stage of tumorogenesis while cytotoxic lymphocyte will convey their message later in the process.

Van montfoort et al, reported a therapeutic benefit in their murine tumor models when they blocked the NKG2A receptor (24). On the other hand, André P et al, reported that antibody blockade of mouse or human NKG2A combined with anti-PD-(L)1, promotes anti-tumor immunity by unleashing both T and NK cells functions in-vivo as well as in-vitro (10). This is in line with our discovery about the roles NK and CD8 T cells in A20 tumor model.

Also, by direct comparison of the both sides of the NKG2A axis as a target for blocking antibody therapy, we observed targeting Qa-1^b/Qdm by EXX-1, increased mice survivability by 35%. However, treating mice with anti NKG2A only cured 11% of their tumors, suggesting a benefit in blocking Qa-1^b/Qdm side of this axis.

André P et al reported that tumor infiltrated CD8+ T cells are often co-expressing the PD-1 with NKG2A receptor. Since PD-1/PD-L1 blockade antibodies are the first line of treatment for many cancers (10), we tried to compare the efficacy of EXX-1with PD-1 in our animal model. BALB/c mice were inoculated with CT26 tumor and treated with EXX-1 (active Fc domain), anti-PD-1

and their isotype controls. The results illustrated that PD-1 blockade did not improve overall survivability of the mice, whereas EXX-1 therapy increased the life span of the tumor bearing mice. These findings provide insight in the distinct cellular mechanisms underlying the mode of action for the blocking antibodies targeting NKG2a and PD-1 axis.

Van montfoort et al, and others have reported that NKG2A receptor are also expressed on a large quantity of the head and neck tumor reactive CD8+ T cells in human (24). Since HLAE is an ortholog of the Qa-1^b and its interaction with NKG2A receptor have an immune inhibitory role in human, likely having an antibody targeting HLAE peptide complex can create a significant benefit in the field of the human immuno-oncology.

Taken together, these data imply an important restraining role of the NKG2A/Qa-1^b axis for therapees, mediate via an increased NKG2A expression on CD8 T cells in the tumor and induction of Qa-1^b on tumor cells. These findings also provide support for the continued preclinical development of TCR-like antibody conjugate to IgG1, with a long-term goal of clinical evaluation in patients with cancer.

FIGURES

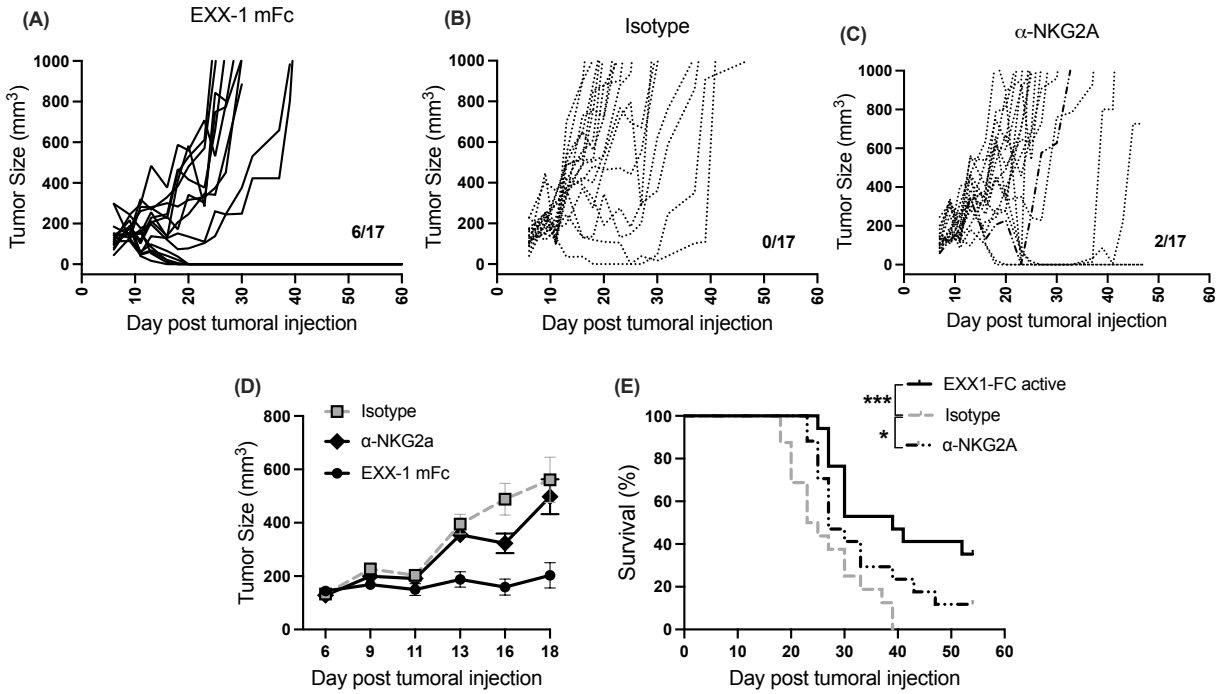

Chapter 5 1: Enhanced cytotoxicity of NK cells against mouse lymphoma through EXX-1 mAb-mediated ADCC

A20 tumor cells were engrafted in BALB/c mice. Tumor bearing mice were then treated on day 9 to 21 in every other day interval (total of 7 doses) with an isotype control, anti-NKG2A and EXX-1 mAb. Graphs shows individual mouse tumor growth in (A) EXX-1, (B) anti NKG2A, (C) isotype control treated groups. (D) comparison of the average tumor growth in each treatment group and (E) combined survival curves. The data presented are the pooled results of two independent experiments. Error bars represent mean±SD (n=17 in each group). (C) Log rank test *p = 0.0142 and ***p=0.0009 was used for statistical analyses.

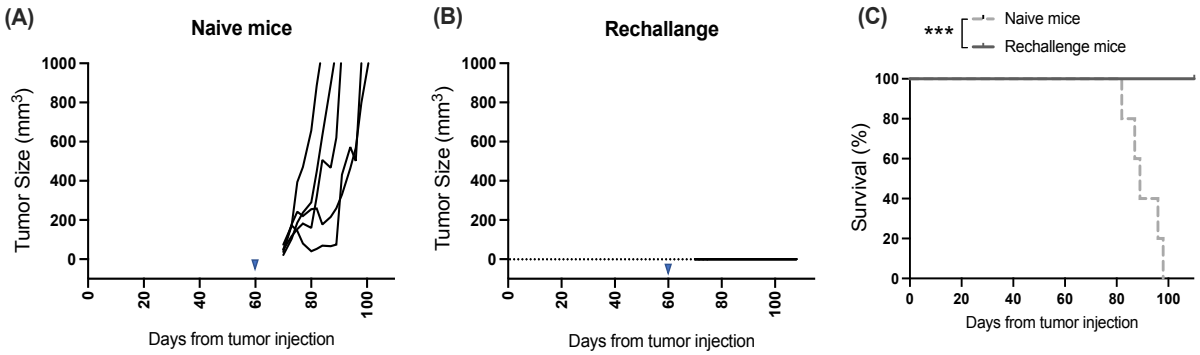

Chapter 5 2: EXX-1 mAb with active Fc promote anti-tumor immunity in A20 tumor-bearing mice.

Graphs shows tumor growth in (A) rechallenged mice with A20 tumor (n=6), (B) Naïve mice engrafted with A20 tumor (n=5). Triangular marks on the graphs indicate the day of tumor engraftment. (C) combined survival curves. (C) Log rank test, ***p = 0.0007 was used for statistical analyses.

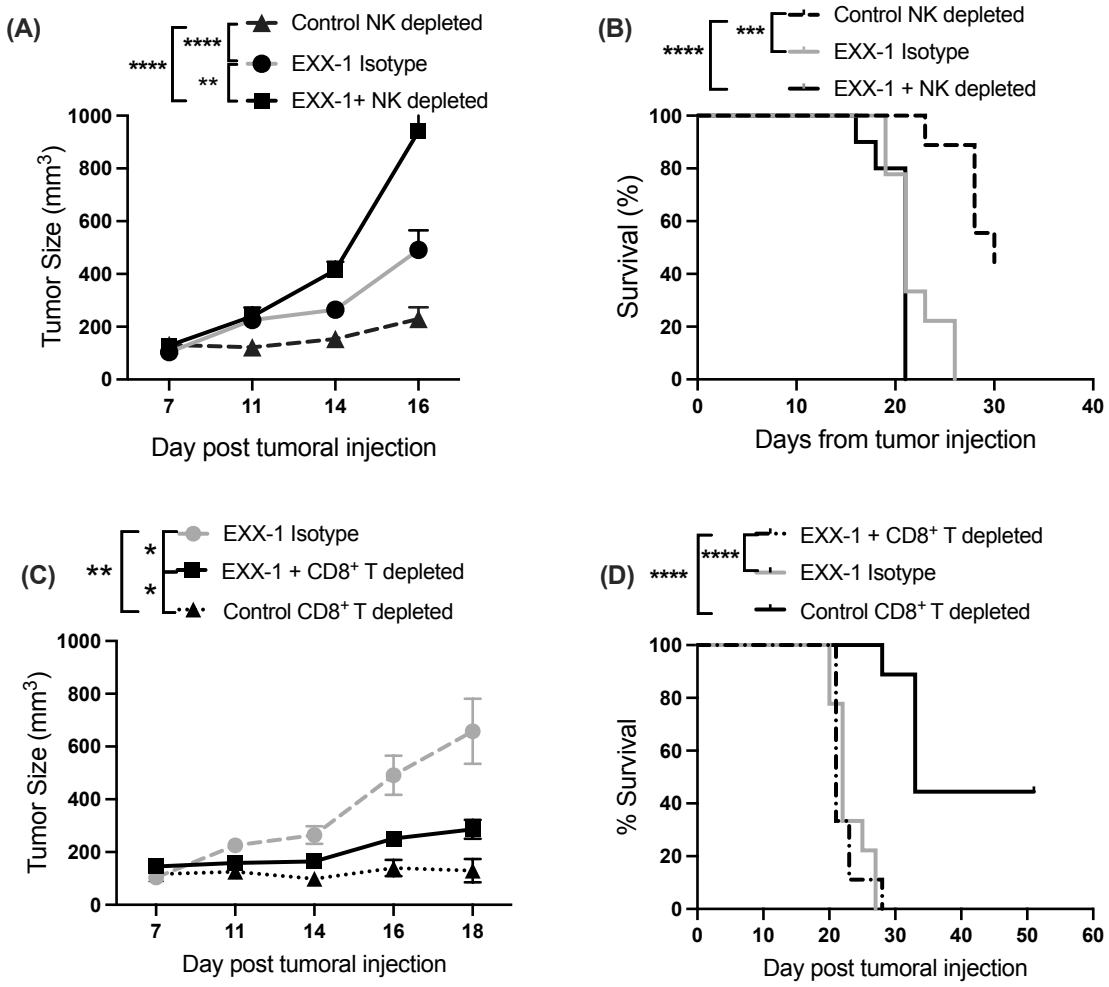

Chapter 5 3: Qa-1^b/Qdm interaction with NKG2A blocks the anti-tumor efficacy of NK and CD8+ T cells

A20 bearing mice were treated with an anti-asialo-GM1 pAbs (NK depleted) or an anti-CD8α (CD8α depleted) one week prior to tumor inoculation. Tumor bearing BALB/c mice were then treated on day 9 through 21 in every other day intervals (total of 7 doses) with EXX-1 mFc mAb. Graphs shows (A) average tumor growth in NK-depleted group, control NK depleted and EXX-1 isotype control, (B) followed by their survival curve (n=10), (C) average tumor growth in CD8α depleted group, control CD8α depleted combined with EXX-1 isotype control and (D) followed by their survival curves (n=10). Data pooled from two independent study. Error bars represent Mean±SD in each group. (A) One-way Anova **p=0.0039, ****p<0.0001 (B) log rank test: ***p=0.0003, ****p<0.0001 were used for analysis of the graphs.

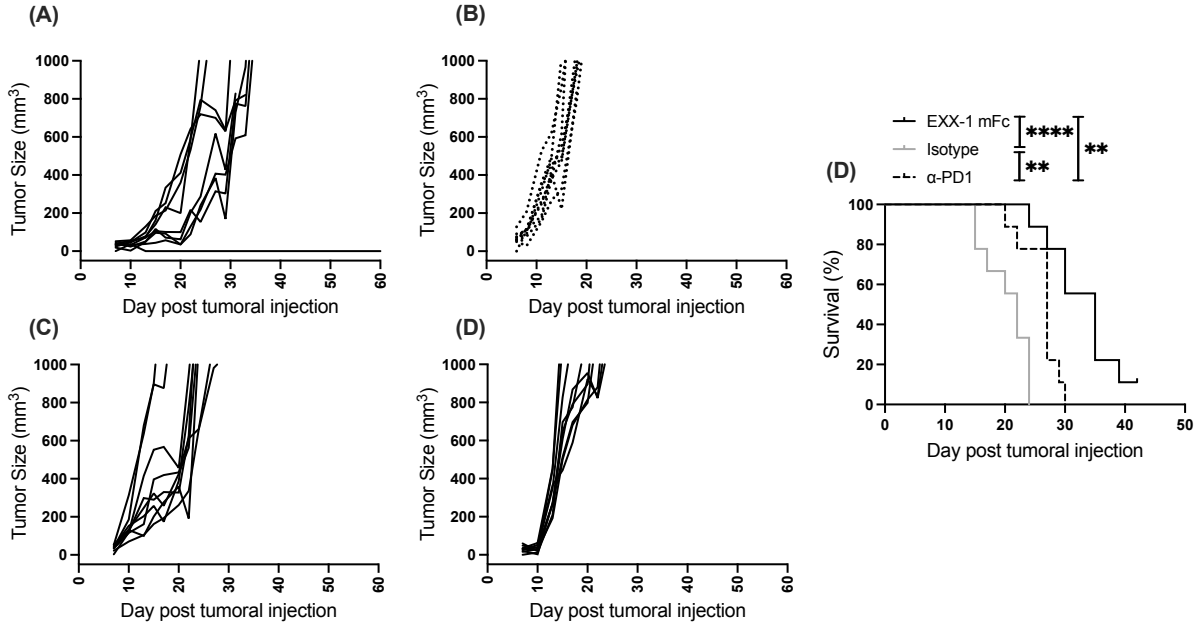

Chapter 5 4: Boosting EXX-1 therapeutic potency in colorectal cancer via ADCC mechanism

CT26_WT tumor cells were engrafted in BALB/c mice. Tumor bearing mice were then treated on day 6 through 18 in every other day interval (total of 7 doses) with isotype control, anti-PD1 and EXX-1 mFc mAb. Graphs shows individual mice tumor groups in (A-B) EXX-1 and isotype control, (C-D) anti-PD1 and isotype control respectively. (E) followed by survival curve (n=10). (E) log rank test **p= 0.0017, ****p<0.0001 used for analysis of the graphs. Data pooled from two independent study.

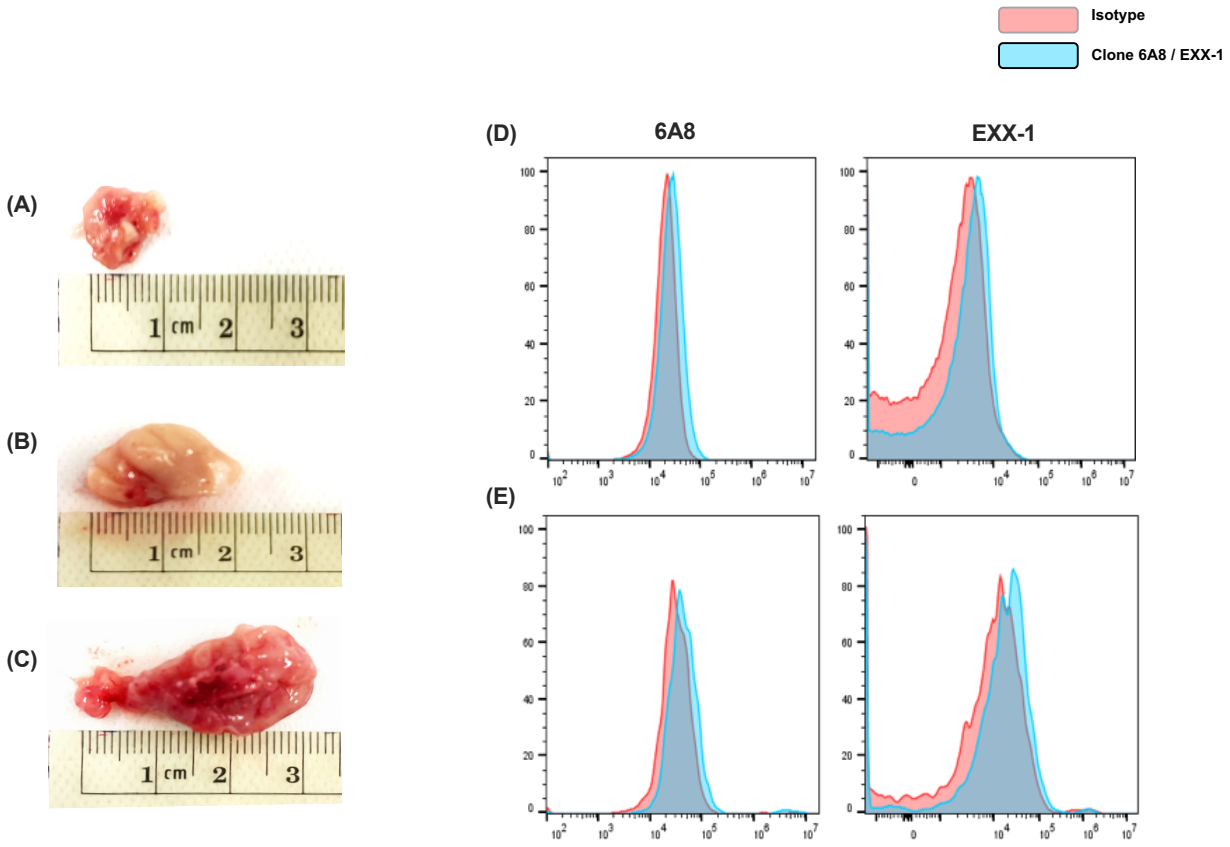

Chapter 5 5: Phenotypic characterization of ex-vivo harvested CT26_WT tumor.

Schematics shows representative tumor size in mice treated with (A) EXX-1 mFc, (B) anti PD-1 and (C) isotype control. Histogram shows flow cytometry characterization of (D) harvested tumor and (E) tumor infiltrating macrophage, determine by anti-Qa-1^{b} clone 6A8 (left panel) and EXX-1 (right panel) binding.

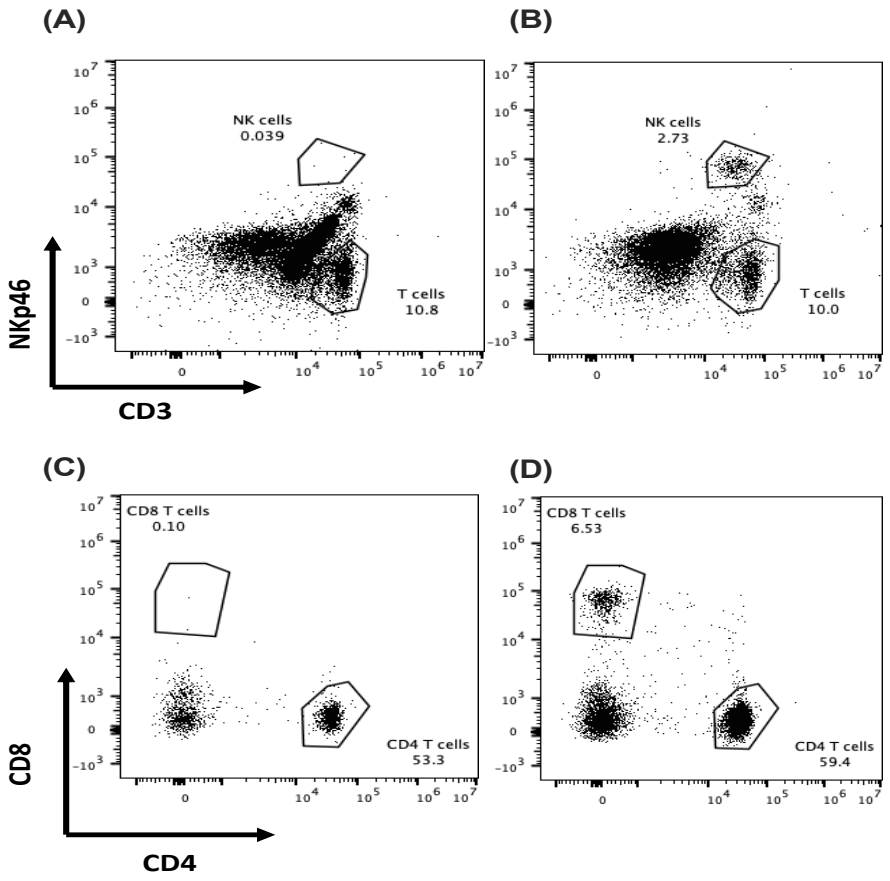

Supplement Figure 5 1: Flow cytometry conformation of NK and CD8+ T cells depletion in mice blood.

Blab/C mice treated with an anti-asialo-GM1 pAbs (NK depleted) or an anti-CD8α (CD8α depleted), bled to evaluate their responses to the injected therapies.
Upper panels: FACS profiles of CD3 and NKp46 expression on NK and T cells in the blood of (A) NK depleted mice, (B) followed by control (Naïve) mice.
Lower panels: FACS profiles of CD8 and CD4 expression on CD3+ T cells in the bloods of (A) CD8α depleted mice and (D) followed by control mice.

REFERENCES

1. Pardoll, Drew M. “The blockade of immune checkpoints in cancer immunotherapy.” Nature reviews. Cancer vol. 12,4 252-64. 22 Mar. 2012, doi:10.1038/nrc3239
2. Topalian, Suzanne L et al. “Immune checkpoint blockade: a common denominator approach to cancer therapy.” Cancer cell vol. 27,4 (2015): 450-61. doi:10.1016/j.ccell.2015.03.001
3. Dietze, Kirsten K et al. “Combining regulatory T cell depletion and inhibitory receptor blockade improves reactivation of exhausted virus-specific CD8+ T cells and efficiently reduces chronic retroviral loads.” PLoS pathogens vol. 9,12 (2013): e1003798. doi:10.1371/journal.ppat.1003798
4. Bertone, S et al. “Transforming growth factor-beta-induced expression of CD94/NKG2A inhibitory receptors in human T lymphocytes.” European journal of immunology vol. 29,1 (1999): 23-9. doi:10.1002/(SICI)1521-4141(199901)29:01<23::AID-IMMU23>3.0.CO;2-Y
5. McMahon, Christopher W et al. “Viral and bacterial infections induce expression of multiple NK cell receptors in responding CD8(+) T cells.” Journal of immunology (Baltimore, Md. : 1950) vol. 169,3 (2002): 1444-52. doi:10.4049/jimmunol.169.3.1444
6. Mingari, M C et al. “HLA class I-specific inhibitory receptors in human T lymphocytes: interleukin 15-induced expression of CD94/NKG2A in superantigen- or alloantigen-activated CD8+ T cells.” Proceedings of the National Academy of Sciences of the United States of America vol. 95,3 (1998): 1172-7. doi:10.1073/pnas.95.3.1172
7. Sheu, Bor-Ching et al. “Up-regulation of inhibitory natural killer receptors CD94/NKG2A with suppressed intracellular perforin expression of tumor-infiltrating CD8+ T lymphocytes in human cervical carcinoma.” Cancer research vol. 65,7 (2005): 2921-9. doi:10.1158/0008-5472.CAN-04-2108

8. Le Dréan, E et al. “Inhibition of antigen-induced T cell response and antibody-induced NK cell cytotoxicity by NKG2A: association of NKG2A with SHP-1 and SHP-2 protein-tyrosine phosphatases.” European journal of immunology vol. 28,1 (1998): 264-76. doi:10.1002/(SICI)1521-4141(199801)28:01<264::AID-IMMU264>3.0.CO;2-O
9. Rapaport, Aaron S et al. “The Inhibitory Receptor NKG2A Sustains Virus-Specific $CD8^+$ T Cells in Response to a Lethal Poxvirus Infection.” Immunity vol. 43,6 (2015): 1112-24. doi:10.1016/j.immuni.2015.11.00
10. André, Pascale et al. “Anti-NKG2A mAb Is a Checkpoint Inhibitor that Promotes Anti-tumor Immunity by Unleashing Both T and NK Cells.” Cell vol. 175,7 (2018): 1731-1743.e13. doi:10.1016/j.cell.2018.10.014
11. TBD
12. L.Q. Chow, et al.“Phase 1b trial of the toll-like receptor 8 agonist, motolimod (VTX-2337), combined with cetuximab in patients with recurrent or metastatic SCCHN.” Clin Cancer Res, 23 (2017), pp. 2442-2450
13. C. Lo Nigro, et a.“Evaluation of antibody-dependent cell-mediated cytotoxicity activity and cetuximab response in KRAS wild-type metastatic colorectal cancer patients.” World J Gastrointest Oncol, 8 (2016), pp. 222-230
14. Weidanz, Jon A et al. “TCR-like biomolecules target peptide/MHC Class I complexes on the surface of infected and cancerous cells.” International reviews of immunology vol. 30,5-6 (2011): 328-40. doi:10.3109/08830185.2011.604880
15. Bossi, Giovanna et al. “Examining the presentation of tumor-associated antigens on peptide-pulsed T2 cells.” Oncoimmunologyvol. 2,11 (2013): e26840. doi:10.4161/onci.26840

16. Purbhoo, Marco A et al. “Quantifying and imaging NY-ESO-1/LAGE-1-derived epitopes on tumor cells using high affinity T cell receptors.” Journal of immunology (Baltimore, Md. : 1950) vol. 176,12 (2006): 7308-16. doi:10.4049/jimmunol.176.12.7308
17. Ghaffari, Soroush et al. “A single-domain TCR-like antibody selective for the Qa-1b/Qdm peptide complex enhances tumoricidal activity of NK cells via the NKG2A immune checkpoint.” Journal of immunology (Baltimore, Md. : 1950) under review.
18. Ossendorp F, Mengedé E, Camps M, Filius R, Melief CJ. Specific T helper cell requirement for optimal induction of cytotoxic T lymphocytes against major histocompatibility complex class II negative tumors. J Exp Med. 1998 Mar 2;187(5):693-702. doi: 10.1084/jem.187.5.693. PMID: 9480979; PMCID: PMC2212165.
19. Mosely, Suzanne I S et al. “Rational Selection of Syngeneic Preclinical Tumor Models for Immunotherapeutic Drug Discovery.” Cancer immunology research vol. 5,1 (2017): 29-41. doi:10.1158/2326-6066.CIR-16-0114
20. Yu, Jong W et al. “Tumor-immune profiling of murine syngeneic tumor models as a framework to guide mechanistic studies and predict therapy response in distinct tumor microenvironments.” PloS one vol. 13,11 e0206223. 2 Nov. 2018, doi:10.1371/journal.pone.0206223
21. Shi, Gang et al. “Modulating the Tumor Microenvironment via Oncolytic Viruses and CSF-1R Inhibition Synergistically Enhances Anti-PD-1 Immunotherapy.” Molecular therapy : the journal of the American Society of Gene Therapy vol. 27,1 (2019): 244-260. doi:10.1016/j.ymthe.2018.11.010

22. Griswold, D P, and T H Corbett. “A colon tumor model for anticancer agent evaluation.” Cancer vol. 36,6 Suppl (1975): 2441-4. doi:10.1002/1097-0142(197512)36:6<2441::aid-cncr2820360627>3.0.co;2-p

23. Kipps, T J et al. “Importance of immunoglobulin isotype in human antibody-dependent, cell-mediated cytotoxicity directed by murine monoclonal antibodies.” The Journal of experimental medicine vol. 161,1 (1985): 1-17. doi:10.1084/jem.161.1.1

24. van Montfoort, Nadine et al. “NKG2A Blockade Potentiates CD8 T Cell Immunity Induced by Cancer Vaccines.” Cell vol. 175,7 (2018): 1744-1755.e15. doi:10.1016/j.cell.2018.10.028

25. Karyampudi L, et al. PD-1 Blunts the Function of Ovarian Tumor-Infiltrating Dendritic Cells by Inactivating NF-κB. Cancer Res. 2016; 76:239–250. DOI: 10.1158/0008-5472.CAN-15-0748 [PubMed: 26567141]

26. Ansell SM, et al. PD-1 blockade with nivolumab in relapsed or refractory Hodgkin’s lymphoma. N Engl J Med. 2015; 372:311–319. DOI: 10.1056/NEJMoa1411087 [PubMed: 25482239]

27. Reichel J, et al. Flow sorting and exome sequencing reveal the oncogenome of primary Hodgkin and Reed-Sternberg cells. Blood. 2015; 125:1061–1072. DOI: 10.1182/blood-2014-11-610436 [PubMed: 25488972]

28. Saederup N, et al. Selective chemokine receptor usage by central nervous system myeloid cells in CCR2-red fluorescent protein knock-in mice. PLoS One. 2010; 5:e13693. [PubMed: 21060874]

29. Maruyama C, et al. Genotyping the mouse severe combined immunodeficiency mutation using the polymerase chain reaction with confronting two-pair primers (PCR-CTPP). Exp Anim. 2002; 51:391–393. [PubMed: 12221933]

30. Takenaka K, et al. Polymorphism in Sirpa modulates engraftment of human hematopoietic stem cells. Nat Immunol. 2007; 8:1313–1323. DOI: 10.1038/ni1527 [PubMed: 17982459]
31. MacDonald KP, et al. An antibody against the colony-stimulating factor 1 receptor depletes the resident subset of monocytes and tissue- and tumor-associated macrophages but does not inhibit inflammation.Blood.2010;116:3955-363.DOI:10.1182/blood-2010-02-266296[PubMd: 20682855].
32. Dobin, A., Davis, C.A., Schlesinger, F., Drenkow, J., Zaleski, C., Jha, S., Batut, P., Chaisson, M., and Gingeras, T.R. (2013). STAR: ultrafast universal RNA-seq aligner. Bioinformatics 29, 15–21.
33. Doisne, J.M., Balmas, E., Boulenouar, S., Gaynor, L.M., Kieckbusch, J., Gardner, L., Hawkes, D.A., Barbara, C.F., Sharkey, A.M., Brady, H.J., et al. (2015). Composition, Development, and Function of Uterine Innate Lymphoid Cells. J. Immunol. 195, 3937–3945. Duzkale, H., Schweighofer, C.D., Coombes, K.R., Barron, L.L., Ferrajoli, A.,
34. O'Brien, S., Wierda, W.G., Pfeifer, J., Majewski, T., Czerniak, B.A., et al. (2011). LDOC1 mRNA is differentially expressed in chronic lymphocytic leukemia and predicts overall survival in untreated patients. Blood 117, 4076–4084.
35. Eixarch, E., Meler, E., Iraola, A., Illa, M., Crispi, F., Hernandez-Andrade, E.,
36. Gratacos, E., and Figueras, F. (2008). Neurodevelopmental outcome in 2- year-old infants who were small-for-gestational age term fetuses with cerebral blood flow redistribution. Ultrasound Obstet. Gynecol. 32, 894–899.
37. Fernandez, N.C., Treiner, E., Vance, R.E., Jamieson, A.M., Lemieux, S., and Raulet, D.H. (2005). A subset of natural killer cells achieves self-tolerance without expressing inhibitory receptors specific for self-MHC molecules. Blood 105, 4416–4423.

38. Filipovic, I., Chiossone, L., Vacca, P., Hamilton, R.S., Ingegnere, T., Doisne, J.M., Hawkes, D.A., Mingari, M.C., Sharkey, A.M., Moretta, L., et al. (2018). Molecular definition of group 1 innate lymphoid cells in the mouse uterus. Nat. Commun. 9, 4492.

39. Goodridge, J.P., Jacobs, B., Saetersmoen, M.L., Clement, D., Hammer, Q., Clancy, T., Skarpen, E., Brech, A., Landskron, J., Grimm, C., et al. (2019). Remodeling of secretory lysosomes during education tunes functional potential in NK cells. Nat. Commun. 10, 514.

Greco, A., Ragucci, M., Coda, A.R., Rosa, A., Gargiulo, S., Liuzzi, R.,Gramanzini, M., Albanese, S., Pappata` , S., Mancini, M., et al. (2013). High frequency ultrasound for in vivo pregnancy diagnosis and staging of placental and fetal development in mice. PLoS ONE 8, e77205.